

การปรับปรุงความเสถียรต่อความร้อนของอะลานีนดีไฮโดรจิเนสจาก
Aeromonas hydrophila โดยวิธี SITE DIRECTED MUTAGENESIS



นาย จีระพันธุ์ มาชาวป่า

วิทยานิพนธ์นี้เป็นส่วนหนึ่งของการศึกษาตามหลักสูตรปริญญาวิทยาศาสตรมหาบัณฑิต

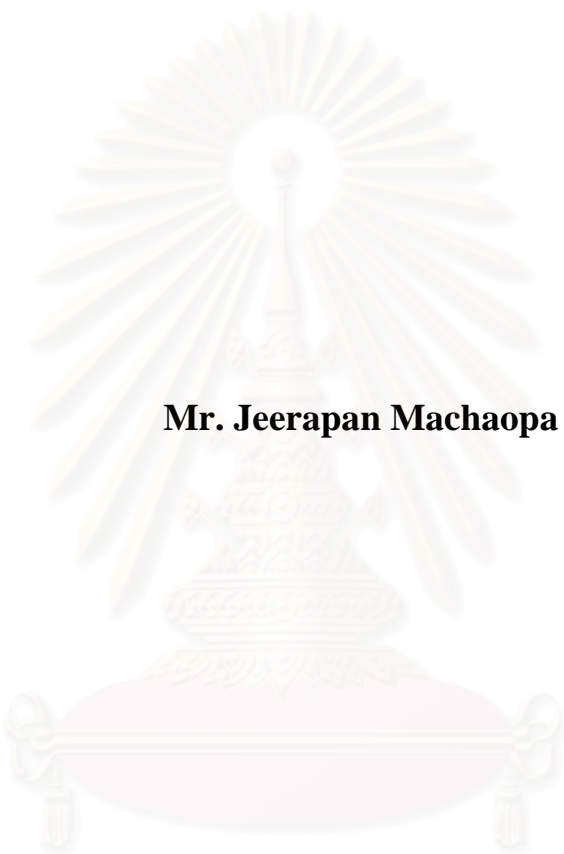
สาขาวิชาชีวเคมี ภาควิชาชีวเคมี
คณะวิทยาศาสตร์ จุฬาลงกรณ์มหาวิทยาลัย

ปีการศึกษา 2546

ISBN 974-17-5383-7

ลิขสิทธิ์ของจุฬาลงกรณ์มหาวิทยาลัย

**THERMOSTABILITY IMPROVEMENT OF
ALANINE DEHYDROGENASE FROM *Aeromonas hydrophila*
BY SITE DIRECTED MUTAGENESIS**



Mr. Jeerapan Machaopa

สถาบันวิทยบริการ
จุฬาลงกรณ์มหาวิทยาลัย
**A Thesis Submitted in Partial Fulfillment of the Requirements
for the Degree of Master of Science in Biochemistry**

Department of Biochemistry

Faculty of Science

Chulalongkorn University

Academic Year 2003

ISBN 974-17-5383-7

Thesis Title THERMOSTABILITY IMPROVEMENT OF
ALANINE DEHYDROGENASE FROM *Aeromonas hydrophila*
BY SITE DIRECTED MUTAGENESIS
By Mr. Jeerapan Machaopa
Field of Study Biochemistry
Thesis Advisor Assistant Professor Kanoktip Packdibamrung, Ph.D.

Accepted by the Faculty of Science, Chulalongkorn University in Partial
Fulfillment of the Requirements for the Master's Degree

..... Dean of the Faculty of Science
(Professor Piamsak Menasveta, Ph.D.)

THESIS COMMITTEE

.....Chairman
(Associate Professor Piamsook Pongsawasdi, Ph.D.)

.....Thesis Advisor
(Assistant Professor Kanoktip Packdibamrung, Ph.D.)

..... Member
(Associate Professor Siriporn Sittipraneed, Ph.D.)

..... Member
(Associate Professor Pairoh Pinphanichakarn, Ph.D.)

จิระพันธุ์ มาชาวป่า : การปรับปรุงความเสถียรต่อความร้อนของอะลานีนดีไฮโดรจิเนสจาก

Aeromonas hydrophila โดยวิธี SITE DIRECTED MUTAGENESIS (THERMOSTABILITY

IMPROVEMENT OF ALANINE DEHYDROGENASE FROM *Aeromonas hydrophila* BY SITE DIRECTED MUTAGENESIS)

อาจารย์ที่ปรึกษา : ผศ.ดร.กนกทิพย์ ภักดีบำรุง, xxx หน้า, ISBN xxx-xxx-xxxx-x

อะลานีนดีไฮโดรจิเนส (EC 1.4.1.1) เร่งปฏิกิริยาการดึงหมู่อะมิโนจากแอล-อะลานีนให้ผลิตภัณฑ์คือ แอมโมเนียม, ไพรูเวท และ NADH ซึ่งเป็นปฏิกิริยาที่ผันกลับได้และต้องการ NAD^+ เป็นโคเอนไซม์ จากปฏิกิริยาดังกล่าวจึงได้มีการนำเอนไซม์นี้มาใช้ในการสังเคราะห์กรดอะมิโน รวมทั้งนำมาประยุกต์ใช้ในการวินิจฉัยโรค อะลานีนดีไฮโดรจิเนสที่แยกได้จาก *Aeromonas hydrophila* มีแอกติวิตีและความจำเพาะต่อสับสเตรทสูงเหมาะสมสำหรับใช้ผลิตกรดอะมิโน แต่อย่างไรก็ตามแอกติวิตีของเอนไซม์ลดลงอย่างรวดเร็วหลังจากการบ่มที่อุณหภูมิสูงกว่า 55 องศาเซลเซียส เป็นเวลา 10 นาที ดังนั้นจึงทำการปรับปรุงอะลานีนดีไฮโดรจิเนสให้มีความเสถียรต่ออุณหภูมิสูงขึ้น โดยใช้วิธี site-directed mutagenesis เพื่อเปลี่ยนกรดอะมิโน ที่ตำแหน่ง โกลซีน 38, ลูซีน 101 และอะลานีน 231 เป็น กรดกลูตามิก นอกจากนี้ยังเปลี่ยนที่ ลูซีน 58 และ โพรลีน 168 เป็นอาร์จินีน เพื่อการเกิดพันธะอิเลกโตรสแตติก ในโปรตีนซึ่งมีรายงานว่าเป็นปัจจัยสำคัญต่อความเสถียรต่อความร้อนของอะลานีนดีไฮโดรจิเนส โดยเปรียบเทียบกับพันธะที่พบในเอนไซม์จากแบคทีเรียทนร้อน *Bacillus stearothermophilus* จากการทดลองในสารละลาย เอนไซม์หยาบพบว่าเอนไซม์ที่เปลี่ยนแปลงตำแหน่ง ลูซีน 101 หรือ อะลานีน 231 เป็นกรดกลูตามิกทนร้อนมากกว่าเอนไซม์ดั้งเดิม แต่ถ้าเปลี่ยนโกลซีน 38 เป็นกรดกลูตามิกไม่มีผลต่อการทนร้อน ในขณะที่การเปลี่ยนลูซีน 58 หรือ โพรลีน 168 เป็นอาร์จินีน มีผลให้เอนไซม์สูญเสียคุณสมบัติทนร้อน ดังนั้นจึงได้ทำการเปลี่ยนกรดอะมิโนทั้งสองตำแหน่งพร้อมกัน (ลูซีน 101 และอะลานีน 231) พบว่าทำให้ความเสถียรเพิ่มสูงขึ้น จากนั้นนำเอนไซม์ที่ให้ผลทนร้อนดีขึ้นมาทำให้บริสุทธิ์ เมื่อวิเคราะห์ด้วยอิเล็กโตรโฟรีซิสแบบไม่เสียดสภาพพบว่าเอนไซม์มีความบริสุทธิ์มากกว่า 90 เปอร์เซ็นต์ และแต่ละเอนไซม์ที่เปลี่ยนแปลงมีการเคลื่อนที่ต่างจากเอนไซม์ดั้งเดิม ซึ่งเป็นผลจากการเพิ่มประจุลบบนโมเลกุลของเอนไซม์ ขณะที่การเคลื่อนที่ของเอนไซม์จากการทำอิเล็กโตรโฟรีซิสแบบเสียดสภาพให้ผลไม่แตกต่างจากเอนไซม์ดั้งเดิม การศึกษาความเสถียรต่อความร้อนซึ่งใช้ค่า T_m เป็นค่าแสดงความเสถียร พบว่าเอนไซม์ที่มีการเปลี่ยนแปลงกรดอะมิโนทั้งสองตำแหน่ง (ลูซีน 101 และอะลานีน 231) แสดงค่า T_m สูงกว่าเอนไซม์ดั้งเดิม 3 องศาเซลเซียส ส่วนเอนไซม์ที่เปลี่ยนแปลงตำแหน่งเดียวให้ผลเพิ่มขึ้น 2 องศาเซลเซียส นอกจากนี้ยังพบว่าอุณหภูมิที่เหมาะสมในการทำปฏิกิริยาของเอนไซม์ที่ถูกเปลี่ยนแปลงทั้งหมดมีการเพิ่มขึ้นจากเดิม 50 องศาเซลเซียส เป็น 52.5 องศาเซลเซียส แต่ผลของ pH ความจำเพาะกับสับสเตรท และค่า K_m ต่อแอล-อะลานีน และ NAD^+ พบว่าไม่แตกต่างกัน ทำให้คาดการณ์ได้ว่าบริเวณเร่งปฏิกิริยาไม่ถูกเปลี่ยนแปลง จากการทดลองทั้งหมดสรุปได้ว่าการเปลี่ยนแปลงกรดอะมิโนลูซีน 101 และอะลานีน 231 เป็นกรดกลูตามิก ทำให้เอนไซม์มีความเสถียรต่อความร้อนเพิ่มขึ้นเนื่องจากการเกิดพันธะอิเลกโตรสแตติกโดยที่การทำงานของเอนไซม์ไม่เปลี่ยนแปลง

ภาควิชาชีวเคมี.....

ลายมือชื่อนิสิต

สาขาวิชา.....ชีวเคมี.....

ลายมือชื่ออาจารย์ที่ปรึกษา

ปีการศึกษา.....2546.....

4272238323 : MAJOR BIOCHEMISTRY

KEY WORD: alanine dehydrogenase/ site directed mutagenesis/ thermostability/ electrostatic interaction

JEERAPAN MACHAOPA: THERMOSTABILITY IMPROVEMENT OF ALANINE DEHYDROGENASE FROM *Aeromonas hydrophila* BY SITE DIRECTED MUTAGENESIS. THESIS ADVISOR: ASST. PROF. KANOKTIP PACKDIBAMRUNG, Ph.D., xxx pp. ISBN xxx-xxx-xxxx-x

Alanine dehydrogenase (EC 1.4.1.1) catalyzes the NAD^+ - dependent reversible oxidative deamination of L-alanine to form ammonia, pyruvate, and NADH. The enzyme is important as a catalyst for the synthesis of amino acids. Moreover, it is therefore applicable to diagnosis of malignant hematopoietic disease. Alanine dehydrogenase from *Aeromonas hydrophila* has high activity and high substrate specificity, so it is suitable for L-alanine production. However, the enzyme activity lost rapidly upon the incubation at temperature above 50°C for 10 min. To improve the enzyme thermostability, site-directed mutagenesis was performed. Uncharged amino acids were replaced by charge residues. G38E, L58R, L101E, P168R and A231E were selected for electrostatic interaction formation based on three dimensional structure of thermophilic counterpart enzyme from *Bacillus stearothermophilus*. In crude enzyme, L101E and A231E showed higher stability than wild type. While G38E showed similar enzyme level with wild type, L58R and P168R showed lower. Thus, residues of Leu 58 and A231 were chosen for double mutation. Alanine dehydrogenase from L101E, A231E and L101E/Arg231 were purified for comparison of their characters with wild type. The purity of wild type and all mutant enzymes were more than 90%, estimated by native PAGE. Mobility of mutant enzymes on native gel was faster than that of wild type. Whereas, no difference was detected by SDS-PAGE. This evidence reflected the net charge on molecule of enzymes. T_m of L101E/A231E increased 3°C while single mutants showed 2°C higher than wild type. Furthermore, optimum temperature of mutants shifted up from 50°C in wild type to 52°C. The optimum pH, substrate specificity and K_m for L-alanine and NAD^+ of all mutants were not differed from wild type, so no change in an active site of enzyme was occurred. Thus, replacement of Leu 101 and Ala 231 with Glu could form electrostatic interaction which could enhance thermostability.

DepartmentBiochemistry.....
Field of study.....Biochemistry.....
Academic year.....2003.....

Student's signature.....
Advisor's signature.....

ACKNOWLEDGEMENT

I would like to express my deepest gratitude to my advisor, Assist. Prof. Dr. Kanoktip Packdibamrung for her generous advice, skillful assistance, and technical helps guidance, encouragement, supporting, fruitful and stimulating discussions through the period of my study.

My appreciation is also expressed to Prof. Haruo Misono and Prof. Shinji Nagata for their supporting and sequencing helps.

Sincere thanks and appreciation are due to Assoc. Prof. Dr. Piamsook Pongsawasdi, Assoc. Prof. Dr. Siriporn Sittipraneed and Assoc. Prof. Dr. Pairoh Pinphanichakarn who serve as the members of the master committees, for their helpful suggestions and comments.

The financially support of research scholarship, Chulalongkorn university, is also gratefully acknowledged.

The special thanks are also extended to Miss Nattawadee Poomipark for *alaDH* gene, furthermore, Miss Arunee Leksakorn and Miss Jittima Chareonpanich for their technical guidance and materials for literature review.

I would like to express my sincere thanks to all teachers for their care and encouragement.

My cordial thanks also go to all friends of the Biochemistry and Biotechnology department for their helps in the laboratory and friendships that make me enjoy and happy throughout my study.

Last but not least, the warmest gratitude is extended to the patience, understanding, helping, encouragement, constant support and warmhearted love of my family whilst I have spent many hours with this thesis rather than with them. My thanks are also extended to my patience and sedulous too.

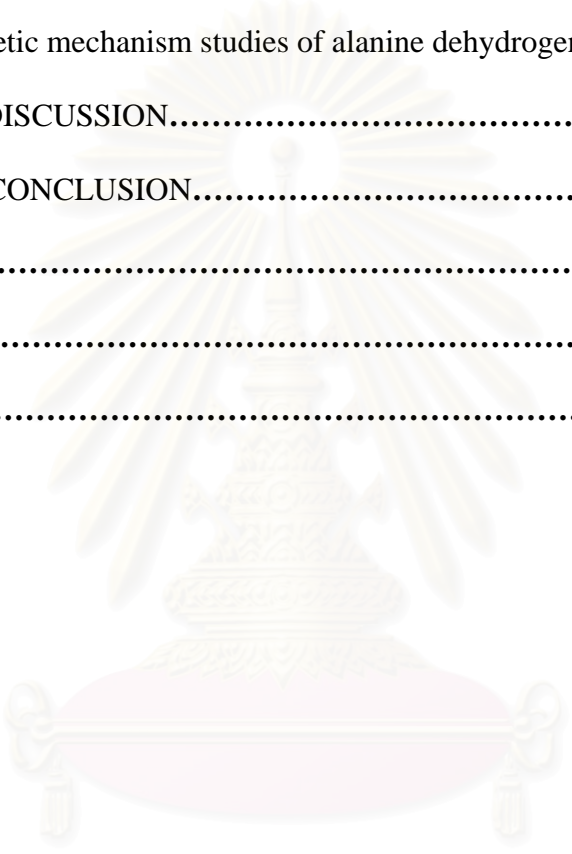
CONTENTS

	Page
THAI ABSTRACT	iv
ENGLISH ABSTRACT	v
ACKNOWLEDGEMENT	vi
CONTENTS	vii
LIST OF TABLES.....	xi
LIST OF FIGURES.....	xii
ABBREVIATIONS.....	xiv
CHAPTER I INTRODUCTION.....	1
1.1 Amino acid dehydrogenase.....	1
1.2 Alanine dehydrogenase (AlaDH).....	5
1.3 Structural basis of protein thermostability.....	15
1.4 Electrostatic interaction of ion pair.....	18
1.5 Sequence and structural differences in thermophilic and mesophilic proteins.....	20
1.6 Engineering proteins for thermostability.....	22
1.7 Protein thermostability and electrostatic interactions.....	25
1.8 Site-directed mutagenesis.....	27
CHAPTER II MATERIALS AND METHODS.....	31
2.1 Equipments.....	31
2.2 Chemicals.....	32
2.3 Enzymes and restriction enzymes.....	35
2.4 Oligonucleotide primers.....	36
2.5 Bacterial strains and plasmids.....	36
2.6 Selection of amino acid residues for contribution of salt bridges.....	37
2.6.1 Construction of three-dimensional structure.....	37
2.6.2 Calculation of electrostatic interaction.....	37

	Page
2.6.3 Selection of amino acid residues.....	38
2.7 Site-directed mutagenesis.....	38
2.7.1 Plasmid extraction.....	38
2.7.2 Agarose gel electrophoresis.....	40
2.7.3 Site directed mutagenesis (QuikChange site-directed mutagenesis kit).....	41
2.7.4 Plasmid extraction of mutant <i>alaDH</i> gene.....	43
2.8 Enzyme activity assay and Protein assay.....	44
2.8.1 Crude extraction preparation.....	44
2.8.2 Enzyme activity assay.....	44
2.8.3 Protein measurement.....	45
2.9 Nucleotide sequencing.....	45
2.10 Transformation into <i>E. coli</i> JM 109.....	46
2.11 Purification of alanine dehydrogenase.....	46
2.11.1 Bacterial cultivation.....	46
2.11.2 Preparation of crude enzyme solution	47
2.11.3 Purification procedures of enzyme	48
2.12 Polyacrylamide gel electrophoresis.....	51
2.12.1 Non-denaturing polyacrylamide gel electrophoresis (Native PAGE).....	51
2.12.2 SDS-polyacrylamide gel electrophoresis.....	53
2.13 Characterization of alanine dehydrogenase and mutate enzymes.....	54
2.13.1 Effect of temperature on AlaDH activity.....	54
2.13.2 Effect of pH on AlaDH activity.....	54
2.13.3 Effect of temperature on AlaDH stability.....	55
2.13.4 Substrate specificity of alanine dehydrogenase.....	55

	Page
2.14 Kinetic parameter of alanine dehydrogenase	55
CHAPTER III RESULTS.....	57
3.1 Selection of amino acid residues for contribution of electrostatic interaction	57
3.1.1 Construction three-dimensional structure.....	57
3.1.2 Calculation of electrostatic interaction and amino acid sequence alignment.....	59
3.2 Site-directed mutagenesis.....	66
3.1.1 Plasmid extraction.....	66
3.1.2 Site-directed mutagenesis (QuikChange site-directed mutagenesis kit).....	66
3.3 Enzyme activity assay and Protein assay.....	69
3.4 Transformation into <i>E. coli</i> JM 109.....	69
3.5 Nucleotide sequencing	74
3.6 Thermostability of crude enzymes	74
3.7 Double site-directed mutagenesis.....	74
3.8 Purification of alanine dehydrogenase.....	77
3.8.1 Preparation of crude enzyme.....	77
3.8.2 Ammonium sulfate precipitation.....	77
3.8.3 DEAE-Toyopearl column chromatography.....	77
3.8.4 Blue Sepharose column chromatography.....	78
3.9 Determination of enzyme purity and protein pattern on polyacrylamidegel electrophoresis.....	78
3.9.1 Non-denaturing polyacrylamide gel electrophoresis.....	78
3.9.2 SDS polyacrylamide gel electrophoresis (SDS-PAGE).....	82
3.10 Characterization of AlaDH wild type and mutants.....	82
3.10.1 Effect of temperature on AlaDH activity.....	82

	Page
3.10.2 Effect of pH on AlaDH activity.....	86
3.10.3 Effect of temperature on AlaDH stability.....	86
3.10.4 Substrate specificity of phenylalanine dehydrogenase.....	86
3.11 Kinetic mechanism studies of alanine dehydrogenase.....	90
CHAPTER IV DISCUSSION.....	101
CHAPTER V CONCLUSION.....	113
REFERENCES.....	114
APPENDICES.....	121
BIOGRAPHY.....	145



สถาบันวิทยบริการ
จุฬาลงกรณ์มหาวิทยาลัย

LIST OF TABLES

Table	Page
1.1 The group of NAD(P) ⁺ - dependent amino acid dehydrogenase.....	3
1.2 Properties of AlaDHs.....	16
3.1 List of created electrostatic interaction in three-dimensional model of mutant AlaDHs	64
3.2 The activity of crude enzyme from <i>E. coli</i> XL1-Blue containing L588R mutant plasmid	70
3.3 The activity of crude enzyme from <i>E. coli</i> XL1-Blue containing P1688R mutant plasmid	70
3.4 The activity of crude enzyme from <i>E. coli</i> JM109 containing L58R and P168R mutant plasmid	71
3.5 The activity of crude enzyme from <i>E. coli</i> JM109 containing G38E, L101E or A231E mutant plasmid.....	72
3.6 The activity of crude enzyme AlaDHs in <i>E. coli</i> JM109.....	73
3.7 The activity of crude enzyme from <i>E. coli</i> JM109 containing L101E/A231E mutant plasmid.....	76
3.8 Purification table of AlaDHs.....	81
3.9 Substrate specificity of AlaDHs.....	89
3.10 The apparent K_m values of AlaDHs.....	99
3.11 Properties of AlaDH wild type and mutants	100

LIST OF FIGURES

Figure	Page
1.1 The general reaction of L-amino acid dehydrogenases.....	2
1.2 The reaction of L-alanine dehydrogenase.....	2
1.3 The production of L-alanine by ultrafiltration membrane reactor	7
1.4 Enzymatic syntheses of D-amino acids by a multienzyme system consisting of the coupling reaction of four enzymes	8
1.5 Kinetic mechanism of alanine dehydrogenase	12
1.6 Assembly of the hexamer of AlaDH.....	13
1.7 Locations of arginine residues in the three-dimensional structural models of AlaDHs.....	17
1.8 Different types of ion pairs in proteins.....	19
2.1 Step of selection of amino acid position for contribution of electrostatic interaction	39
2.2 QuikChange™ site-directed mutagenesis kit method	42
2.3 Flow chart of purification process of alanine dehydrogenase	49
3.1 Three-dimensional structure of AlaDHs.....	58
3.2 Linear alignment of the amino acid sequence of alanine dehydrogenase from various sources.....	60
3.3 Linear alignment of the amino acid sequence of alanine dehydrogenase from <i>Aeromonase hydrophila</i> and published <i>Bacillus stearothermophilus</i>	62
3.4 Location of mutated residues in the three-dimensional structure model of AlaDH from <i>Aeromanas hydrophila</i>	65
3.5 Agarose gel electrophoresis of plasmids template.....	67
3.6 Agarose gel electrophoresis of <i>EcoRI/HindIII</i> digested mutant plasmids	68
3.7 Thermostability of crude AlaDH from wild type and mutants.....	75
3.8 Purification of alanine dehydrogenase by DEAE-Toyopearl column.....	79
3.9 Purification of alanine dehydrogenase by Blue Sepharose column.....	80
3.10 Non-denaturing PAGE of alanine dehydrogenase from Blue sepharose column....	83
3.11 SDS-polyacrylamide gel electrophoresis of alanine dehydrogenase.....	84

Figure	Page
3.12 Effect of temperature on AlaDH activity.....	85
3.13 Effect of pH on AlaDH activity.....	87
3.14 Effect of temperature of AlaDH thermostability activity.....	88
3.15 Initial velocity patterns for oxidative deamination of wild type when varied L-alanine.....	91
3.16 Initial velocity patterns for oxidative deamination of wild type when varied NAD ⁺	92
3.17 Initial velocity patterns for oxidative deamination of L101E varied L-alanine....	93
3.18 Initial velocity patterns for oxidative deamination of L101E when varied NAD ⁺	94
3.19 Initial velocity patterns for oxidative deamination of A231E varied L-alanine...95	
3.20 Initial velocity patterns for oxidative deamination of A231E when varied NAD ⁺	96
3.21 Initial velocity patterns for oxidative deamination of L101E/A231E varied L-alanine.....	97
3.22 Initial velocity patterns for oxidative deamination of L101E/A231E when varied NAD ⁺	98
4.1 Glu 231 of <i>A. hydrophila</i> (upper) coincided with Glu 230 of <i>P. lapideum</i> (lower).....	109
4.2 Glu 101 and Arg 105 formation in <i>A. hydrophila</i> AlaDH (upper) and Glu 101 and Arg 102 formation in <i>B. stearrowthermophilus</i> AlaDH (lower).....	110

ABBREVIATIONS

A	absorbance, 2'-deoxyadenosine (in a DNA sequence)
Ala	alanine
AlaDH	alanine dehydrogenase
bp	base pairs
BSA	bovine serum albumin
C	2'-deoxycytidine (in a DNA sequence)
°C	degree Celsius
cm	centrimeter
Da	Dalton
DNA	deoxyribonucleic acid
dNTP	2'-deoxynucleoside 5'-triphosphate
EDTA	ethylene diamine tetraacetic acid
G	2'-deoxyguanosine (in a DNA sequence)
IPTG	isopropylthio- β -D-galactosidase
kb	kilobase pairs in duplex nucleic acid,
kDa	kiloDalton
K_m	Michaelis constant
l	liter
LB	Luria-Bertani
μ g	microgram
μ l	microliter
μ M	micromolar
M	mole per liter (molar)
mg	milligram
min	minute
ml	milliliter
mM	millimolar
MW	molecular weight
N	normal
NAD ⁺	nicotinamide adenine dinucleotide (oxidized)

NADH	nicotinamide adenine dinucleotide (reduced)
NADP ⁺	nicotinamide adenine dinucleotide phosphate (oxidized)
NADPH	nicotinamide adenine dinucleotide phosphate (reduced)
ng	nanogram
nm	nanometer
OD	optical density
PAGE	polyacrylamide gel electrophoresis
PCR	polymerase chain reaction
pmol	picomole
PMSF	phenyl methyl sulfonyl fluoride
rpm	revolution per minute
RNase	ribonuclease
SDS	sodium dodecyl sulfate
T	2'-deoxythymidine (in a DNA sequence)
TB	tris-borate buffer
TE	tris-EDTA buffer
T_m	melting temperature, melting point
UV	ultraviolet
V	voltage
v/v	volume by volume
w/w	weight by weight
X-gal	5-bromo-4-chloro-3-indolyl- β -D-galactopyranoside

CHAPTER I

INTRODUCTION

1.1 Amino acid dehydrogenase

Amino acid dehydrogenases (EC 1.4.1.-) catalyze the reversible deamination of amino acids to the corresponding keto acids in the presence of pyridine nucleotide coenzymes, NAD(P)^+ . The general equation for this reaction can be illustrated as shown in Figure 1.1 (Brunhuber and Blanchard, 1994). They catalyze the removal of the amino group, generally from L-amino acids, to formation of the corresponding keto acids by reductive amination. Keto acid and ammonia can be converted to L-isomer of amino acid. Many kinds of amino acid dehydrogenase are found in an extensive number of diverse prokaryotic and eukaryotic organisms (Table 1.1). They are known as important enzymes, which provide a route for interconversion of inorganic nitrogen with organic nitrogen. In other words, they serve as a connecting link between amino acid and organic acid metabolism. Their metabolic function can be described as the balance of both amino acid and keto acid syntheses. The amino group is firstly removed as free ammonia before the carbon skeleton of an amino acid can be metabolized for energy through glycolysis and/or TCA cycle. Coenzymes, NAD(H) and NADP(H) , are involved in reaction. They can be dissociated easily and need second reaction with another metabolite for generation. These properties are one of the means by which nature directs the flow of intermediates in response to biosynthetic needs. The participation of NAD(P)^+ makes these enzyme systems a valuable tool for the analysis of L-amino acids or their corresponding keto acids. By reductive amination of the keto acid, L-amino acid can be obtained in a lot of

Table 1.1 The group of NAD(P)⁺ - dependent amino acid dehydrogenase

EC number	Enzyme	Coenzymes	Major source
1.4.1.1	AlaDH	NAD	Bacteria (<i>Bacillus</i> , <i>Streptomyces</i> , <i>Anabena</i> , <i>Pseudomonas</i> , <i>Rhodobacter</i> , <i>Arthrobacter</i> , <i>Thermus</i> , <i>Enterobacter</i> , <i>Phormidium</i>) chrorella
1.4.1.2	GluDH	NAD	Plants, fungi, yeasts, bacteria
1.4.1.3	GluDH	NAD(P)	Animals (bovine liver, chicken liver), tetrahymena, bacteria (<i>Clostridium</i> , <i>Thiobacillus</i>)
1.4.1.4	GluDH	NADP	Plants, <i>Euglena gracilis</i> , <i>Chrorella sarokiniana</i> , fungi, yeasts, bacteria
1.4.1.5	L-Amino acidDH	NADP	Bacteria (<i>Clostridium sporogenes</i>)
1.4.1.7	SerDH	NAD	Plants (parsley)
1.4.1.8	ValDH	N A D , NADP	Bacteria (<i>Streptomyces</i> , <i>Alcaligenes faecalis</i> , <i>Planococcus</i>), plants (pea, wheat)
1.4.1.9	LeuDH	NAD	Bacteria (<i>Bacillus</i> , <i>Clostridium</i> , <i>Thermoactinomyces</i>)
1.4.1.10	GlyDH	NAD	Bacteria (<i>Mycobacterium tuberculosis</i>)
1.4.1.11	DAHDH	N A D , NADP	Bacteria (<i>Clostridium</i> , <i>Brevibacterium</i>)
1.4.1.12	DAPDH	NAD(P)	Bacteria (<i>Clostridium</i>)
1.4.1.15	LysDH	NAD	Human liver
1.4.1.16	DAPMDH	NADP	Bacteria (<i>Corynebacterium glutamicum</i> , <i>Brevibacterium</i> sp., <i>Bacillus sphaericus</i>)
1.4.1.17	MethylalaDH	NADP	Bacteria (<i>Pseudomonas</i> sp.)
1.4.1.18	L y s D H (Lys-6-DH)	NAD	Bacteria (<i>Agrobacterium tumefaciens</i> , <i>Klebsiella pneumoniae</i>)
1.4.1.19	TryDH	NAD(P)	Plants (<i>Nicotiana tabacum</i> , <i>Pisum sativum</i> , <i>Spinacia oleracea</i>)
1.4.1.20	PheDH	NAD	Bacteria (<i>Sporosarcina ureae</i> , <i>Bacillus sphaericus</i> , <i>Rhodococcus marinas</i> , <i>Thermoactinomyces intermedius</i>)
1.4.1.-	AspDH	NADP	Bacteria (<i>Klebsiella pneumoniae</i>)

DH, dehydrogenase; NAD(P), NAD and NADP-nonspecific; DAHDH: L-erythro-3,5-diaminohexanoate dehydrogenase; DAPDH, 2,4-diaminopentanoate dehydrogenase; DAPMDH, meso-2,6-diaminopimelate dehydrogenase; MethylalaDH, N-methyl-L-alanine dehydrogenase.

Source: Ohshima and Soda, 2000

yield because the equilibrium of the reaction favors amino acid formation. Thus, amino acid dehydrogenases have been extensively studied in the past and have found widespread application in amino acid production for clinical and food analyses.

Nowadays, L-amino acids are widely used in various compounds synthesis, for example, L-glutamic acid, L-lysine, L-alanine and L-leucine. It appears technically feasible to carry out such reaction also on a large scale. Economic consideration shows, however, that the enzyme-catalyzed production of L-amino acid competes with the fermentation or biotransformation route, which employs cheap substrates, such as molasses or methanol and ammonia, and highly producing strains optimized by classical mutation methods or genetic engineering. In recent years, enzyme and whole-cell bioreactor methods as well as chemical methods have been developed for L-amino acid production. For example, leucine dehydrogenase (LeuDH), alanine dehydrogenase (AlaDH) and phenylalanine dehydrogenase (PheDH) are used for the continuous production of L-leucine, L-alanine and L-phenylalanine, respectively (Ohshima and Soda, 1990). The products, L-amino acids are used as food and feed additives such as L-phenylalanine, an important starting material for an artificial sweetener, aspartame (Suye *et al.* 1992). Moreover, PheDH can be used in the synthesis of DOPA (3, 4 dihydroxyphenylalanine) which is the precursor of many chemical compounds such as melanine in hair and skin which the defect of DOPA also cause Parkinson's disease (Reinhold *et al.*, 1987). In addition, a continuous production of L-amino acids and their derivatives, amino acid dehydrogenases are used for the preparation of ^{15}N -labeled amino acids such as L- ^{15}N -alanine (Mocanu *et al.*, 1982), L- ^{15}N -glutamate (Bojan *et al.*, 1980) and L- ^{15}N -leucine (Wandrey *et al.*, 1984).

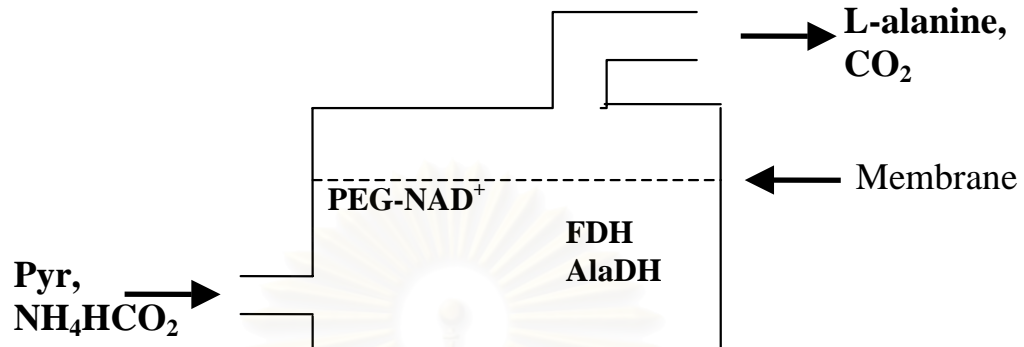
Enzymatic analysis of amino acids, keto acids and ammonia is an important tool in clinical chemistry, bioprocess control and nutrition studies. The methods are based on the increase and decrease in concentration of NADH in the enzyme reaction of amino acid dehydrogenase which can be detected by spectrophotometer. Amino acid dehydrogenase are applicable in the assay of marker enzyme of human diseases, for example LeuDH is used for the assay of serum leucine aminopeptidase (Takamiya *et al.*, 1983), which is related to liver disease and AlaDH is for erythrocytic γ -glutamyl cyclotransferase, which is a marker of malignant hematopoietic disease (Takahashi *et al.*, 1987). Furthermore, PheDH is used for the specific determination of L-phenylalanine and phenylpyruvate, and is therefore applicable to diagnosis of neonatal hyperphenylalaninemia and phenylketonuria (Ohshima *et al.*, 1990b). Thermostable amino acid dehydrogenases are advantageous for these analyses because of their high stability. Nowadays, the genes for thermostable amino acid dehydrogenases have been cloned into *E. coli*. Since enzyme productivity has been enhanced and purification has been facilitated, the thermostability enzymes are proved to be very useful as industrial and analytical biocatalysts.

1.2 Alanine dehydrogenase (AlaDH)

Alanine dehydrogenase catalyzes the reversible oxidative deamination of L-alanine to pyruvate by using NAD(P)⁺ as coenzyme (Figure 1.2). L-alanine itself is an important product, which approximately 250 tons were consumed in 1980 (Calton *et al.*, 1992). It is used in seasonings, enteral and parenteral nutrition, and drug synthesis. Isotopically labeled alanines and pyruvate, such as the ¹⁵N-, ¹¹C-, and ¹³C-labeled species, have been produced using AlaDH for biological research application of NMR and

positron emission tomography (PET) (Mosanu *et al.*, 1982). The enzyme also has been employed for synthesis of 3-fluoro-alanines, L- β -chloroalanine, (R)-3-fluorolactate, and (S)-2-amino-5-(1,3-dioxolan-2-yl)-pentanoic acid, which are useful unnatural amino acid drug intermediates. In application of AlaDH to industrial production of amino acids, multienzyme reaction system for simultaneous coenzyme regeneration has been proposed. Yamamoto *et al.*, (1980) studied continuous production of L-alanine from pyruvate and ammonia using an ultrafiltration membrane reactor containing AlaDH, formate dehydrogenase and NAD(H) which bound covalently to polyethyleneglycol (PEG) (Figure 1.3). The formate dehydrogenase is used to catalyze the regeneration of the PEG-NADH co-enzyme. The system can be used to produce several L-amino acids. Otherwise, the synthesis of various D-amino acids by a multienzyme system has been developed. In this system, D-amino acids are produced from the corresponding keto acids and ammonia by coupling four enzyme reactions catalyzed by L-alanine dehydrogenase, D-amino acid aminotransferase, alanine racemase, and formate dehydrogenase as shown in Figure 1.4. This is based on the high substrate specificity of alanine racemase and the strict enantioselectivity and low structural specificity for the substrates of D-amino acid aminotransferase. D-alanine and NADH are regenerated with alanine dehydrogenase and formate dehydrogenase, respectively (Galkin *et al.*, 1997b). Furthermore, Vadas *et al.*, (2002) synthesized L-alanine by reductive amination of pyruvate using AlaDH from hyperthermophilic archaeon *Archaeoglobus fulgidus*. The reaction mixture included yeast formate dehydrogenase for regeneration of NADH. The synthesis of L-alanine at room temperature was accompanied by no detectable loss of alanine dehydrogenase activity over 139 h with $\geq 99\%$ consumption of pyruvate.

A.



B.

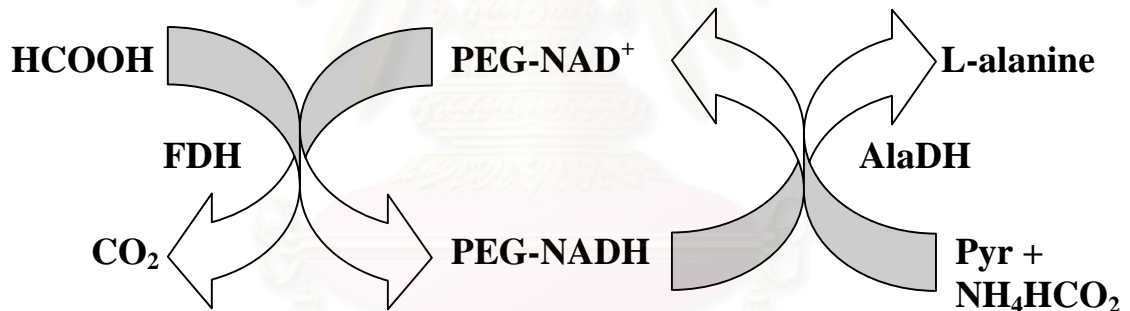


Figure 1.3 The production of L-alanine by ultrafiltration membrane reactor

A. enzyme membrane reactor

B. The reaction of L-alanine producing catalyzed by enzyme

AlaDH : alanine dehydrogenase

FAD : formate dehydrogenase

PEG : polyethyleneglycol

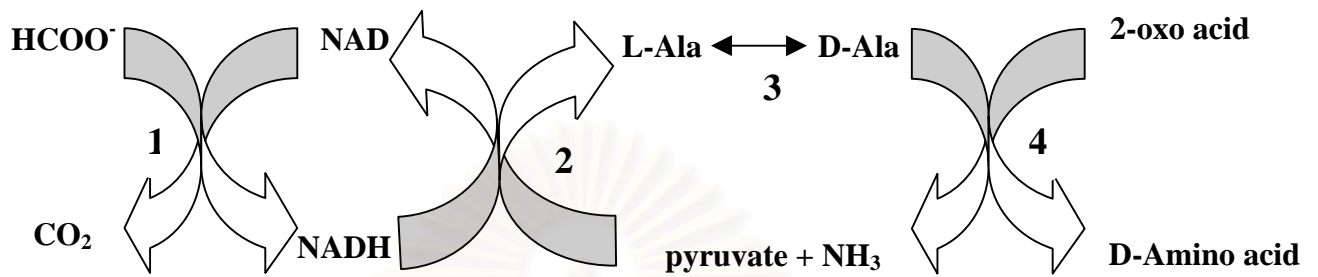


Figure 1.4 Enzymatic syntheses of D-amino acids by a multienzyme system consisting of the coupling reaction of four enzymes.

1 : formate dehydrogenase

2 : alanine dehydrogenase

3 : alanine racemase

4 : D-amino acid aminotransferase

Source: Galkin *et al.*, 1997b

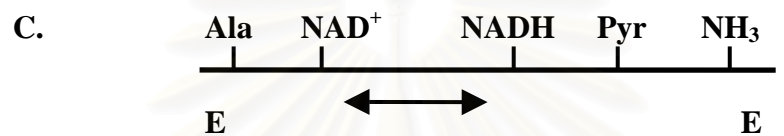
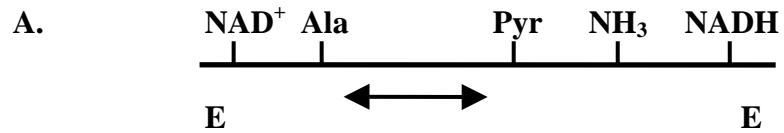
สถาบันวิทยบริการ
จุฬาลงกรณ์มหาวิทยาลัย

Among amino acid dehydrogenase, Alanine dehydrogenase is the first enzyme that has been studied. It was found in *Bacillus subtilis* by Yoshida and Freeze (1964). The enzyme was purified and its molecular mass was estimated by the sedimentation equilibrium method to be 228 kDa. Subsequently, Vali *et al.*, (1980) studied AlaDH in *Thermus thermophilus*. The enzyme has a molecular mass of 290 kDa as detected by the sedimentation equilibrium method, and is composed of six subunits of identical. The thermostability of the *T. thermophilus* enzyme is much greater than that of *B. subtilis* enzyme. Ohshima *et al.*, (1990) studied the production of AlaDH from *Bacillus sphaericus* and found that the enzyme has molecular mass 230 kDa and composes of six subunits (38 kDa). The enzyme has high specificity on L-alanine (K_m 18.9 μ M). The pH optimum for reductive amination is around 9.0 and between 10.0-10.5 for oxidative deamination. The properties of the enzyme are closely to those of *Bacillus subtilis*, but it is more stable at high temperature. In 1994, Sawa *et al.*, purified and characterized alanine dehydrogenase from cyanobacterium *Phormidium lapideum* and found that the molecular mass of native enzyme was 240 kDa, and SDS-PAGE revealed a minimum molecular mass of 41 kDa, suggesting a six-subunit structure. The pH optima are 8.4 for reductive amination of pyruvate and 9.2 for oxidative deamination of L-alanine. The K_m values are 5.0 mM for L-alanine and 0.04 mM for NAD^+ , 0.33 mM for pyruvate, 60.6 mM for NH_4^+ (pH 8.7), and 0.02 mM for NADH. Not only in vegetative cells, had AlaDH also been found in spores of various bacteria. Siranosian *et al.*, (1993) found the sporulation defect caused by null mutations in AlaDH. This defect was partly relieved by the addition of pyruvate at a high concentration, indicating that the normal role of alanine dehydrogenase in sporulation might be to generate pyruvate as provide an energy source for sporulation.

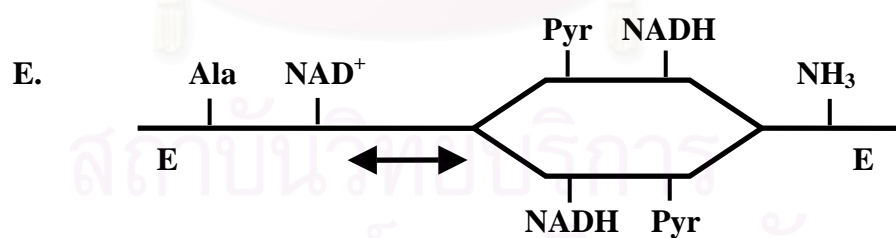
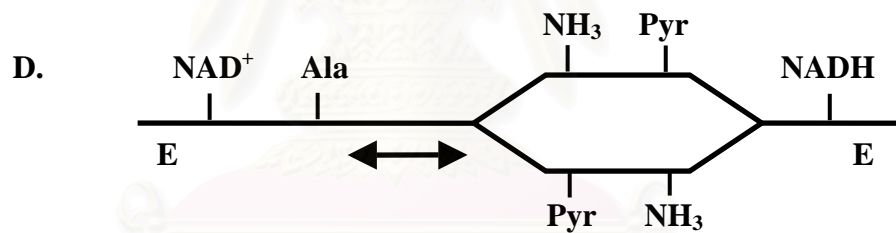
For gene cloning, there are few reports about alanine dehydrogenase available. In 1990, Sakamoto *et al.* studied gene cloning, purification and characterization of thermostable AlaDH of *Bacillus stearothermophilus*. The *alaDH* gene was cloned and expressed in *E. coli* C600. The enzyme was purified 30 fold with 46 % yield. It showed immunochemically identical with that of *B. stearothermophilus*. The enzyme has a molecular mass of 240 kDa and consists of six subunits identical in molecular mass (40 kDa). The enzyme is not inactivated by heat treatment at pH 7.2 and 75°C for 30 min; at 55°C and various pHs between 6.0 and 11.5 for 10 min. The enzymological properties of AlaDH from *B. stearothermophilus* are very similar to those of the mesophilic *B. sphaericus* enzyme except for thermostability. This research group also reported gene cloning of *B. sphaericus* in the same year (Kuroda *et al.*, 1990). *alaDH* gene from *B. sphaericus* and *B. stearothermophilus* were analyzed for their nucleotide sequences. They found that each *alaDH* gene consists of a 1,116 bp and encodes 372 amino acid residues corresponding to subunits of the hexamer. The similarity of amino acid sequence between two AlaDH is very high (>70%) whereas the both enzymes differed in thermostability. The *B. stearothermophilus* enzyme retained about 50% of its initial activity when heated at 85°C for 5 min, whereas the *B. sphaericus* enzyme lost its activity when heated at 65°C for 5 min. Moreover, Chowdhury *et al.*, (1998) purified AlaDH from *Enterobacter aerogenes* ICR 0220. The enzyme has a molecular mass of about 245 kDa and consists of six identical subunits. The enzyme showed maximal activity at about pH 10.9 for the deamination of L-alanine and about pH 8.7 for the amination of pyruvate. Initial-velocity and product inhibition studies suggested that the deamination of L-alanine proceeded through a sequential ordered binary-ternary mechanism in which NAD⁺ bound first to the enzyme followed by L-alanine and the products were released in the order of ammonia,

pyruvate, and NADH (Figure 1.5). The K_m were 0.47 mM for L-alanine, 0.16 mM for NAD^+ , 0.22 mM for pyruvate, 0.067 mM for NADH, and 66.7 mM for ammonia. The enzyme gene was cloned into *Escherichia coli* JM109 cells and the nucleotides were sequenced. The deduced amino acid sequence was very similar to that of the alanine dehydrogenase from *B. subtilis*.

Chemical modification of alanine dehydrogenase in *B. subtilis* was studied by Delforge *et al.*, (1997) and its amino acid sequence was also compared with those of AlaDH from various bacteria and pyridine nucleotide transhydrogenase from various species. From this report, Lys- 74 was found to be the substrate binding site and the enzyme probably has a different active site from other B-stereospecific amino acid dehydrogenase, since alanine dehydrogenase is A-stereospecific and no sequence similarity was found between alanine dehydrogenase and other B-stereospecific amino acid dehydrogenase such as glutamate dehydrogenase and leucine dehydrogenase, except the coenzyme binding site. The three dimensional structure of alanine dehydrogenase from *Phormidium lapideum* was studied by Baker *et al.* (1998). It was found that the enzyme subunit folds compact into two domains. Both domain 1 (residues 1-128 and 306-361) and domain 2 (residues 129-305) are constructed from a mainly parallel central β -sheet, flanked by helices (Figure 1.6). Six subunits of AlaDH pack together to form a hexamer, a trimer of dimer. The refined structure of the L-alaDH- NAD^+ binary complex revealed that the NAD^+ binds to the C-terminal end of the strands in domain 2 of each in a manner similar to that seen in other dehydrogenases. The adenine ring of NAD^+ site in a mainly hydrophobic pocket bound by Ile 198, Val 238, Leu 248, Ser 219 and Gly 174 with formed a hydrogen bond between the side chain of Ser 219 and nitrogen of adenine



Sequential ordered binary-ternary mechanism



Sequential random binary-ternary mechanism

Figure 1.5 Kinetic mechanism of alanine dehydrogenase

- A. Mesophilic *Bacillus sphaericus*
- B. *Bacillus subtilis*
- C. *Mycobacterium*
- D. Thermophilic *Bacillus sphaericus*
- E. *Propionibacterium*

Source: Ohshima and Soda, 2000

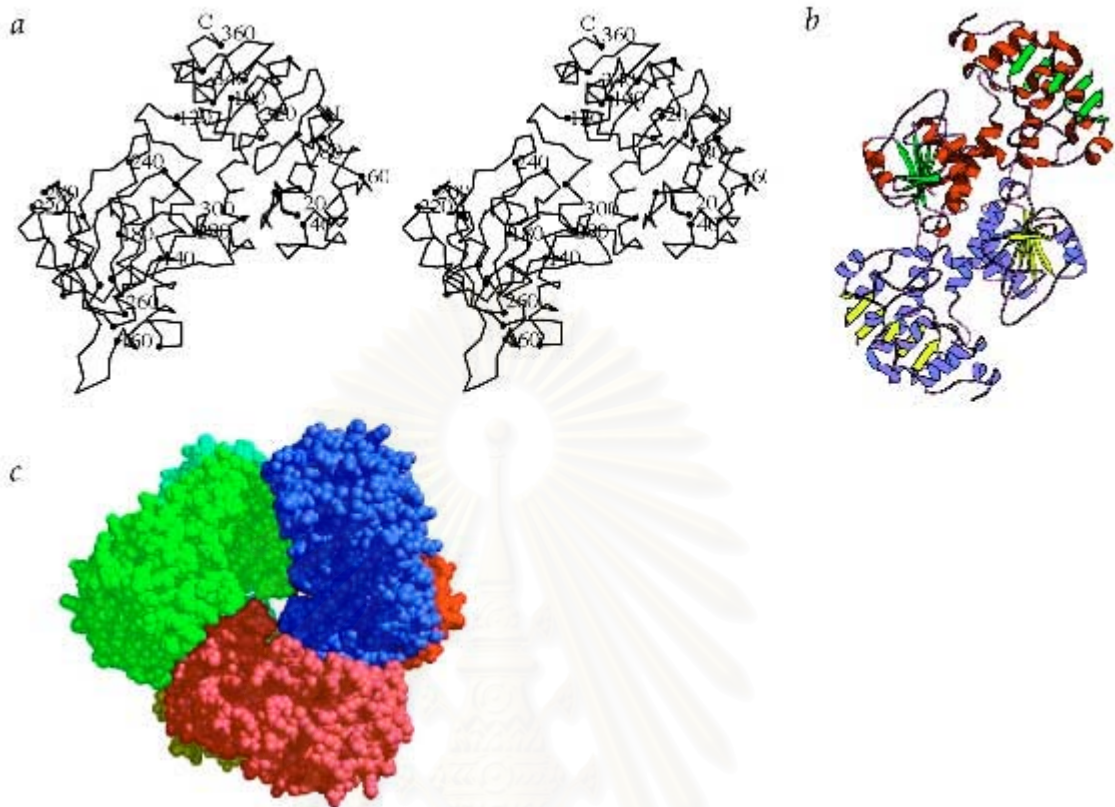


Figure 1.6 Assembly of the hexamer of AlaDH. *a*, The $C\alpha$ stereo backbone of a single subunit, with every 10th residue drawn as a black dot and every 20th numbered. *b*, A schematic diagram of the dimer, with domain 1 furthest from the two-fold axis and the dinucleotide binding domain 2 closest to the two-fold axis. *c*, A space filling representation of the hexamer viewed down the three-fold axis.

Source: Baker *et al.*, 1998

ring. In addition, the refined structure of the L-AlaDH-pyruvate binary complex showed that the pyruvate binding site locates near the binding site of the nicotinamide ring and deep in the cleft between the two domains. The methyl group packs against the hydrophobic residues Tyr 93, Met 132 and Leu 129 with the carboxyl hydrogen bonded to the side chain of Arg 15. The side chain amino acid group of Lys 74 interacts with both the carbonyl oxygen of the pyruvate and one of its carboxyl oxygen. A hydrogen bond is also made between the carbonyl oxygen of the pyruvate and the side chain of His 95, and N δ 2 from the side chain of Asn 299 interacts with one of the carboxylate oxygens of the pyruvate. All of the above residues are identical in all the L-AlaDHs sequenced. Baker *et al.* also proposed that in the binary complex of pyruvate with AlaDH, the pyruvate carboxyl is bound by the side chain of both Lys 74 and Arg 15. The close proximity of the imidazole ring of His 95 to the pyruvate carbonyl group suggested that this residue could well act as the acid base catalyst.

In 1999, Galkin *et al.* studied the cold-adapted alanine dehydrogenase from *Shewanella* sp. stain Ac10 (SheAlaDH) and *Carnobacterium* sp. stain St2 (CarAlaDH). The enzyme gene were cloned and expressed in *Escherichia coli*. SheAlaDH has molecular mass of 240 kDa and consists of 6 identical subunits like *Bacillus* enzymes. The amino acid sequences of SheAlaDH and CarAlaDH were compared with the sequences of AlaDH from other bacterial sources. CarAlaDH exhibited the highest overall levels of identity (58.5 to 62.8%) with the enzymes from members of the same group of bacteria (the low-G+C-content gram-positive bacteria), such as *B. stearothermophilus*, while, SheAlaDH was most similar (level of identity, 76.5%) to *Vibrio proteolyticus*, that is a mesophilic gram-negative bacterium. The optimum temperature for catalytic activity of SheAlaDH and CarAlaDH are in the same range as

the half-inactivation temperatures (Table 1.2). SheAlaDH was more stable than CarAlaDH but less stable than all of the AlaDHs from mesophilic (*B. subtilis*) and thermophilic stains (*B. stearothermophilus*). The total numbers of salt bridges declined in the order thermophilic AlaDH-mesophilic AlaDHs-psychrotrophic AlaDHs when AlaDHs from members of the same bacterial subgroups (SheAlaDH and VprAlaDH; and BstAlaDH, BsuAlaDH, and CarAlaDH) were compared (Table 2). The structural model for CarAlaDH indicates that it has two and five fewer arginine residues forming salt bridges per subunit than BsuAlaDH and BstAlaDH, respectively (Fig. 1.7). The thermal instability of CarAlaDH may be explained by the lower total number of salt bridges, in particular salt bridges formed by arginine residues, in the enzyme. However, other structural features often found in proteins isolated from cold-adapted organisms, such as lower numbers of extended surface loops and aromatic-aromatic interactions, were not evident in the structural models of the psychrotrophic AlaDHs. Thus, salt bridge content is proposed to be the primary factor on thermal stability of AlaDHs.

1.3 Structural basis of protein thermostability

Numerous studies have identified a number of potential interactions that nature may use to render proteins extremely thermostable (Jaenicke and Bohm, 1998). Among them are (1) an increase in the number of hydrogen bond, (2) additional or improved electrostatic interactions caused by salt bridges or networks there of, (3) optimized hydrophobic interactions, (4) increased compactness or packing densities, (5) increased polar compared with non-polar surface areas, (6) increases in α -helical content and α -helix stability, (7) the (improved) binding of metal ions, (8) improved fixation of the polypeptide chain termini to the protein core, (9) replacement of residues with

Table 1.2 Properties of AlaDHs

Parameter	Source of <i>alaDH</i> gene				
	γ -Subdivision of the <i>Proteobacteria</i>		Low-G+C-content gram-positive bacteria		
	<i>V. proteolyticus</i>	<i>Shewanella</i> sp. strain Ac10	<i>B. stearothermophilus</i>	<i>B. subtilis</i>	<i>Carnobacterium</i> sp. strain St2
Optimum growth temp (°C)	37	20	57	37	20
Thermostability (°C) ^a	63	59	81	64	41 ^b
Maximum activity temp (°C)	53-57	47-50	60-64	60-64	35-38 ^b
K_m for L-alanine (mM)	30	7.6	ND ^c	1.73	3.8 ^b
Arg/(Arg + Lys) ratio	0.39	0.47	0.5	0.34	0.19
Proline content (%)	4.5	4.3	4.3	5.0	5.0
Glycine content (%)	8.8	9.4	10.8	10.1	10.1
No. of salt bridges	117	87	132	99	60
No. of aromatic interactions	36	30	54	42	48
No. of hydrogen bonds	1,892	1,986	1,936	1,947	1,962
Hydrophobic interactions	2.2	2.1	2.2	2.2	2.1
No. of loop insertions/no. of deletions	2/0	2/0	3/1	2/1	2/1

^a Temperature at which the enzyme loses 50% of its original level of activity after 30 min of incubation.

^b The values were estimated from the results obtained with a crude enzyme preparation.

^c ND, Not determined.

Source: Galkin *et al*, 1999

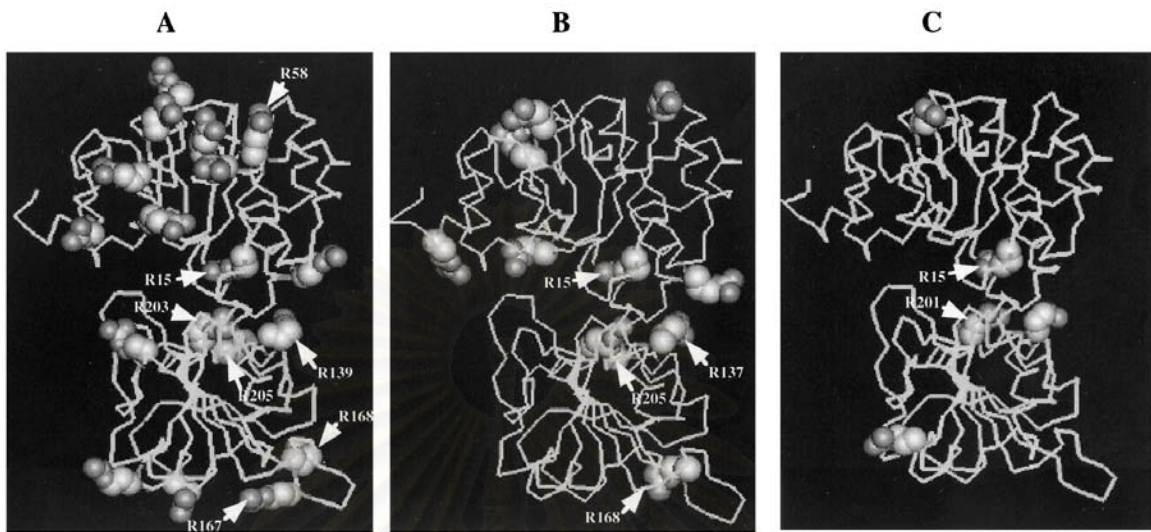


Figure 1.7 Location of arginine residues in the three-dimensional structural models of AlaDHs from the thermophilic organism *B. stearotherophilus* (A), the mesophilic organism *B. subtilis* (B), and the psychrotrophic organism *Carnobacterium* sp. strain St2 (C). The arginine residues are shown as space-filling models, and the residues that form salt bridges are indicated by arrows. The lines indicate the C α traces of the protein monomers.

Source: Galkin *et al.*, (1999)

energetically unfavorable conformations by glycine, (10) truncation of solvent-exposed loops, (11) a higher number of prolines and β -branched amino acids in loops, (12) association to oligomers, (13) reduction of the content of the thermally labile amino acids asparagines, glutamine, cysteine and methionine. These stabilizing features can occur at all structure levels, from the amino acid sequence to the quaternary structure of proteins. The growing amount of whole genome sequences from mesophilic and (hyper) thermophilic organisms and the enormous speed with which new X-ray structure become available, now allow systematic comparison between proteins from mesophiles and (hyper) thermophiles that promises a more general insight into the problem.

1.4 Electrostatic interaction of ion pair

The electrostatic interactions such as salt bridge or ion pair play important roles in protein structure and function, such as in oligomerization, molecular recognition, domain motions, α -helix capping, and thermostability (Kumar and Nussunov, 2002). Oppositely charged residue pairs often form ion pairs in protein. In NMR conformers, the ion pair is classified as salt bridges, nitrogen-oxygen (N-O) bridges and longer-range ion pair on the basis of geometrical criteria (Figure 1.8). In salt bridge, centroids of the side-chain positive charged groups (basic amino: Arg, Lys or His) and side-chain negative charged groups (acidic amino: Asp or Glu), as well as at least a pair of nitrogen and oxygen atom of the ion-pair residues are within a 4 Å distance. In N-O bridges, at least a pair of the side-chain nitrogen and oxygen atom of the ion-pairing residues is within 4 Å distance, but the distance between the side-chain charged group centroids is greater than 4 Å. In the longer-range ion pairs, the side chain charged groups centroids as well as the side-chain nitrogen and oxygen atoms are more than 4 Å apart. The electrostatic

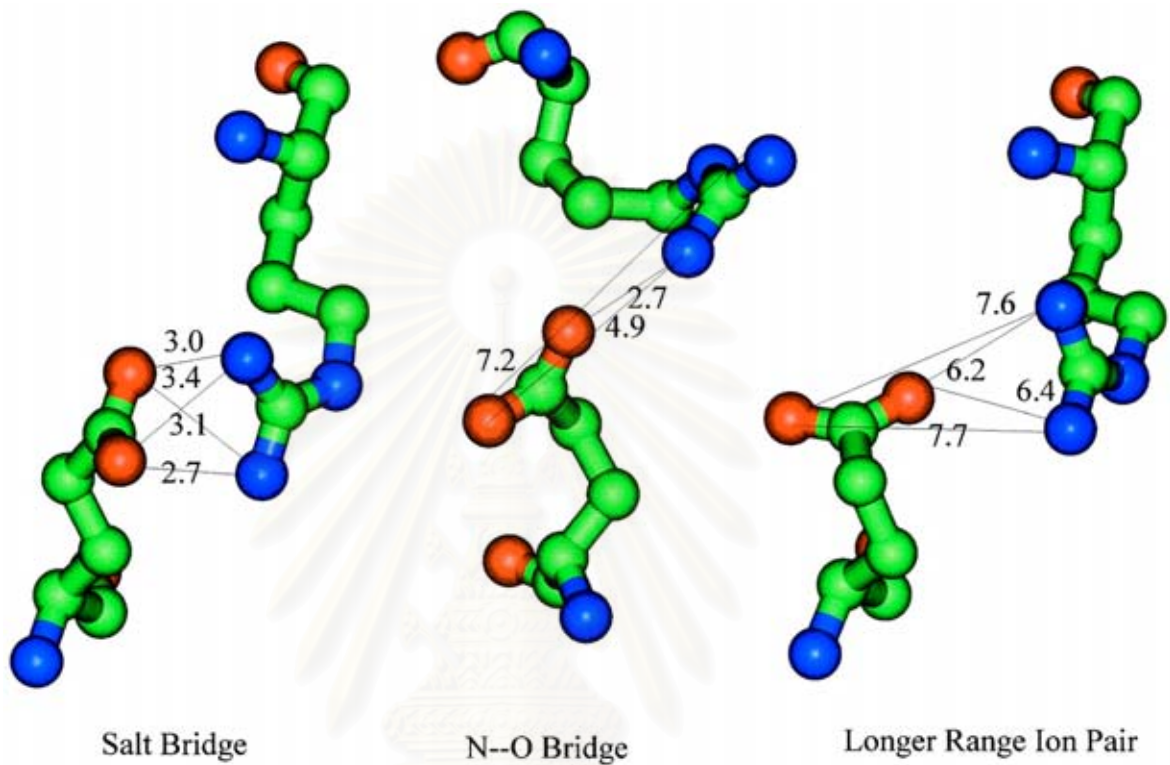


Figure 1.8 Different types of ion pairs in proteins. Salt bridge, N-O bridge, and longer-range ion pair types are shown for Glu-Arg. The separation of side-chain charged groups increases in N-O bridges and longer-range ion pair. Atoms are color coded. Oxygen atoms are in red, nitrogen in blue, and carbon in green.

Source: Kumar and Nussunov (2002)

interaction between side-chain charged groups of the ion-pairing residues is the strongest for salt bridges, considerably weaker for N-O bridges, and the weakest for longer-range ion pairs.

1.5 Sequence and structural differences in thermophilic and mesophilic proteins

Recently, different strategies adopted by thermophilic proteins to achieve stability and activity at high temperatures have been proposed. These principles are behind the various sequence and structural factors seen in thermostable proteins, with different thermophilic proteins adopting different single or combination of strategies. Interactions that impart thermostability are of tin characteristic of a protein family. Hence, comparison of a number of families containing homologous proteins from hyperthermophilic, thermophilic, and mesophilic organisms is a powerful method to understand the microscopic sequence/structure basis of protein thermostability. Furthermore, such comparisons may be useful for the rational design of thermostable proteins and interpreting directed-evolution experiments.

Kumar *et al.*, (2000) studied structural and sequence parameters in representatives of 18 non-redundant families of thermophilic and mesophilic proteins. They looked for systematic differences among thermophilic and mesophilic proteins across the families. They observed that both thermophilic and mesophilic proteins have similar hydrophobicities, compactness, oligomeric states, polar and non-polar contribution to surface areas, main-chain and side-chain hydrogen bonds. Insertion/deletions and proline substitutions do not show consistent trends between the thermophilic and mesophilic of the families. On the other hand, salt bridges and side chain-side chain hydrogen bonds

increase in the majority of the thermophilic proteins. Additionally, comparison of the sequences of the thermophile-mesophile homologous protein pairs indicate that Arg and Tyr are significantly more frequent, while Cys and Ser are less frequent in thermophilic proteins. Thermophiles have both a larger fraction of their residues in the α -helical conformation and avoid Pro in the α -helices to a greater extent than the mesophiles. In addition, Szilagy and Zavodszky (2000) compared 13 different structure features in 64 mesophilic and 29 thermophilic proteins representing 25 protein families. They also observed increased ion pair formation in thermophiles and hyperthermophiles and found that hyperthermophilic proteins are stabilized in a different way than the moderately thermophilic proteins. Moreover, the number of ion pairs, atom packing, exposed polar surface area, and secondary-structure content were different in these two groups. The same results were reported by Cambillau and Claverie (2000). They compared the composition of proteins from 30 complete genomes (22 mesophiles, 1 thermophile, and 7 hyperthermophiles) and found a statistically significant increase in the proportion of charged residues (Lys, Arg, Asp, Glu) for proteins in the hyperthermophiles and in the thermophile. A decrease in the proportion of uncharged polar residues (Asn, Gln, Ser, and Thr) was also statistically significant. The comparison of water-accessible surface areas for each amino acid in 131 mesophilic proteins and 58 hyperthermophilic proteins showed that the hyperthermophilic proteins have a greater proportion of charged residues at the surface.

Furthermore, the number of amino acid differences in counterpart soluble proteins from thermophilic and mesophilic organism were reported by Chakravarty and Vardarajan (2000). They compared amino acid sequences of soluble proteins in complete genomes of 8 thermophilic and 12 mesophilic organisms. On average, thermophilic

proteins were found to contain fewer residues (268 ± 38) than the mesophilic proteins (310 ± 16). The increase in proportion of charged residues (Arg, Lys, His, Asp, Glu) and hydrophobic β -branched amino acids and decrease in proportion of uncharged polar residues (Ser, Thr, Gln, Asn, Cys) in thermophilic proteins are statistically significant. Whereas, factor such as the relative proportion of residues in loops, proline and glycine content and helix capping do not appeared to be important. In addition, Thompson and Eisenberg (1999) found a statistically significant trend for shorter sequence lengths in thermophilic proteins in a comparison involving the complete genomes of 20 mesophilic, thermophilic, and hyperthermophilic organism. The sequence deletion sites in thermophilic proteins correspond to the exposed loop regions. Hence, they concluded that deletion of exposed loops is a natural mechanism for enhancing protein thermostability, in addition to improving electrostatic interactions. From several studies of sequence and structural differences in thermophilic and mesophilic proteins which have been reported, an increase in the proportion of charged residues and electrostatic interaction are the most consistent mechanisms for increasing protein thermal stability.

1.6 Protein thermostability and electrostatic interactions

While there may be several strategies to attain thermostability, nature appears to use an improvement in electrostatic interaction most frequently. Electrostatic interaction such as salt bridges and their network have important roles in protein folding, structure, and function. Yip *et al.* (1998) carried out homology-based modeling studied using sequences of a range of glutamate dehydrogenases. They also observed a similar correlation between salt bridge networks and thermostabilities from several hyperthermophilic, thermophilic, and mesophilic enzymes. The results of analysis

indicated that the ion pair network become more fragmented as the temperature stability of the enzyme decreases and are consistent with a role for the involvement of such networks in the adaptation of enzyme to extreme temperature. In addition, Takano *et al.* (2000) elucidated the net contribution of a surface salt bridge to the conformational stability of a protein by determination of 1) systematic mutant human lysozymes, containing one Glu to Gln (E7Q) and five Asp to Asn mutations (D18N, D49N, D67N, D102N, and D120N) at residues where a salt bridge is formed near the surface in the wild-type structure and 2) the thermodynamic parameters for denaturation between pH 2.0 and 4.8. They found that the contribution of salt bridge correlate with the solvent inaccessibility. Strop and Mayo (2000) presented NMR structure for analyzed two salt bridges in a hyperthermophilic rubredoxin by double mutant cycles. The analysis showed that the surface side-chain to side-chain salt bridge between Lys 6 and Glu 49 dose not stabilize rubredoxin.

Contribution of electrostatic interactions such as salt bridges and their networks toward protein stability can be stabilizing or destabilizing. Makhathdze *et al* (2003), analyzed the net strength of lysine 11 (K11) / glutamic acid 34 (E34) and mutant, inverted E11/K34 surface salt bridge of ubiquitin. They found that the salt bridge of E11/K34 can be formed with similar strength to that of the K11/E34 pair. However, the global stability of K11/E34 (wild type) was higher than that of E11/K34. The difference in the contribution of opposing salt bridge orientations to the overall stability of the ubiquitin molecule is attributed to the difference in the charge-charge interactions between residues forming the salt bridge and the rest of the ionizable groups in this protein. Thus, the surface salt bridges are stabilizing, but their contribution to the overall protein stability is strongly context-dependent, with charge-charge interactions being the

largest determinant. Lebbink *et al.*, (1998) demonstrated that the engineered ion-pair interactions in the hinge region of glutamate dehydrogenase from *Thermotoga maritima* did not affect the stability towards temperature or guanidinium chloride-induced denaturation but rather affected the specific activity of the enzyme and the temperature at which it functioned optimally. In contrast Vetrant *et al.* (1998) improved stability of hexameric glutamate dehydrogenase of *Thermococcus litoralis* by comparison of its structure with the enzyme from hyperthermophilic *Pyrococcus furiosus* using homology-based modeling. Glu 138 of *P. furiosus* can form triple ion-pair interaction with Arg 35, subunit c; Arg 165, subunit b; and Lys 66, subunit b; however, none of these interactions is joined at Thr 138 of and *T. litoralis* enzyme. Thus substitution of Thr with Glu, which was performed T138E, itself could not raise the thermostability. On the contrary, T_m of T138E was decreased from 109.0°C (wild type) to 103.5°C. With the assistance of Asp 167 which was unshielded and its carboxyl group were buried away from the lumen on the three fold axis, T138E/D167T mutant of GDH from *T. litoralis* could elevate the T_m value to 111.5°C. These result suggested that extensive ion pair networks may provide a general strategy for manipulating enzyme thermostability of multisubunit enzymes. In addition, Trejo *et al.*, (2001) engineered electrostatic interactions to stabilize cytosolic malate dehydrogenase from *Thermus thermophilus*. Since comparison between homologous thermophilic and mesophilic enzymes from a given structural family can reveal structural features responsible for the enhanced stability of thermophilic proteins, structures from pig heart cytosolic and *Thermus flavus* malate dehydrogenases (MDH) were compared. Three potential salt bridges were selected on the basis of their location in the protein (surface R176-D200, inter-subunit E57-K168 and intrasubunit R149-E275). Mutant containing E275 were not produced any detectable amount of activity. The salt

bridge R149-E275, if formed, did not enhance stability enough to overcome this effect. The remaining mutants were expressed and no differences from wild-type other than stability were found. Of the mutants assayed, Q57E/L168K led to increase stability. This results in a 15°C shift in the optimum temperature, thus confirming that the inter-subunit salt bridge was formed in cytosolic MDH. Wada *et al.*, (2001) replaced Ser 89 with glycine, alanine, threonine, glutamic acid, or aspartic acid using PCR-mutagenesis method to enhance thermostability of inorganic pyrophosphatase (PPase) from thermophilic bacterium PS-3. S89G, S89A and S89T as well as the wild type PPase were stable in the presence of 5 mM MgCl₂ at 70° for 1 hour, but were inactivated rapidly at 80°C. On the other hand, S89D and S89E were stable at 80°C, 1 hour incubation.

1.7 Proteins engineering for thermostability

Protein thermostability has been vigorously studied in the biophysical and biotechnological research areas, because protein instability at high temperature is main bottleneck in extending the application of protein. The industrial use of enzymes is often limited by lack of stability. Additionally, high stability can be utilized to increase reaction rates, control reaction specificity, and to reduce microbial contamination. Understanding the structural basis for enhanced thermostability is an important practical goal in the industrial application of enzymes. However, protein engineering demonstrated that it is possible to utilize the information gained from naturally occurring thermostable enzymes to engineer enhanced thermal stability. Engineering proteins for thermostability is a particularly exciting and challenging field, as it is crucial for broadening the industrial use of recombinant proteins.

With the advent of mutation techniques, protein engineering has received a fresh impetus. Protein engineering is currently a very active area of research, thus the basis assumption of protein engineering based on rational design principle or directed evolution (Lehmann and Wyss, 2001). Rational design principle is one strategy for identifying thermostability mutations involves the comparison of more stable proteins with less stable ones, with the goal of identifying amino acid sequence patterns that correlate with thermostability. In addition, the rational approaches for thermostability engineering can be grouped in two main classes: (1) comparison of the amino acid sequence of protein of interest with that of a more thermostable, homologous counterpart, followed by replacement of selected amino acids by site-directed mutagenesis; and (2) detailed inspection of the 3D structure of the protein of interest, structure-based prediction of promising amino acid exchanges by applying current concepts of thermostability engineering, and subsequent verification as single mutations in the wild type protein. Perl *et al.* (2000) compared the cold shock proteins from the thermophile *Bacillus caldolyticus* and the mesophile *Bacillus subtilis*, which differ in only 12 out of 67 residues but display a considerable difference in stability. Site-directed mutagenesis of all 12 residues in the *Bacillus caldolyticus* enzyme revealed that the difference in thermostability can be fully accounted for by only two amino acid substitutions (E3R, E66L) on the surface of the molecule. In this illustrative example, with small proteins that exhibit high homology and a pronounced difference in thermostability, it is noted that less than 20% of the amino acid substitutions actually contribute to the difference in stability. This observation highlights the problem of identifying the relevant thermostabilising mutations in larger and less homologous sets of proteins.

The term 'directed evolution' encompasses a series of experimental techniques that reproduce, on an accelerated timescale in the test tube, the evolution of natural diversity and environmental adaptation. This is achieved through mutation and recombination and by giving the process a 'direction' towards the optimization of one or more properties of interest. Either a selective pressure is applied, or in each round of mutagenesis and/or recombination the library of variants obtained is screened for the desired trait. Giver *et al.*, (1998) studied directed evolution of ρ -nitrobenzyl esterase from *Bacillus subtilis* by random mutagenesis and DNA shuffling. They succeeded to engineer the thermostable enzyme which increased in T_m over 14°C with 8 amino acid substitutions in six generation of directed evolution.

1.8 Site-directed mutagenesis

Protein engineering, usually performed through site-directed mutagenesis, is the favorite mode of experiment analysis and stability enhancement. Specific mutations were introduced into a part of a gene by using oligonucleotide primers for change nucleotide sequence. There are many types of mutagenesis protocols available such as Kunkel method (Kunkel, 1985) which uses circle single strand DNA from M13 as a template. However this method has disadvantage since preparation of single strand DNA is difficult. Nowadays, many researches usually used PCR site-directed mutagenesis or PCR mutagenesis which bases on principle of PCR. The advent of PCR has greatly simplified DNA manipulations. One of the most basic of these manipulations is mutagenesis of a gene in order to characterize its function. Oligonucleotide-directed mutagenesis during PCR is a wonderfully simple and efficient technique for introducing specific, site-directed mutations. Misses, nonsense, deletion and substitution mutations can be created.

Site directed mutagenesis is also a powerful tool for producing mutants to assess the importance of specific amino acid residues in a protein's structure and function.

Currently, one of protocols that are frequently used in research labs is the Quik-Change Site Directed Mutagenesis made by the local biotech company, Stratagene (La, Jolla CA). This protocol requires a doubled stranded plasmid that contains the gene to be mutated and two complementary synthetic oligonucleotide primers, one of which contains the desired mutation. A high fidelity *Pfu Turbo* DNA polymerase is used to extend the primers during temperature cycling. The resulting PCR product and the plasmid template is then treated with *Dpn* I restriction enzyme that cuts at methylated GATC sequences. Since the PCR product is created *in vitro*, and hence is not methylated, only the template plasmid DNA is digested. The whole reaction is then transformed into bacterial competent cells. Bacterial DNA repair enzymes repair the *Dpn* I-nicked plasmid using the PCR product containing the mutation as a template.

Although the Quik-Change protocol is usually successful, Wang and Malcolm (1999) developed a two-stage procedure, base on the Quik-Change Site-directed mutagenesis. The plasmid pUC4K containing two antibiotic-resistant genes: *bla* conferring ampicillin resistance and *Tn903* yielding kanamycin resistance was used as the mutagenesis template. The mutagenesis primers were designed to disrupt the *bla* gene by introducing nonsense mutation through point mutations, frameshifts, insertions or deletion, so that the mutagenesis could be easily scored by antibiotic selection. They found that the mutagenesis efficiency determined by antibiotic selection ranged from 65% to 95%, which was comparable to the efficiency of a standard mutagenesis using the Quik-Change Site-directed mutagenesis. In 2000, Sawano and Miyawaki developed transformation efficiency by using an *in vitro* technique, LDA (ligation-during-

amplification) with added *Taq* DNA ligase for increase efficiency to 70%. This technique allows introduction of 2 or more mutations by random mutagenesis with degenerative primers.

Aeromonas hydrophila, screened from soil in Bangkok (Phungsangthum, 1997), is one of bacteria with high activity of alanine dehydrogenase. The previous research presented that alanine dehydrogenase from this bacterium has molecular mass of about 230 kDa and consists of 6 identical subunits. The enzyme is highly specific for L-alanine and NAD^+ . Optimum temperature for reductive amination and oxidation deamination are 45 and 55°C, respectively. For thermostability the enzyme dose not lose activity after incubation at 55°C for 16 hours. The optimum pH for reductive amination is 8.0 while the reverse reaction rate is highest at pH 10.5. The steady state kinetic studies including product inhibition on the enzyme reaction indicate that the oxidative deamination proceeds through a sequential ordered binary-ternary mechanism in which NAD^+ binds first to the enzyme followed by L-alanine and products are released in the order of pyruvate, ammonia and NADH, respectively. The K_m values for NAD^+ , L-alanine, pyruvate, ammonia and NADH, were 0.17, 20, 1.33, 77 and 0.24 mM, respectively. Subsequently, Poomipark (2000) sequenced and cloned the enzyme gene into *E. coli* JM109. This gene has open reading frame of 1,113 base pair which encodes for 371 amino acids. Comparison of deduced amino acid sequence with AlaDHs from other bacteria shows over 50% similarity. The transformant has specific activity 50 times higher that of the enzyme from wild type.

In this study, improvement thermostability of alanine dehydrogenase from *Aeromonas hydrophila* by site-directed mutagenesis, based on structure and amino acid sequence comparison with thermophilic *Bacillus stearothermophilus* will be performed.



สถาบันวิทยบริการ
จุฬาลงกรณ์มหาวิทยาลัย

CHAPTER II

MATERIALS AND METHODS

2.1 Equipments

Autoclave: Model H-88LL, Kokusan Ensinki Co., Ltd., Japan

Autopipette: Pipetman, Gilson, France

Camera: Pentax super A, Asahi Opt. Co., Japan

Centrifuge, refrigerated centrifuge: Model J2-21, Beckman Instrument
Inc., U.S.A.

Centrifuge, microcentrifuge: Model MC-15A, Tomy Seiko Co., Ltd., Japan
and KUBOTA 1300, KUBOTA, Japan

Centrifuge tube: Nelgene, U.S.A.

Concentrator centrifuge: UNIVAPO, UNIEQUIP, Germany

DNA Sequencer Applied Biosystem 3100 with a PRISM kit:
Perkin Elmer, U.S.A.

Electrophoresis unit: HoeferTM miniVE, Amersham Pharmacia Biotech.,
U.S.A.; 2050 MIDGET, LKB, Sweden; Mini protein, Bio-Rad,
U.S.A. and submarine agarose gel electrophoresis unit

Filter paper No.1, Whatman, England

Gene Pulser^R/*E. coli* PulserTM Cuvettes: Bio-Rad, U.S.A.

Gel Document: SYNGEND, England

Heating box: Type 17600 Dri-Bath, Thermolyne, U.S.A.

Incubator, waterbath: Model M20S, Lauda, Germany and BioChiller
2000, FOTODYNE Inc., U.S.A. and ISOTEMP 210, Fisher Scientific, U.S.A.

Incubator shaker: Innova™ 4080, New Brunswick Scientific, U.S.A.

Light box: 2859 SHANDON, Shandon Scientific Co., Ltd., England.

Lamina flow: HT123, ISSCO, U.S.A.

Magnetic stirrer: Model Fisherbrand, Fisher Scientific, U.S.A.

Membrane filter: cellulose nitrate, pore size 0.45 µm, Whatman, England

Microcentrifuge tubes 0.5 and 1.5 ml, Axygen Hayward, U.S.A.

Microwave oven: Model TRX1500, Turbora International Co., Ltd., Korea

Orbital incubator: Model 1H-100, Gallenkamp, England

Orbital shaker: Orbital shaker 03, Stuart Scientific, England

pH meter: Model PHM95, Radiometer Copenhagen, Denmark

Power supply: Model POWER PAC 300, Bio-Rad, U.S.A.

Shaking waterbath: Model G-76, New Brunswick Scientific Co., Inc., U.S.A.

Sonicator: SONOPULS Ultrasonic homogenizers, BANDELIN, Germany

Spectrophotometer: DU Series 650, Beckman, U.S.A.

Thermal cycle: Gene Amp PCR system 2400, Perkin Elmer Cetus, U.S.A.

Thin-wall microcentrifuge tubes 0.2 ml, Axygen Hayward, U.S.A.

Ultrafilter: Suprec^{Tm-01, Tm-02}, pore size 0.20 µm and 0.22 µm,
Takara Shuzo Co, Ltd., Japan

UV transilluminator: Model 2011 Macrovue, San Gabriel California, U.S.A. and M-26,
UVP, U.S.A.

Vortex: Model K-550-GE, Scientific Industries, Inc, U.S.A.

2.2 Chemicals

Acrylamide: Merck, Germany

Agar: Merck, Germany

Agarose: SEKEM LE Agarose, FMC Bioproducts, U.S.A.

Ammonium persulphate: Sigma, U.S.A.

Ammonium sulphate: Carlo Erba Reagent, Italy

Ampicillin: Sigma, U.S.A.

Boric acid: Merck, Germany

Bovine serum albumin: Sigma, U.S.A.

5-Bromo-4-chloro-3-indolyl- β -D-galactosidase (X-gal): Sigma, U.S.A.

Bromphenol blue: Merck, Germany

Casein hydrolysate: Merck, Germany

Chloroform: BDH, England

Coomassie brilliant blue R-250: Sigma, U.S.A.

Copper sulfate: Merck, Germany

di-Potassium hydrogen phosphate anhydrous: Carlo Erba Reagenti, Italy

di-Sodium ethylene diamine tetra acetic acid: M&B, England

DNA marker: Lamda (λ) DNA digested with *Hind*III, BioLabs, Inc., U.S.A.

100 base pair DNA ladder, Promega Co., U.S.A.

dNTP mix: Stratagene, U.S.A.

Ethidium bromide: Sigma, U.S.A.

Ethyl alcohol absolute: Carlo Erba Reagenti, Italy

Ethylene diamine tetraacetic acid (EDTA): Merck, Germany

Ficoll type 400: Sigma, U.S.A.

Glacial acetic acid: Carlo Erba Reagenti, Italy

Glycerol: Merck, Germany

Glycine: Sigma, U.S.A.

Glucose: BDH, England

Hydrochloric acid: Carlo Erba Reagenti, Italy

8-Hydroxyquinolin: Merck, Germany

Isoamyl alcohol: Merck, Germany

Isopropanol: Merck, Germany

Isopropylthio- β -D-galactosidase (IPTG): Sigma, U.S.A.

L-Alanine: Sigma, U.S.A.

Magnesium sulphate: BDH, England

2- Mercaptoethanol: Fluka, Switzerland

Methylalcohol: Merck, Germany

N,N-Dimethyl-formamide: Fluka, Switzerland

N,N'-Methylene-bis-acrylamide: Sigma, U.S.A.

N,N,N',N'-Tetramethyl-1, 2-diaminoethane (TEMED): Carlo Erba Reagent, Italy

β -Nicotinamide adenine dinucleotide (oxidized form) (NAD^+): Sigma, U.S.A.

β -Nicotinamide adenine dinucleotide (reduced form) (NADH^+): Sigma, U.S.A.

Nitroblue tetrazolium: Koch-Light Laboratories Ltd., Japan

Peptone from casein pancreatically digested: Merck, Germany

Phenazine methosulfate: Nacalai Tesque, Inc., Japan

Phenol: BDH, England

Phenylmethylsulfonyl fluoride (PMSF): Sigma, U.S.A.

Potassium acetate: Merck, Germany

Potassium chloride: Merck, Germany

Potassium hydroxide: Carlo Erba Reagenti, Italy

Potassium phosphate monobasic: Carlo Erba Reagenti, Italy

QIA quick Gel Extraction Kit: QIAGEN, Germany

Sodium acetate: Merck, Germany

Sodium carbonate anhydrous: Carlo Erba Reagenti, Italy

Sodium chloride: Carlo Erba Reagenti, Italy

Sodium citrate: Carlo Erba Reagenti, Italy

Sodium dodecyl sulfate: Sigma, U.S.A.

Sodium hydroxide: Merck, Germany

Standard protein marker: Amersham Pharmacia Biotech Inc., U.S.A.

Sucrose: Sigma, U.S.A.

Tris (hydroxymethyl)-aminomethane: Carlo Erba Reagenti, Italy

Yeast extract: Scharlau microbiology, European Union

2.3 Enzymes and Restriction enzymes

QuikChange[®] Site-Directed Mutagenesis Kit: Stratagene, U.S.A. consists of

PfuTurbo[®] DNA polymerase and *Dpn* I restriction enzyme

Proteinase K: Sigma, U.S.A.

Restriction enzymes: GIBCOBRL, U.S.A., Amersham Pharmacia Biotech Inc., U.S.A.,

New England BioLabs, Inc., U.S.A. and Zibenzyme, Sweden.

RNaseA: Sigma, U.S.A.

T₄ DNA ligase: GIBCOBRL, U.S.A., New England BioLabs, Inc., U.S.A. and

Zibenzyme, Sweden.

2.4 Oligonucleotide primers

G38E For 5' CGT TTT CGT CCA AAG CGA AGC AGG AAA TGG CAT TGG 3'

G38E Rev 5' CCA ATG CCA TTT CCT GCT TCG CTT TGG ACG AAA ACG 3'

L58R For 5' GAT CCG GGC CTC TGC GG 3'

L58R Rev 5' CCG CAG AGG CCC GGA TC 5'

P168R For 5' GCG TGG AAC GGG CCA AGG TG 3'

P168R Rev 5' CAC CTT GGC CCG TTC CAC GC 3'

L101E For 5' CTG GCG CCA GAC GAG GCC CAG ACC CGG GAG CTG 3'

L101E Rev 5' CAG CTC CCG GGT CTG GGC CTC GTC TGG CGC CAG 3'

A231E For 5' GGA GCG CCA TCT GCT GGA GGC AGA CCT GGT CAT CG 3'

A231E Rev 5' CGA TGA CCA GGT CTG CCT CCA GCA GAT GGC GCT CC 5'

Note: Position of mutated sequences are shown by underline

2.5 Bacterial strains and plasmids

Escherichia coli JM109 contained pUC18 carrying alanine dehydrogenase gene (*alaDH* gene) from *Aeromonas hydrophila* (Poomipark, 2000) was used as a source of *alaDH* gene.

Escherichia coli JM109, genotype: F' [*traD36 proAB*⁺ *lacI*^q *lacZ*ΔM15] *recA1 supE44 endA1 hsdR17 gyrA96 relA1 thi* Δ (*lac-proAB*) was used as a host for transformation.

Escherichia coli XL1-Blue, genotype: F' [*proAB*+ *lacZ*ΔM15,::Tn10(Tet^r)] *recA1 supE44 endA1 hsdR17 gyrA96 relA1 thi lac* was used as a host for transformation.

pUC18 was used as a vector for cloning alanine dehydrogenase gene into *E. coli* JM109 (Appendix A).

2.6 Selection of amino acid residue for contribution of electrostatic interaction

2.6.1 Construction of three-dimensional structure

Three-dimensional structure (3D-structure) was constructed by homology modeling program from SWISS MODEL (<http://swissmodel.expasy.org>) that is a server for automate comparative modeling of three-dimensional protein structure. All homology-modeling methods consist of the following four steps: (i) template selection; (ii) target template alignment; (iii) model building; (iv) evolution. Protein sequences of thermophilic alanine dehydrogenase (AlaDH) from *Bacillus stearothermophilus* and mesophilic AlaDH from *Aeromonas hydrophila* were submitted to the SWISS MODEL using protein structure of alanine dehydrogenase from *Phormidium lapideum* deposited in Protein Data bank (accession number 1PJB) as template. The resulting protein structure model can be visualized and analyzed using the integrated tool (Swiss PdbViewer 3.7 and Rastop program).

2.6.2 Calculation of electrostatic interaction

Three-dimensional structures of AlaDHs from SWISS MODEL in section 2.6.1 were submitted to <http://www.cmbi.kun.nl/gv/servers/WIWWWI/> for calculation of electrostatic interaction which is occurred between a negative atom (side chain oxygens in Asp or Glu) and a positive atom (side chain nitrogens in Arg, Lys or His) with an interatomic distance less than 7.0 Ångstrom. The number and position of electrostatic interaction were compared between AlaDH from *Aeromonas hydrophila* and AlaDH from thermophilic *Bacillus stearothermophilus*.

2.6.3 Selection of amino acid residue

All amino acid sequences of AlaDHs from GENBANK were aligned by using Clustal X. Conserved sequences, especially the amino acid residues in an active site of this enzyme referred to X-ray crystallography structure of *Phormidium lapideum* AlaDH (Baker and Sawa. *et. al.*1998) were determined. The information from three-dimensional structure (section 2.6.1), number and position of electrostatic interaction (section 2.6.2) and amino acid alignment of mesophilic AlaDH (*A. hydrophila*) compared to its thermophilic counterpart from *B. stearothermophilus* were used for engineering of the interaction thought to be responsible for thermostability into *A. hydrophila* AlaDH.

This study points toward the increased position of electrostatic interaction which is not conserved sequence or important amino acids in an enzyme active site as a critical factor in an enhancement of thermostability. After replacement target uncharged amino acid in *A. hydrophila* AlaDH with charged amino acid (Glu, Asp, Arg or Lys), the mutated sequences were then submitted for construction of their three dimensional structure and calculation of electrostatic interaction (Figure 2.1). The suitable positions which led to the increment of electrostatic interaction were selected for site-directed mutagenesis.

2.7 Site-directed mutagenesis

2.7.1 Plasmid extraction

In this study, the *E. coli* JM 109 harboring *alaDH* gene in plasmid pUC18 which cloned by Poomipark (2000) was used as a source of DNA template for site-directed mutagenesis. The bacteria clone was grown in LB-medium (1 % peptone, 0.5 % NaCl and 0.5 % yeast extract, pH 7.2) containing 100 µg/ml ampicillin overnight at 37°C

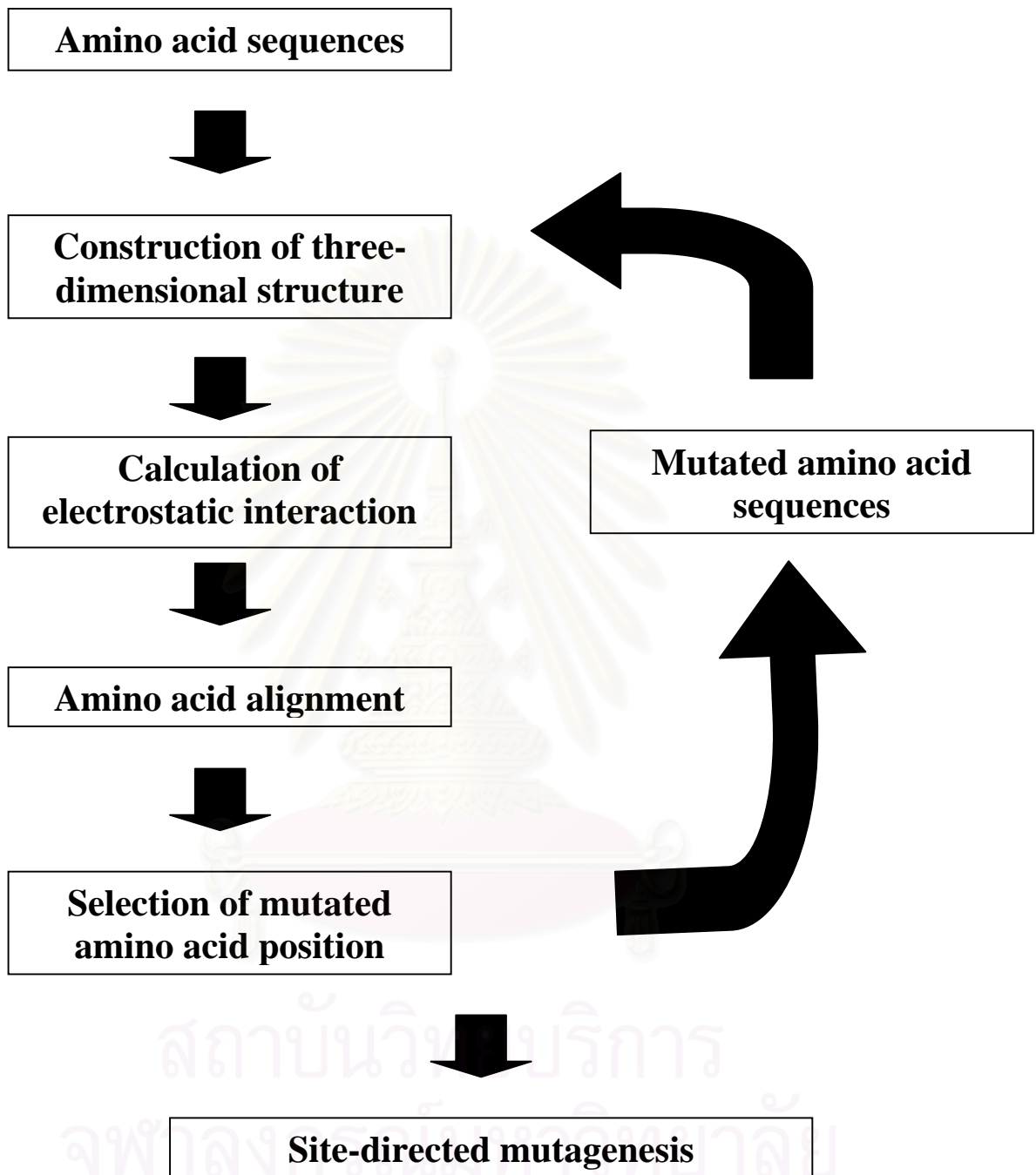


Figure 2.1 Steps of selection of amino acid positions for contribution of electrostatic interaction

with rotary shaking. The cell culture was collected by centrifugation at 10,000 rpm for 5 minutes. Then 100 µl of ice-cold Solution I (50 mM glucose, 25 mM Tris-HCl and 10 mM EDTA, pH 8.0) was added and the cell pellet was resuspended and left at room temperature for 10 minutes. After that, the 200 µl of freshly prepared Solution II (0.2 N NaOH and 1 % SDS) was added, gently mixed by inverting the tube for five times and placed on ice for 10 minutes. Then the 150 µl of cooled Solution III (3 M sodium acetate, pH 4.8) was added and the tube was placed on ice for 10 minutes. The mixture was centrifuged at 10,000 rpm for 10 minutes and then the supernatant was transferred to a new tube. An equal volume of phenol-chloroform-isoamyl alcohol (25: 24: 1) was added, mixed and centrifuged at 12,000 rpm for 10 minutes. The upper-phased liquid was transferred to a new tube. The plasmid DNA was precipitated with absolute ethanol and washed with 70 % ethanol. After drying, the pellet was finally dissolved in an appropriate volume of TE buffer, pH 8.0 containing 20 µg/ml of DNase-free pancreatic RNase.

2.7.2 Agarose gel electrophoresis

Electrophoresis through agarose is the standard method used to separate, identify, and purify DNA fragments. The 0.7% of agarose powder was added to 100 ml electrophoresis buffer (89 mM Tris-HCl, 8.9 mM boric acid and 2.5 mM EDTA, pH 8.0) in an Erlenmeyer flask and heated until complete solubilization in a microwave oven. The agarose solution was cooled down below to 60°C until all air bubbles were completely eliminated. The solution was then poured into an electrophoresis mould. After the gel was completely set, the comb and seal of the mould was carefully removed. When ready, the DNA samples were mixed with one-fifth volume of the desired gel-loading buffer (0.025% bromphenol blue, 40% ficoll 400 and 0.5% SDS) and slowly loaded the mixture

into an appropriate percentage of agarose gel. Electrophoresis had been performed at constant voltage of 10 volt/cm until the faster migration dye (bromphenol blue) migrated to approximately 1 cm from the bottom of the gel. The gel was stained with 2.5 µg/ml ethidium bromide solution for 5 minutes and destained to remove unbound ethidium bromide in distilled water for 10 minutes. DNA fragments on agarose gel were visualized under a long wavelength UV light and photographed through a red filter using Kodak Tri X pan 400 film. The concentration or molecular weight of DNA sample was compared with the intensity and relative mobility of the standard DNA fragment.

2.7.3 Site directed mutagenesis (QuikChange site-directed mutagenesis kit)

Recombinant plasmid from section 2.7.1 was used as template for site directed mutagenesis. The QuikChange site-directed mutagenesis kit was used to make point mutations (see Figure 2.2). The 50 µl of reaction mixture contained 50-200 ng of a supercoiled double-stranded DNA (dsDNA) pUC18 vector with an insert of *alaDH* gene, each 125 ng of two synthetic oligonucleotide primers containing the desired mutation 1 µl dNTP stock solution and 2.5 U of *PfuTurbo* DNA polymerase in the 1× QuikChange site-directed mutagenesis buffer. The extension reaction was initiated by preheating the reaction mixture 95°C for 30 seconds and then continued with 12 cycles of 95°C for 30 seconds, 55°C for 1 minute and 68°C for 4 minutes. The reaction for synthesized mutant strand and QuikChange mutagenesis control (see in Appendix B) were performed at the same time. The oligonucleotide primers, each complementary to opposite strands of the vector, were extended during temperature cycling. Incorporation of the oligonucleotide primers generated a mutant plasmid containing staggered nicks. After temperature

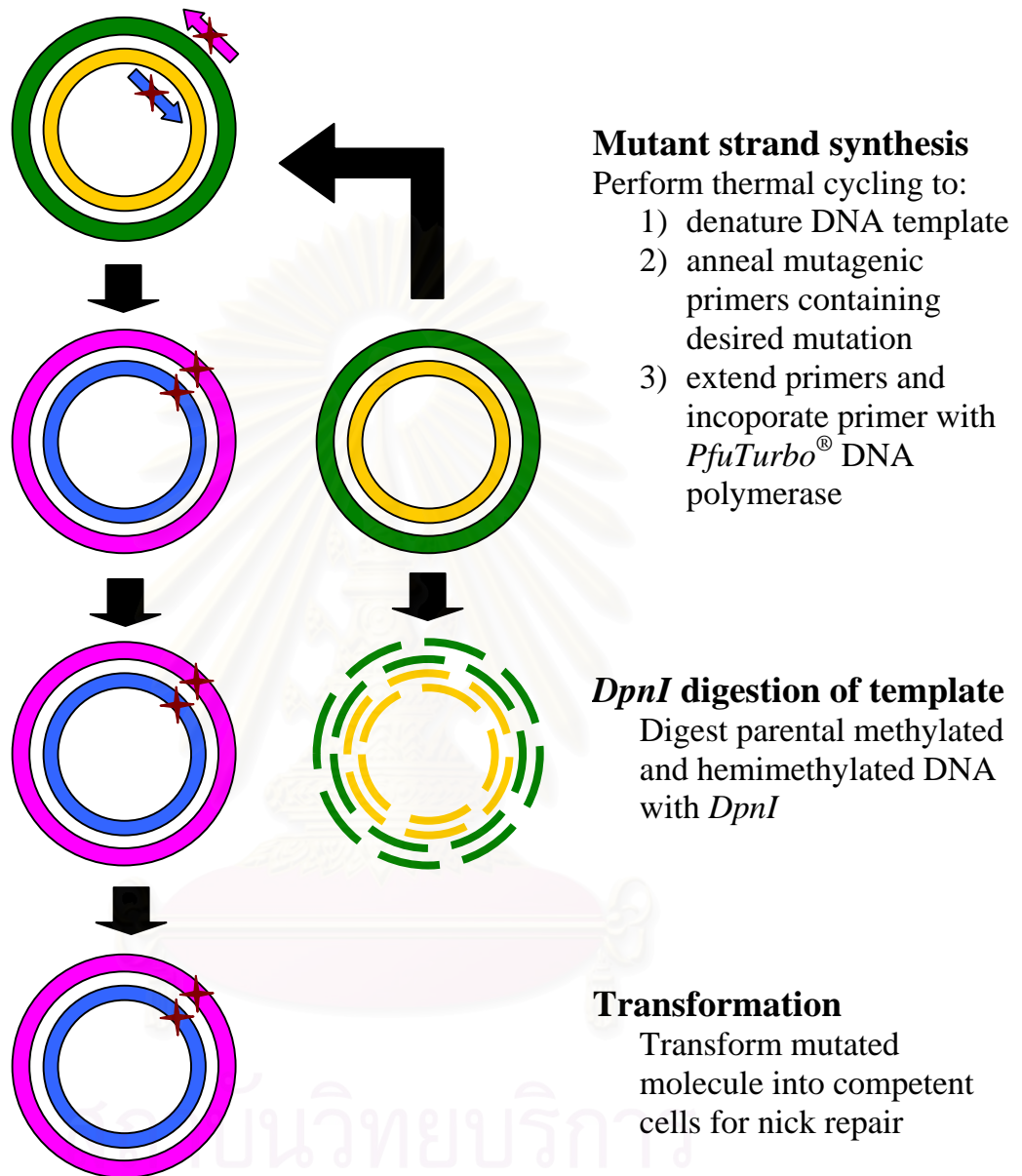


Figure 2.2 QuikChange[™] site-directed mutagenesis kit method

cycling, PCR product was treated with 10 U of *Dpn* I, at 37°C for 1 hour before transformation. The *Dpn* I endonuclease (target sequence: 5'-Gm6ATC-3') specific for methylated as well as hemimethylated DNA, is used to digest the parental DNA template to select for mutation-containing synthesized DNA. DNA isolated from almost all *E. coli* strains is dam methylated and therefore susceptible to *Dpn* I digestion. The nicked plasmid of the *Dpn* I-treated DNA containing the desired mutations was then transformed into *E. coli* XL1-Blue supercompetent cells. The transformation reaction was gently mixed and incubated on ice for 30 minutes. After that the transformation reaction was heated at 42°C for 45 seconds and then placed on ice for 2 minutes. The transformed reaction was added to 0.5 ml of NZY⁺ broth (Appendix C) which was preheated at 42°C and incubated at 37°C for 1 hour with shaking at 250 rpm. Finally, this transformed culture was spread onto the LB agar plate containing 80 µg/ml ampicillin, 25 µg/ml IPTG and 20 µg/ml X-gal, and then incubated at 37°C for 16 hours. Cells containing the recombinant plasmids, which formed white colonies, were picked and the plasmids were further extracted.

2.7.4 Plasmid extraction of mutant *alaDH* gene

The recombinant plasmids, which harbored mutant *alaDH* gene, were extracted from *E. coli* XL1-Blue by the method described in section 2.7.1. The plasmids were completely digested with *Eco*RI and *Hind*III. The size of recombinant plasmid was estimated by submarine agarose gel electrophoresis compared with relative mobility of DNA marker for checking size of mutant plasmids.

2.8 Enzyme activity assay and Protein assay

2.8.1 Crude extraction preparation

E. coli XL1-Blue cells, which contained the recombinant plasmid, were grown at 37°C in 10 ml of LB-medium supplemented with 100 µg/ml ampicillin overnight in a rotary shaker. After that, 10% of the cell culture was inoculated into 100 ml LB-medium containing 100 µg/ml ampicillin and 75 µg/ml isopropylthio-β-D-galactosidase (IPTG). Cell culture was grown at 37°C with shaking speed 250 rpm for 20 hours. The cells were harvested by centrifugation at 8,000 rpm for 15 minutes, then washed with cold 0.85% NaCl and centrifuged at 8,000 rpm for 15 minutes. After that, the cell pellet was washed once in cold extraction buffer (0.1 M potassium phosphate buffer, pH 7.4 containing 0.1 mM PMSF, 0.01 % 2-mercaptoethanol and 1.0 mM EDTA) and centrifuged again. The cell pellet was stored at -80°C until the next step. For enzyme extraction, the cell pellet was resuspended in 5 ml of cold extraction buffer and broken by discontinuously sonication on ice with half second pulse and half second stop interval for 10 minutes by sonic dismembrator (3 mm diameter-stepped microtip, 10 amplitude). Unbroken cell and cell debris were removed by centrifugation at 10,000 rpm for 45 minutes. The supernatant was stored at 4°C for enzyme and protein assays.

2.8.2 Enzyme activity assay

The activity of alanine dehydrogenase for oxidative deamination of alanine was spectrophotometrically assayed. One milliliter of reaction mixture of comprised 200 µmol of glycine-potassium chloride-potassium hydroxide buffer, pH 10.5, 20 µmol of L-alanine, 1 µmol of NAD⁺, and enzyme. In a blank tube, L-alanine was replaced by distilled water. Incubation was carried out at 30°C in a cuvette of 1-cm light

path. The reaction was started by addition of NAD^+ and was monitored by measuring the initial change in absorbance of NADH at 340 nm.

One unit of the enzyme is defined as the amount of enzyme that catalyzes the formation of 1 μmol of NADH in 1 minute. Specific activity is expressed as units per milligram of protein.

2.8.3 Protein measurement

Protein concentration was determined by the method of Lowry *et al.* (1951), using bovine serum albumin (BSA) as the protein standard. The reaction mixture 5 ml containing 20-300 μg of protein, 100 μl of solution A, 5 ml of solution B was mixed and incubated at 30°C for 10 minutes. After that, the solution mixture was incubated with 0.5 ml of solution C at room temperature for 20 minutes. Preparation of the solutions was described in Appendix D. The protein concentration was derived from the absorbance at 610 nm and calculated from the curve of protein standard (BSA).

2.9 Nucleotide sequencing

After plasmid extraction and enzyme assay, the nucleotide sequence of mutant were determined in the both directions by the dideoxynucleotide chain termination method of Sanger *et al.*, using an Applied Biosystems 373 A DNA sequencer with a PRISM kit (Perkin Elmer, U.S.A.). The universal primers, M13 Forward and M13 Reverse, were used for nucleotide sequencing. The nucleotide sequences of mutant gene were then compared with that of wild type using the CLUSTAL X program.

2.10 Transformation into *E. coli* JM 109

The recombinant plasmids from section 2.7.4 were introduced into a competent of *E. coli* strain JM 109 by electroporation. In the electroporation step, 0.2 cm cuvettes and sliding cuvette holder were chilled on ice. The Gene Pulser apparatus was set to the 25 μ F capacitor, 2.5 kV, and the pulse controller unit was set to 200 Ω . Competent cells which were prepared by the method of Dower (1988) (see Appendix E). were gently thawed on ice. One to five microliter of recombinant plasmid from section 2.7.4 was mixed with 40 μ l of the competent cells and then placed on ice for 1 minute. This mixture was transferred to a cold cuvette. The cuvette was applied one pulse at the above settings. Subsequently, one milliliter of LB medium was added immediately to the cuvette. The cells were quickly resuspended with a Pasteur pipette. Then the cell suspension was transferred to new tube and incubated at 37°C for 1 hour with shaking. Finally, this suspension was spread onto the LB agar plates containing 100 μ g/ml ampicillin, 25 μ g/ml IPTG and 20 μ g/ml X-gal, and was incubated at 37 °C for 16 hours. Cells containing the recombinant plasmids, which formed white colonies, were picked. Subsequently, the recombinant plasmids were extracted and completely digested with *Eco*RI and *Bam*HI. The size of recombinant plasmid was estimated by submarine agarose gel electrophoresis compared with relative mobility of DNA marker.

2.11 Purification of alanine dehydrogenase

2.11.1 Bacterial cultivation

2.11.1.1) Starter inoculum

One colony of *E. coli* JM109 containing *alaDH* gene in pUC18 from agar slant was grown in 50 ml LB-medium supplemented with 100 μ g/ml

ampicillin, at 37°C with 250 rpm shaking overnight before the culture was inoculated into LB-medium 500 ml containing 100 µg/ml ampicillin. Cell culture was grown at 37°C with 250 rpm overnight.

2.11.1.2) Enzyme production

The starting inoculum from section 2.11.1.1 was transferred into 5 liters of LB-medium, pH 7.2 containing 100 µg/ml ampicillin and 75 µg/ml (IPTG). Cell culture was grown at 37°C for 20 hours. The bacteria cells were harvested after 20 hrs by centrifugation at 8,000 xg for 15 minutes at 4°C. The collected cells were washed with 0.85% sodium chloride before rewashing with extraction buffer (0.1 M potassium phosphate buffer, pH 7.4 containing 0.1 mM PMSF, 0.01% 2-mercaptoethanol and 1 mM EDTA). Harvested cells were stored at -80°C before the purification.

2.11.2 Preparation of crude enzyme solution

The seventeen grams of collected cells from section 2.11.1.2 were resuspended in 80 ml of cold extraction buffer and then broken by discontinuously sonication on ice for 10 minutes; stop 10 minutes with 6 cycles by high intensity ultrasonic processor (6 mm diameter-stepped microtip, 25 amplitude). Unbroken cells and cell debris were removed by centrifugation at 10,000 xg for 30 minutes at 4°C. The crude enzyme solution was collected for the determination of oxidative deamination activity and protein concentration as described in section 2.8.2 and 2.8.3, respectively.

2.11.3 Purification procedures of enzyme

The crude enzyme from section 2.11.2 was purified according to Figure 2.3. All operations were done at 4°C. The buffer used in all steps was 10 mM potassium phosphate buffer (KPB), pH 7.4 containing 0.01% 2-mercaptoethanol and 1 mM EDTA.

2.11.3.1) Ammonium sulfate precipitation

The precipitation of crude enzyme was done by slowly added the initial concentration 0 - 20% saturated ammonium sulfate into enzyme solution with gentle stirred by magnetic stirrer. After 30 minutes, the supernatant was removed by centrifugation at 10,000 xg for 30 minutes then brought to final concentration at 40% saturated with solid ammonium sulfate and left for 30 minutes and centrifugation at 10,000 xg for 30 minutes. The precipitate was dissolved in 10 mM KPB, pH 7.4. The protein solution was dialyzed against the same buffer, at least 4 hours with 3 changes of buffer at 4°C before determination of the enzyme activity and protein concentration as described in section 2.8

2.11.3.2) DEAE-Toyopearl column chromatography

DEAE-Toyopearl was activated by washing with 0.5 N sodium hydroxide for 2-3 times before rewashing by deionized water until the pH reached 8.0. The activated DEAE-Toyopearl was resuspended in the buffer and pack into 2.2 x 20 cm column followed by equilibrating with the same buffer for 5-10 column volume at flow rate 1 ml/min. The dialyzed protein solution from section 2.11.3.1 was applied to the DEAE-Toyopearl column. The unbound proteins were eluted from the column with the buffer. Normally, keep washing until the absorbance at 280 nm of eluant

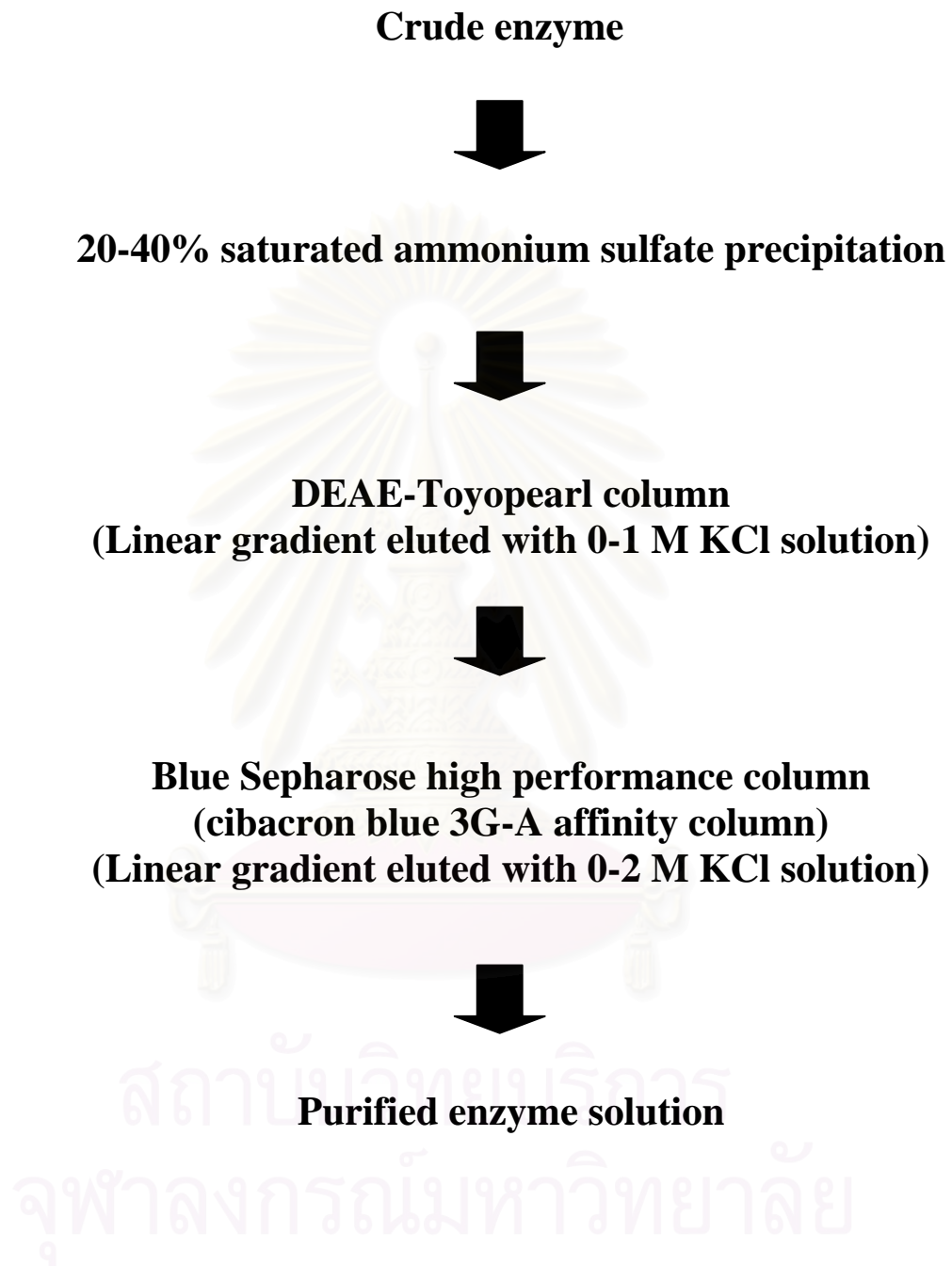


Figure 2.3 Flow chart of purification process of alanine dehydrogenase

decreased to a low value. After the column was washed thoroughly with the buffer, the bounded proteins were eluted from column with linear salt gradient of 0 to 1 M potassium chloride in the same buffer. The fractions of 5 ml were continuously collected using fraction collector. The elution profile was monitored for protein by measuring the absorbance at 280 nm. The enzyme activity was determined as described in section 2.8.2. The potassium chloride concentration was investigated by measuring the conductivity. The active fraction were pooled for further purification step and then dialyzed against the buffer at least 4 hours for 3 times. The enzyme activity and protein concentration were measured as described in section 2.8.

2.11.3.3) Blue Sepharose column chromatography

Blue Sepharose column was used to separate the pyridine nucleotide-dependent enzyme. It contained cibacron blue 3G-A which is specific for NAD(P)⁺-dependent enzyme. The other protein such as albumin are bound to the column with weak force, hydrophobic interaction and/or electrostatic force, than NAD(P)⁺-dependent dehydrogenase so separation of NAD(P)⁺-dependent dehydrogenase from other protein was occurred by eluted with the lower concentration of coenzyme or increasing the ionic strength of elute. In this experiment, the Blue Sepharose column (Pharmacia) with void volume 5 ml was used. The column was equilibrated with 10 mM KPB, pH 7.4 for 5 column volume (25 ml) at flow rate 1 ml per min. The dialyzed enzyme from 2.11.3.2 was filtered through a 0.45 µm filter and then applied into Blue Sepharose column by pumping with flow rate 1 ml per min. The 10 mM KPB, pH 7.4 were used to elute the unbound protein, fraction of 2 ml were continuously collected and measured for the protein at absorbance 280 nm until the absorbance decreased to low

value. The bound proteins were eluted with 0-2 M potassium chloride linear salt gradient elution. Fractions of 1.0 ml were collected. The determination of the enzyme activity, protein and conductivity of potassium chloride were similar to section 2.11.3.2. The active fractions were pooled before concentrating with aquacide, and then dialyzed against 10 mM KPB, pH 7.4 for 4 hours, at 4°C with 3 times changes. The protein concentration and enzyme activity were determined as described in section 2.8.

2.12 Polyacrylamide gel electrophoresis

2.12.1 Non-denaturing polyacrylamide gel electrophoresis (Native PAGE)

2.12.1.1 Pouring the separating gel (7 % acrylamide)

The gel sandwich was assembled according to the manufacturer's instruction. For 2 slab gels, the 2.33 ml of solution A (30 % (w/v) acrylamide, 0.8 % (w/v) Bis-acrylamide) and 2.5 ml of solution B (1.5 M Tris-HCl, pH 8.8) were mixed with 5.17 ml of distilled water in a 25 ml Erlenmeyer flask. Then 50 µl of 10 % ammonium persulfate and 10 µl of TEMED were added and mixed rapidly by swirling or inverting gently. Care by introduced solution into gel sandwich by using a pasteur pipette. After the appropriate amount of separating gel solution was added, water was gently layered on top of the separating gel solution about 1 cm height. The gel was allowed to polymerize, distinguished by clear interface between the separating gel and the water. The water was then poured off.

2.12.1.2 Pouring the stacking gel (5 % acrylamide)

The 0.67 ml of solution A (30 % (w/v) acrylamide, 0.8 % (w/v) Bis-acrylamide) was mixed with 1.0 ml of solution C (0.5 M Tris, pH 6.8) and 2.3 ml of

distilled water in a 25 ml Erlenmeyer flask and mixed. Subsequently, 30 μ l of 10 % ammonium persulfate and 5 μ l of TEMED were added and mixed rapidly. This stacking gel solution was loaded onto separating gel until solution reached top of short plate. Then the comb was carefully inserted into gel sandwich. After stacking gel was polymerized, the comb was removed carefully. Then the gel was placed into electrophoresis chamber. The electrophoresis buffer (25 mM Tris, 192 mM glycine, pH 8.8) was added into the inner and outer reservoir. The air bubbles, which were occurred in the well, were removed.

2.12.1.3) Sample preparation

The protein sample was mixed with 5 x sample buffer (0.3 mM Tris-HCl, 50 % glycerol and 0.05 % bromophenol blue) in an Eppendorf tube and mixed. Then the sample solution was introduced into well by using syringe.

2.12.1.4) Running the gel

An electrode plugs were attached to proper electrodes. Current was flowed towards the anode for pH 8.8 gels. The power supply was turned on at constant current (30 mA). For activity staining electrophoresis, the experiment was done at 4°C. Electrophoresis was continued until the dye front reached the bottom of the gel. Power supply was turned off and then the electrode plugs were removed from electrodes. The gel plates were removed from electrophoresis chamber. Then the gel was removed from glass plates and transferred to a small container.

2.12.1.5) Staining Procedure

Protein staining

The gel from 2.12.1.4 was transferred to a small container containing Coomassie stain solution (1 % Coomassie Blue R-250, 45 % methanol, and 10 % glacial acetic acid). The gel was agitated for 10-20 minutes on a shaker. The stain solution was poured out and the Coomassie destain solution (10 % methanol and 10 % glacial acetic acid) was added. The gel was shaken slowly. To complete destain, the destain solution was changed many times and agitated overnight or until the blue-clearly bands of protein were occurred.

Activity staining (Gabriel, 1971 cited in Bollag *et al.*, 1993)

After electrophoresis at 4°C was done, the gel was transferred to a small container containing 10 ml of activity staining solution (4.25 mmole of Tris-HCl, pH 8.5, 40 µmole of L-phenylalanine, 50 µmole of NAD⁺, 25 µg/ml of phenazine methosulfate and 250 µg/ml of nitroblue tetrazolium) and agitated for 30 minutes at room temperature. After purple bands were occurred, the gel was then destained with distilled water.

2.12.2 SDS-polyacrylamide gel electrophoresis

The SDS-polyacrylamide system was performed according to the section 2.12.1. For 2 slab gels, separating gel (12 % acrylamide) consisted of 3.0 ml of solution A (30 % (w/v) acrylamide, 0.8 % (w/v) bis-acrylamide), 2.5 ml of solution B (1.5M Tris-HCl, pH 8.8, 4% SDS) and 1.89 ml of distilled water. Stacking gel (4 % acrylamide) consisted of 0.67 ml of solution A (30 % (w/v) acrylamide, 0.8 % (w/v) bis-acrylamide), 1.0 ml of solution C (0.5 M Tris, pH 6.8, 4% SDS) and 3.27 ml of distilled water. Protein

sample was mixed with 5 x sample buffer (0.3 mM Tris-HCl, 50 % glycerol, 20% SDS, 5% 2-mercaptoethanol and 0.05 % bromophenol blue) in an Eppendorf tube and was boiled 10 min at 95°C and cooled at room temperature. Then the sample solution was introduced into gel by using syringe. The electrophoresis buffer (25 mM Tris, 192 mM glycine and 0.1% SDS, pH 8.8) was used for gel running. After electrophoresis, proteins in the gel were visualized by protein staining as described in section 2.12.1.5.

2.13 Characterization of alanine dehydrogenase and mutated enzymes

2.13.1 Effect of temperature on AlaDH activity

The purified AlaDHs were used to investigate the effect of temperature on their activity. The enzyme was assayed as described in section 2.8.2 at various temperatures from 30 to 62°C, in oxidative deamination. The result was expressed as a percentage of the relative activity. The temperature at which maximum activity was observed for each reaction was set as 100%.

2.13.2 Effect of pH on AlaDH activity

The purified AlaDHs was used to study the effect of pH on their activity. The enzyme was assayed as described in section 2.8.2 at various pHs. The 200 mM of glycine-KCl-KOH were used as reaction buffer for 8.5 - 12.5, in oxidative deamination. The pH of each reaction mixture was measured with a pH meter at room temperature after reaction. The result was expressed as a percentage of the relative activity. The temperature at which maximum activity was observed for each reaction was set as 100%.

2.13.3 Effect of temperature on AlaDH stability

The thermostability of the enzyme was investigated over the range of 30 to 70°C. The purified enzyme was preincubated at various temperatures for 10 minutes before determination of enzyme activity in oxidative deamination as described in section 2.8.2. The result was expressed as a percentage of the relative activity. The highest activity was defined as 100% for T_m determination.

Thermostability (T_m) of enzyme was determined from temperature at which the enzyme loses 50% of its original level activity after incubation.

2.13.4 Substrate specificity of alanine dehydrogenase

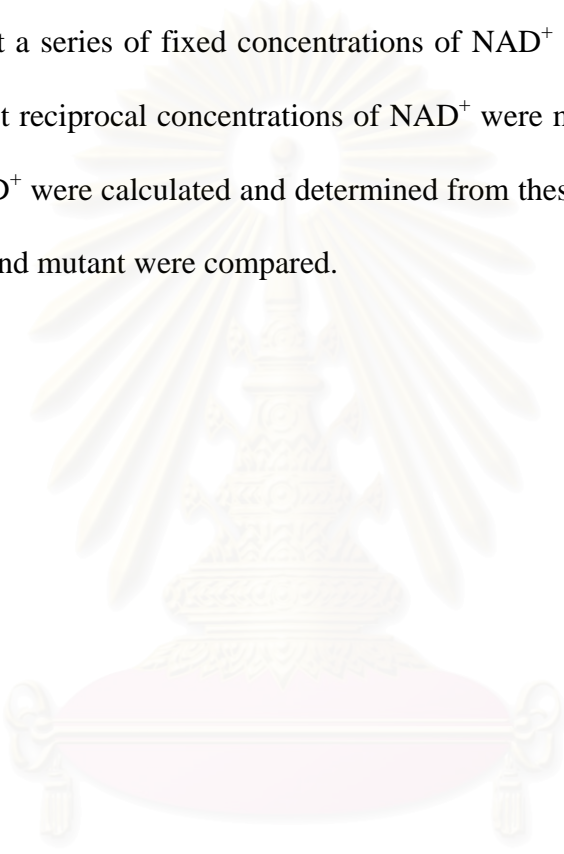
The ability of the enzyme to catalyze the oxidative deamination of various amino acids and L-alanine analogs was determined at a final substrate concentration of 20 mM for D-alanine, D-aspartate, L-aspartate, L-phenylalanine, L-leucine, D-leucine, L-methionine, L-Threonine, L-isoleucine, D-tryptophan, L-valine, glycine, L-glutamate, L-cysteine, L-asparagine, L-lysine, L-serine D-serine and L- α -amino-*N*-butyrate. L-alanine was replaced by various amino acids and L-alanine analogs as substrates for the reaction and enzyme activities were determined as described in section 2.8.2. The result was expressed as a percentage of the relative activity.

2.14 Kinetic parameter of alanine dehydrogenase

Steady-state kinetic analyzes were carried out to investigate the kinetic parameters and reaction mechanism as described below.

Initial velocity analysis for the oxidative deamination

Initial velocity studies for the oxidative deamination reactions were carried out under the standard reaction condition (as described in section 2.8.2) except that various amounts of L-alanine and NAD^+ were used. The concentrations of L-alanine used were 2.5, 5, 10 and 20 mM and those of NAD^+ used were 0.25, 0.5 and 1.0 mM. The Lineweaver-Burke plots (double-reciprocal plots) of initial velocities against L-alanine concentrations at a series of fixed concentrations of NAD^+ and the secondary plots of y intercepts against reciprocal concentrations of NAD^+ were made from the data. K_m of L-alanine and NAD^+ were calculated and determined from these two plots, respectively. K_m from wild type and mutant were compared.



สถาบันวิทยบริการ
จุฬาลงกรณ์มหาวิทยาลัย

CHAPTER III

RESULTS

3.1 Selection of amino acid residues for contribution of electrostatic interaction

3.1.1 Construction of three-dimensional structure

Amino acid sequences of AlaDH from *A. hydrophila* and *B. stearothermophilus* were submitted and three-dimensional structures were constructed by SWISS-MODEL automate protein homology-modeling server. The X-ray crystallography structure of AlaDH from *Phormidium lapideum* deposited in the Protein Data Bank (accession number 1PJB), was used as template. The SWISS-MODEL automate modeling procedure is started when at least one modeling template that has a sequence identity of more than 25% with target sequence is available. The server builds the model based on the given amino acid alignment with template. However, the model reliability decreases as the sequence identity decreases and that target-template pair shares less than 50% sequence identity. The resulting model can be visualized and analyzed using Swiss-pdb Viewer. Since amino acid sequence of AlaDH from *A. hydrophila* and *B. stearothermophilus* resulted in 53.10% and 54.03% identity with that of the *P. lapideum* template respectively, their three-dimensional structures were constructed with high accuracy. Their structures looked very similar as shown in Figure 3.1.

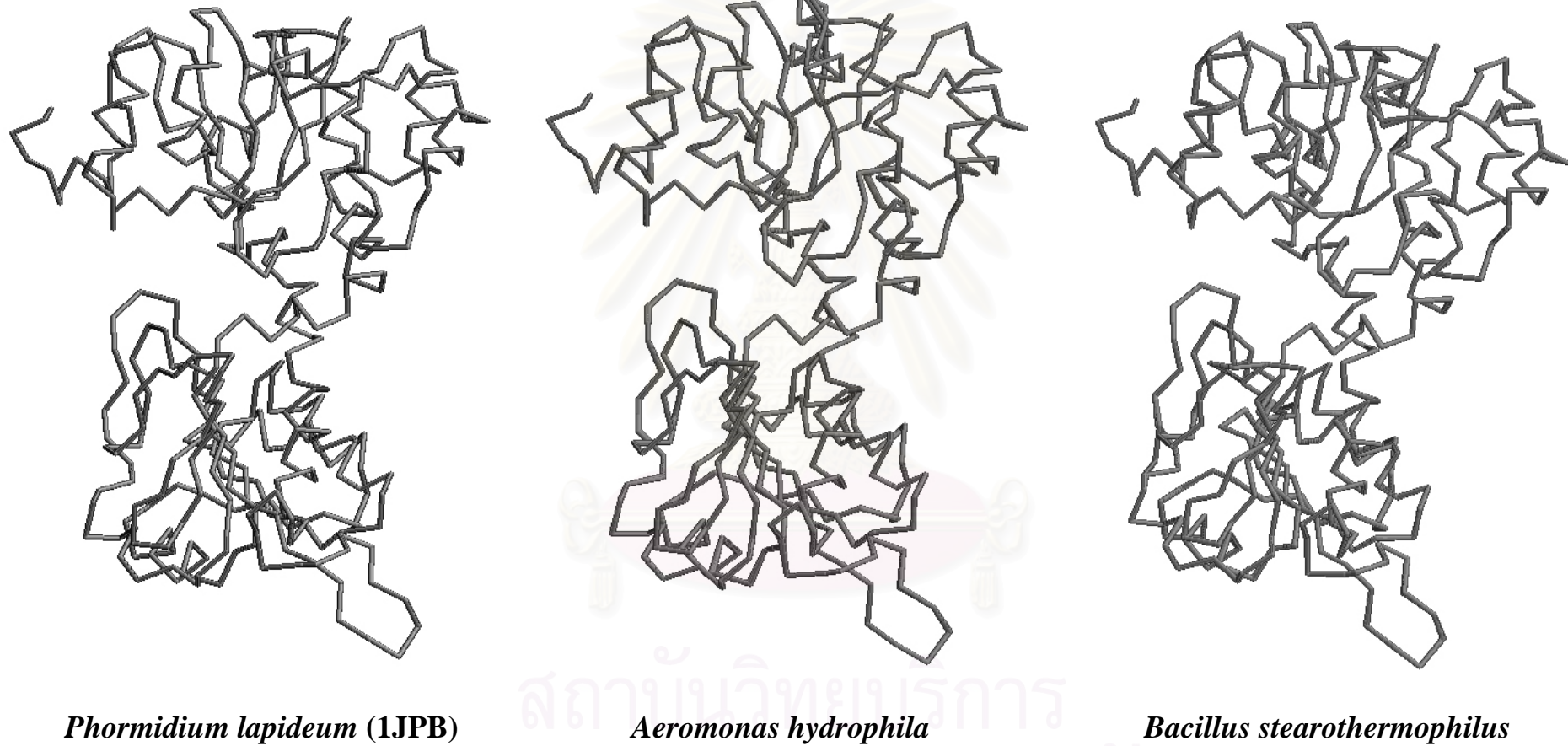


Figure 3.1 Three-dimensional structure of AlaDHs. Structures of AlaDH from *Aeromonas hydrophila* and *Bacillus stearothermophilus* constructed by SWISS-MODEL automated homology-model serve using X-ray diffraction structure of AlaDH from *Phormidium lapideum* (1JPB) deposited in Protein Data Bank as a template.

3.1.2 Calculation of electrostatic interaction and amino acid sequence alignment

Comparison of three-dimensional structure of alanine dehydrogenase from SWISS-MODEL between *A. hydrophila* and *B. stearothermophilus* AlaDH revealed several electrostatic interaction differences as shown in Appendix F. From these data, the constructed structures were analyzed for which position of amino acid residue from *B. stearothermophilus* AlaDH should be introduced to form salt bridge or electrostatic interaction in *A. hydrophila* AlaDH. Rational design technique was used to choose amino acid residues for site-directed mutagenesis. Firstly the amino acid residues located on surface of enzyme subunit which were appeared to form electrostatic interaction in *B. stearothermophilus* AlaDH but missed from that of *A. hydrophila* were considered. Subsequently, the amino acid residues which were conserved among amino acid sequence of AlaDH from various organisms (Figure 3.2) were omitted. Five selected uncharged amino acids were then chosen to be substituted with charge residues according to the sequence of thermophile as G38E, L58R, L101E, P168R and A231E (Figure 3.3). Electrostatic interaction formed in mutant models with the distance of side chain basic amino acid and acidic amino acid $\leq 7 \text{ \AA}$ were shown in Table 3.1. All selected residues are located on surface of molecule far from an active site as shown in Figure 3.4.

CLUSTAL X (1.64b) multiple sequence alignment

```

A.hyd      MIIGVPKEIKNHEYRVGMVPASVRELTARNHT-VFVQSGAGNGIGFSDADYLAAG-AEIL
Shew       MIIGVPTEIKNHEYRVGMVPSSVRELTIKGHV-VYVQSDAGVIGFTDQDYIDAG-ASIL
V.pro      MIIGVPKEIKNHEYRVGMIPASVRELISHGHQ-VFVETNAGAGIGFSDDDYIYAVG-ASIL
E.aer      MIIGVPKEIKNNENRVAMTPAGVVHLLNAGHK-VIETNAGLGSFTNNEYKQAG-AEII
B.sub      MIIGVPKEIKNNENRVALTPGGVSQLISNGHR-VLVETGAGLGSGFENEAYESAG-AEII
B.ste      MKIGIPKEIKNNENRVAITPAGVMTLVKAGHE-VYVETEGGAGSGFSDSEYEKAGAADCRC
B.sph      MKIGIPKEIKNNENRVAMTPAGVVSLTHAGHERLAIETGGGIGSSFTDAEYVAAG-AAZR
Carn       MKIGIPKEIKNNENRVAISPAGVYSLTEGGHE-VLVEASAGKTAGFTDAEFEESG-AKIV
P.lap      MEIGVPKEIKNQEFRVGLSPSSVRTLVEAGHT-VFIETQAGIGAGFADQDYVQAG-AQVV
M.tub      MRVGIPTETKNNFRVAITPAGVAELTRRGHE-VLIQAGAGEGSAITDADFKAAG-AQLV
*  :*:*. * **:* **.: *..* *  . *  : ::: .*  .: :  :  * *

A.hyd      ASAADVFAKAEMIVKVKEPQAVERAMLRPGQTLFTYLHLAPDLAQRELVDSGAICIAYE
Shew       ATAAEVFAKSDMIIVKVKEPQAVERAMLRHDQILFTYLHLAPDLPQTEELITSGAVCIAYE
V.pro      PTAAEVFAQADMIIVKVKEPQAVERAMLRKQGQILFTYLHLAPDFPQTEDLIKSKAVCIAYE
E.aer      ESASDVWTKADMIMKVKEPLASEYGYFRKGLILFTYLHLAAEPQLKALVDSEVIAIAYE
B.sub      ADPKQVWD-AEMVMKVKEPLPEEYVYFRKGLVLFYTLHLAAEPQLAKDKGVTAIAYE
B.ste      RTWRDAWT-AEMVLKVKEPLAREFRYFRPGLILFTYLHLAAAEVTKAVVEQKVVGIAIYE
B.sph      CIGKEAWA-QEMILKVKEPVASEYDYFYEGQILFTYLHLAPRAELTQALIDKKVVGIAIYE
Carn       NNADDVWA-ADMVIKVKEPLPEEYGYFREGLIIFTYLHLAAAKELTEKLMETGVTAIGYE
P.lap      PSAKDAWS-REMVVKVKEPLPAEYDLMQKDQLLFTYLHLAAARELTELQMLRVGLTAIAYE
M.tub      GTADQVWADADLLLKVKEPIAAEYGRLRHGQILFTFLHLAASRACTDALLDSGTTSIAYE
      .: :  :::***** . *  :  .  :*:*****.  :  :  *..*

A.hyd      TVTDGRGGLPLLAPMSEVVGRMSIQAGAQALESRGGSGVLLGGVPGVEPAKVVIIGGGV
Shew       TVTDDRGGGLPLLAPMSEVAGRMSIQAGARALEKSLGGRGMLLGGVPGVEPAKVVIIGGGM
V.pro      TVTDNMGRLPLLAPMSEVAGRMSIQAGAQTLEKSHGGRGMLLGGVPGVEPAKVVIIGGGV
E.aer      TVTVNR-TLPLLSPMSEVAGRMAAQVGAQFLEKTQGGKGIILSGVPGVKRGKVTIIGGGM
B.sub      TVSEGR-TLPLLPMSSEVAGRMAAQVGAQFLEKPKGGKGIILLAGVPGVSRGKVTIIGGGV
B.ste      TVQLANGSLPLLPMSSEVAGRMSVQVGAQFLEKPHGGKGIILGGVPGVRRGKVTIIGGGT
B.sph      TVQLANGSLPLLPMSSEVAGKMATQVGAQFLEKNHGGKGIILGGVSGVHARKVTVIIGGGI
Carn       TMEKDG-VLPLLPMSQVAGRMAVQVGAQFLENNYGGKGLLGGTTPGVSTGNVVIIGGGV
P.lap      TVELPNRSLPLLPMSI IAGRLSVQFGARFLERQQGGRGVLLGGVPGVKPGKVVILGGGV
M.tub      TVQTADGALPLLAPMSEVAGRLAAQVGAHYHLMRTQGGRGVLMGGVPGVEPADVVVIGAGT
* :  *****:* * :.: : * * * * . * * * : : * * * * . * . : : * *

A.hyd      VGSNAARMAIGLRADVTILDNNIDTLRRLDSEFQGAAKVVYSNRETLEHLLAADLVIGG
Shew       VGTNAAQMAVGMGADVVDLDRSIDALRRLNVQFGSAVKAIYSTADAIERHVLEADLVIGG
V.pro      VGANAARMAVGMRADVTILDNRIDTLRKLDEEFQGRAKVVYSTEDAIKHKVLAADLVIGA
E.aer      VGTNAAKIAVGLGADVTIIDLNPDRRLRQLEDIFGTSVQTLMSNPYNI AEAVKESDLVIGS
B.sub      VGTNAAKMAVGLGADVTIIDLNADRLRQLDDIFGHQIKTLISNPVNIADAVAEADLLICA
B.ste      AGTNAAKIGVGLGADVTILDINAERLRELDLFGDHVTTLMSNSYHIAECVRESDLVVGGA
B.sph      AGTNAAKIAVGMGADVVIDLSPERLRQLEDMFGRDVQTLMSNPYNIAESVKHSDLVVGA
Carn       SGMHAAKMAVGLGADVTILDVNPARLAELGNI FGNSVTTLMSNEYNIAEQVKTADLVIGA
P.lap      VGTEAAKMAVGLGAQVQIFDINVERLSYLETLFGSRVELLYSNSAEIETAVAEADLLIGA
M.tub      AGYNAARIANGMGATVTVLDINIDKLRQLDAEFCGRIHTRYSSAYELEGAVKRADLVIGA
* .*: : . * : * * : : *  * * * * *  *  :  :  : * : : .

```

(Continued)

Figure 3.2 Linear alignment of the amino acid sequence of alanine dehydrogenase from various sources. A. hyd = *Aeromonas hydrophila*, Shew = *Shewanella sp.*, V .pro = *Vibrio proteolyticus*, E. aer = *Enterobacter aerogenes*, B. sub = *Bacillus subtilis*, B. ste = *Bacillus stearothermophilus*, B. sph = *Bacillus sphaericus*, Carn = *Carnobacterium sp.*, P. lap = *Phormidium lapideum*, M. tub = *Mycobacterium tuberculosis*.

Conserve residues are indicated by asterisks.

CLUSTAL X (1.83) multiple sequence alignment

```

A. hyd      MIIGVPKEIKNHEYRVGMVPASVRELTARNHTVVFVQSGAGNGIGFSDADYLAAGAEILAS 60
B. ste      MKIGIPKEIKNNENRVAITPAGVMTLVKAGHEVYVETEGGAGSGFSDSEYEKAGAADRCR
* *:*****:* **.:**.* * . * *:*.:. * * *****:.* *** .

A. hyd      AADVFAKAEMIVKVKEPQAVRAMLRPGQTLFTYLHLAPDLAQRELVDSGAICIAYETV 120
B. ste      TWRDAWTAEMVLKVKEPLAREFRYFRPGLILFTYLHLAAAERVTKAVVEQKVVGIAYETV
:      .***:***** * * :*** *****. * : :*. . : *****

A. hyd      TDGRGGLPLLAPMSEVGRMSIQAGAQALESRRGGSGVLLGGVPGVEPAKVVIIGGGVVG 180
B. ste      QLANGSLPLLTPMSEVAGRMSVQVGAQFLEKPHGGKGILLGGVPGVRRKVTIIGGGTAG
. *.*****:*****.*****:*.*** ***.:**.*:*****. .**.******. .*

A. hyd      SNAARMAIGLRADVTILDNNIDTLRRLDSEFQGAAKVVYSNRETLERHLLAADLVIGGVL 240
B. ste      TNAAKIGVGLGADVITILDINAERLRELDLFGDHVTTLMSNSYHIAECVRESDLVVGAVL
:***:..:** ***** * : **.*. * . . . : ** : . : .***:*.**

```

Figure 3.3 Linear alignment of the amino acid sequences of alanine dehydrogenase from *Aeromonas hydrophila* and *Bacillus stearothermophilus* (Kuroda *et al.*, 1990). A. hyd = *Aeromonas hydrophila*, B. ste = *Bacillus stearothermophilus*. Conserve residues are indicated by asterisks. Mutated residues are boxed

```

A. hyd      VPGATAPKLVSRDHIARMKPGSAIVDVAIDQGGCVETS-HATTHEDPTFIVDDVHYCVA 300
B. ste      IPGAKA-KLVTEEMVRSMTPGSVLVDIAIDQGGIFETTDRTVTHDDPTYVKHGVVHYAVA
           :***.* ***:.: : *.***.:**:* ** .**: :.***:***: : ..***.**

A. hyd      NMPGAVARTSTVALN NATLPFI I KLAEQGYRNALLSDPHLRHGLNVMAGKITCKEVAVAH 360
B. ste      NMPGAVPRTSTFALTNVTI PYALQIANKGYRAGCLDNPALLKGIN TLDGHI VYEAVAAAH
           ***** .***** .**.*.*: : : : : : : . * . : * * : * : . : * : * . : **.*

A. hyd      NLAYTDPLTLLN-
B. ste      NMPYTDVHSL LHG
           * : .*** : ** :

```

Figure 3.3 (Continued) Linear alignment of the amino acid sequences of alanine dehydrogenase from *Aeromonas hydrophila* and *Bacillus stearothermophilus* (Kuroda *et al.*, 1990). A. hyd = *Aeromonas hydrophila*, B. ste = *Bacillus stearothermophilus*.

Conserve residues are indicated by asterisks.

Mutated residues are boxed

Table 3.1 List of created electrostatic interactions in three-dimensional model of AlaDHs

AlaDH mutant	Electrostatic interaction	
	Pairs amino acid residue ^a	Distance (Å)
G38E	Glu38 OE2 - Lys7 NZ	6.67
L58R	Arg58 NH1 - Asp 63 OD1	5.44
	Arg58 NH2 - Asp 63 OD1	3.31
	Arg58 NH1 - Asp 63 OD2	3.92
	Arg58 NH2 - Asp 63 OD2	5.72
L101E	Glu101 OE1 - Arg105 NH2	5.56
	Glu101 OE2 - Arg105 NH1	6.02
	Glu101 OE2 - Arg105 NH2	3.87
P168R	Arg168 NH1 - Asp193 OD1	5.05
	Arg168 NH1 - Asp193 OD2	6.07
	Arg168 NH2 - Asp193 OD1	6.45
A231E	Glu231 OE1 - Lys170 NZ	4.98
	Glu231 OE2 - Lys170 NZ	5.87
	Glu231 OE1 - Lys216 NZ	6.10
	Glu231 OE1 - Arg227 NH1	4.08
	Glu231 OE1 - Arg227 NH2	6.27
	Glu231 OE2 - Arg227 NH1	5.06

^a Groups of side chain of amino acid residue are indicated by

OE = carboxyl group of Glu

OD = carboxyl group of Asp

NH = amino group of Arg

NZ = amino group of Lys

Source: <http://www.cmbi.kun.nl/gv/servers/WIWWWI/>

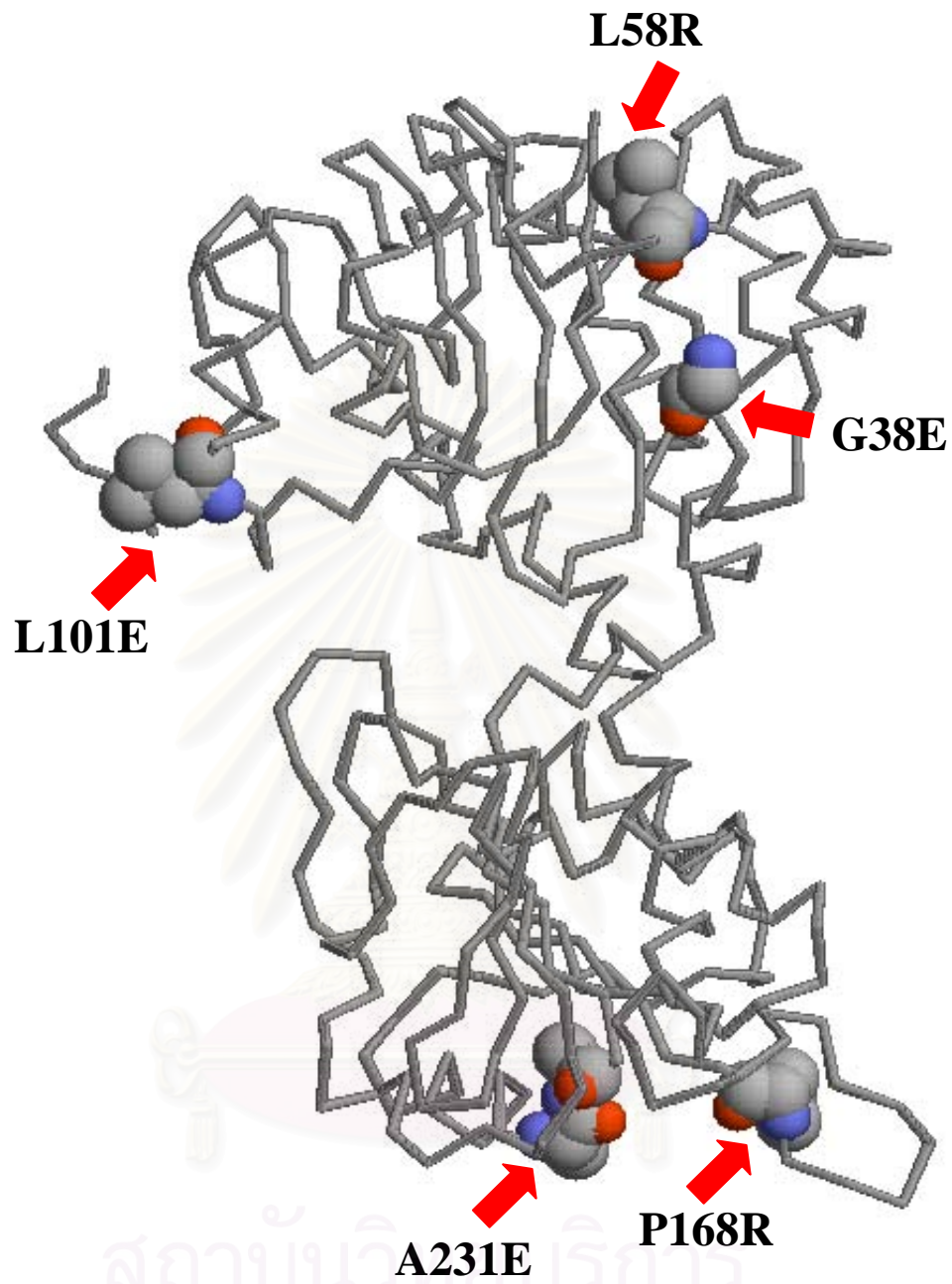


Figure 3.4 Location of mutated residues in the three-dimensional structure model of AlaDH from *Aeromonas hydrophila*.

3.2 Site-directed mutagenesis

3.2.1 Plasmid extraction

The plasmid pUC18 contained *alaDH* gene was extracted from *E. coli* JM 109 in order to use as a template for site-directed mutagenesis, by the method described in section 2.7.1. From agarose gel electrophoresis double digestion with *EcoRI* and *HindIII* showed that the recombinant plasmid contained 1,116 bp of *alaDH* gene (Figure 3.5). The DNA concentration was about 1 µg/µl. The quality of extracted DNA was suitable for further molecular procedures.

3.2.2 Site-directed mutagenesis (QuikChange site-directed mutagenesis kit)

Site-directed mutagenesis was performed by QuikChange site-directed mutagenesis kit as described in section 2.7.3. The oligonucleotide primers used for construction of the AlaDH mutants were summarized in section 2.4. The reactions of mutant and control strand syntheses (Appendix B) were performed at the same time. The concentration of PCR products could not be determined by agarose gel electrophoresis in this stage because low amount of DNA was obtained. The PCR products were then treated with *DpnI*. For cloning of mutant clones L58R and P168R, the mutant plasmids were transformed into *E. coli* XL1-Blue according to the recommendation of QuikChange protocol. In transformation, 50-80 white colonies of mutant clone per 1 µl of PCR reaction were obtained. Mutagenesis efficiency of control determined by antibiotic selection was in the range of 85 - 89%. All target transformants were checked for their plasmid size by agarose gel electrophoresis (Figure 3.6). All mutant plasmids gave the same mobility to their wild type.

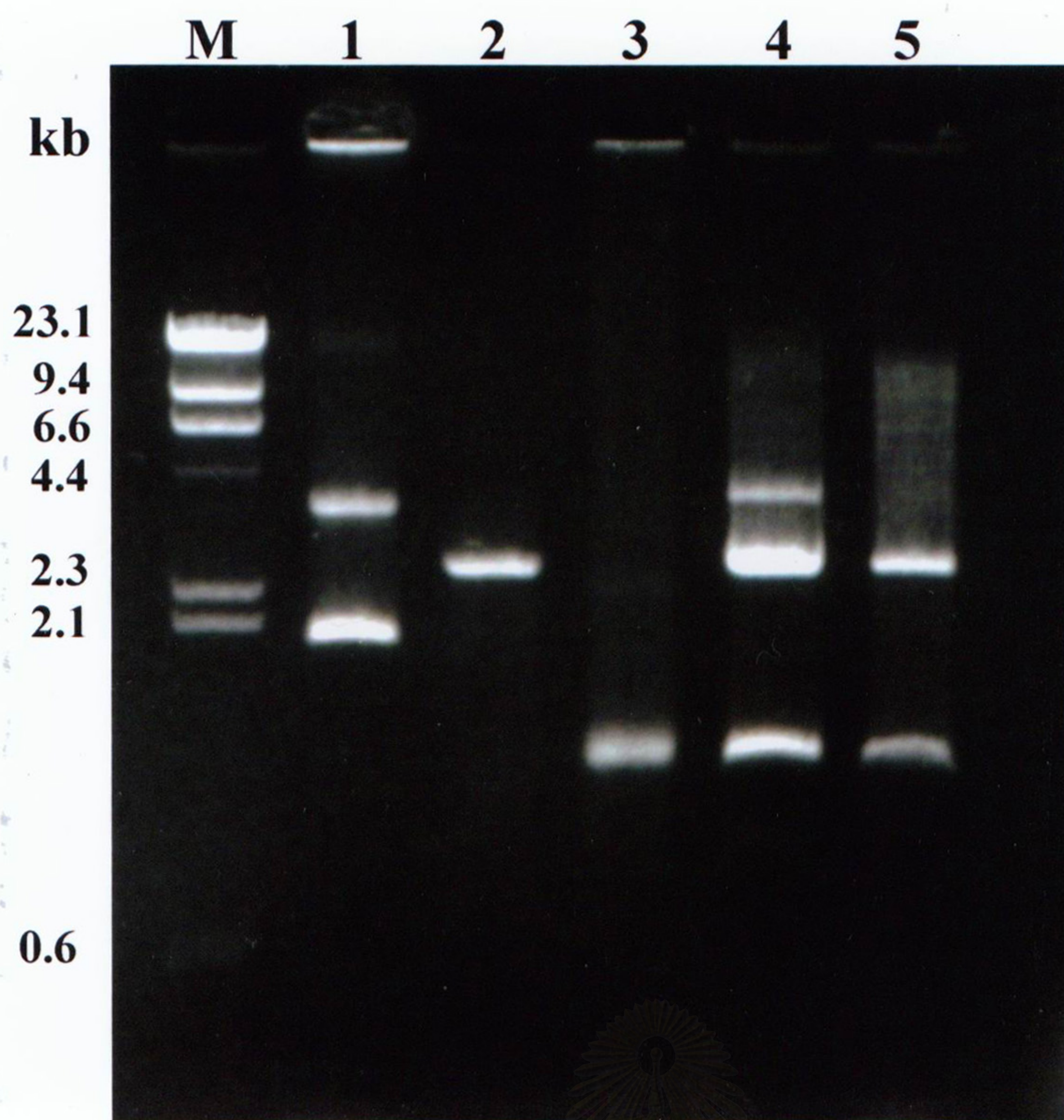


Figure 3.5 Agarose gel electrophoresis of template plasmids harboring *alaDH* gene

Lane M λ Hind III standard DNA marker

Lane 1 undigested pUC18

Lane 2 *EcoRI-HindIII* digested pUC18

Lane 3 amplified product of the alanine dehydrogenase gene

Lane 4-5 *EcoRI-BamHI* digested recombinant plasmid

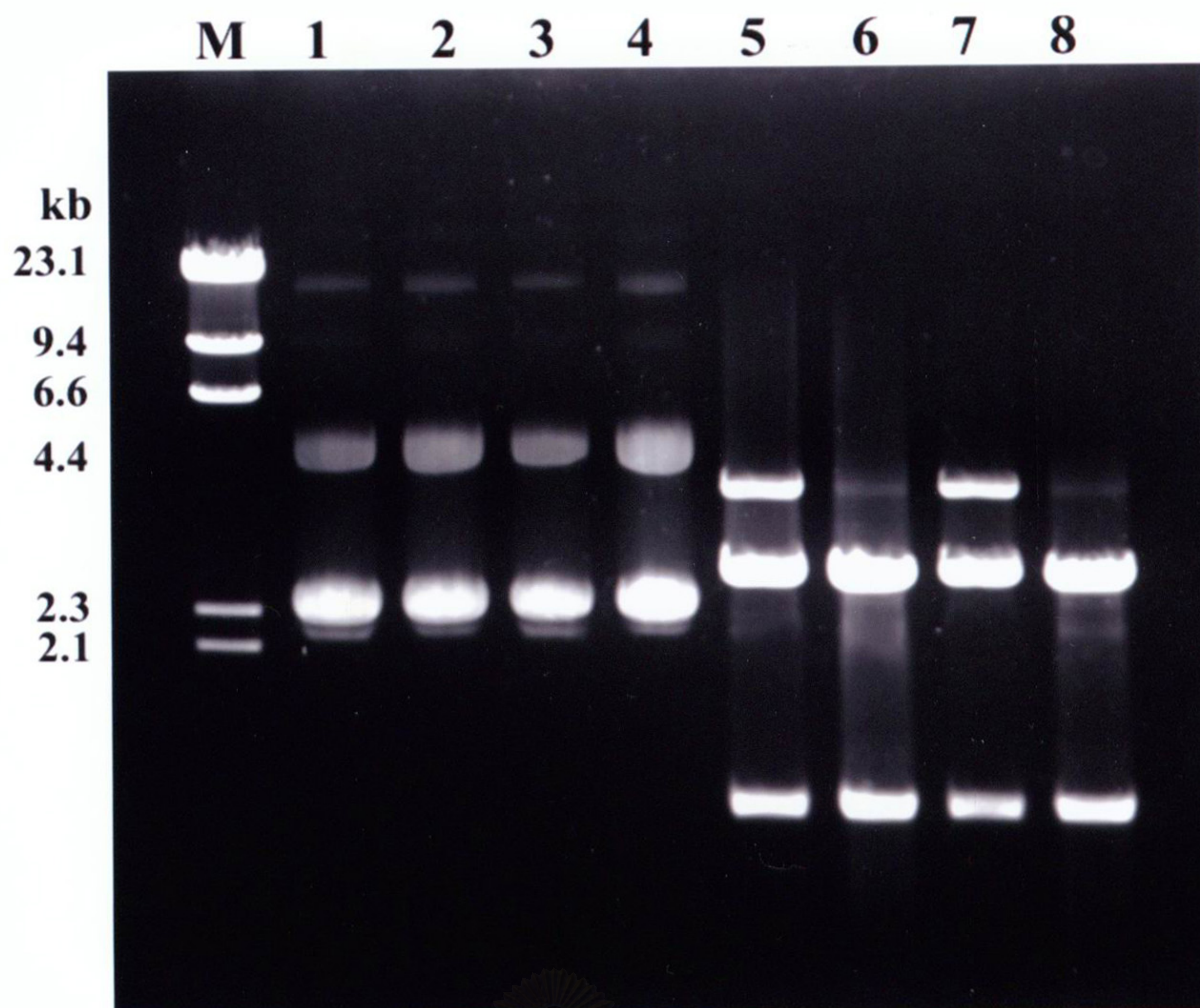


Figure 3.6 Agarose gel electrophoresis of *EcoRI/HindIII* digested mutant plasmids

- Lane M = λ /*Hind III* standard DNA marker
- Lane 1 = undigested wild type plasmid
- Lane 2 = undigested G38E plasmid
- Lane 3 = undigested L58R plasmid
- Lane 4 = undigested P168R plasmid
- Lane 5 = *EcoRI-BamHI* digested wild type
- Lane 6 = *EcoRI-BamHI* digested G38E plasmid
- Lane 7 = *EcoRI-BamHI* digested L58R plasmid
- Lane 8 = *EcoRI-BamHI* digested P168R plasmid

3.3 Enzyme activity assay and Protein assay

The mutant L58R and P168R were determined for their expression in *E. coli* XL1-Blue as described in section 2.8. From 11 random picked clones, the total activity of the crude extracts were about 0 - 42.1 unit for L58R and 0 - 180.6 unit for P168R while that activity of wild type, *E. coli* JM109 harboring *alaDH* gene, was 244.9 - 290.7 unit as shown in Table 3.2 and 3.3. Since the activity of mutant AlaDHs in *E. coli* XL1-Blue were markedly lower than that of wild type in *E. coli* JM109, recombinant plasmids from mutant clones with the highest activity were further cloned into *E. coli* JM109.

3.4 Transformation into *E. coli* JM 109

The selected plasmids of L58R and P168R from section 3.3 were transformed into *E. coli* JM109 by electroporation as described in section 2.10. Subsequently, the enzyme activities were determined, the expression of mutant AlaDHs in *E. coli* JM109 were at the same level with that of wild type in the same host (Table 3.4)

To shorten cloning step of G38R, L101E and A231E mutants, the mutated plasmids from section 3.2.2 were directly transformed into *E. coli* JM109 by electroporation. The transformant clones were random picked for plasmid extraction and then assayed for AlaDH activity. As shown in Table 3.5, the activity AlaDH from mutant G38E varied from clone to clone, whereas the activity from L101E and A231E seemed to be consistent.

The activity of crude enzyme from AlaDH wild type and various mutants in *E. coli* JM109 prepared from 500 ml of LB culture are summarized in Table 3.6

From this stage, the mutants which expressed the highest activity from of each type were selected.

Table 3.2 The activity of crude enzyme from *E. coli* XL1-Blue containing L58R mutant plasmid

Crude extract	Total activity (unit)	Total protein (mg)	Specific activity (unit/mg protein)
AlaDH wt in <i>E. coli</i> JM 109	244.9	31.14	7.86
L58R -1	42.1	31.40	1.34
L58R -2	-	28.79	-
L58R -3	4.6	29.71	0.15
L58R -4	-	31.79	-
L58R -5	18.0	26.39	0.67
L58R -6	3.1	33.33	0.10
L58R -7	38.3	29.99	1.27
L58R -8	1.0	32.13	0.03
L58R -9	1.4	16.57	0.08
L58R -10	1.7	26.04	0.06
L58R -11	1.0	24.70	0.04

Table 3.3 The activity of crude enzyme from *E. coli* XL1-Blue containing P168R mutant plasmid

Crude extract	Total activity (unit)	Total protein (mg)	Specific activity (unit/mg protein)
AlaDH wt in <i>E. coli</i> JM 109	290.7	33.54	8.78
P168R -1	3.2	38.86	0.08
P168R -2	3.1	33.99	0.09
P168R -3	170.9	24.21	7.05
P168R -4	109.1	26.88	0.07
P168R -5	31.2	30.33	1.03
P168R -6	-	37.43	-
P168R -7	180.6	27.10	6.87
P168R -8	2.7	38.34	0.07
P168R -9	4.7	46.98	0.01
P168R -10	3.8	34.86	0.11
P168R -11	126.4	20.00	6.32

Table 3.4 The activity of crude enzyme from *E. coli* JM109 containing L58R or P168R mutant plasmid

Crude extract	Total activity (unit)	Total protein (mg)	Specific activity (unit/mg protein)
AlaDH wild type	279.3	29.50	9.47
L58R'-1	83.2	21.45	3.88
L58R'-2	95.5	23.55	4.05
L58R'-3	92.4	27.38	3.39
L58R'-4	77.0	27.56	2.79
L58R'-5	98.6	30.70	3.21
L58R'-6	86.2	25.86	3.33
P168R'-1	277.3	29.44	9.41
P168R'-2	328.7	32.56	10.10
P168R'-3	287.6	28.99	9.92
P168R'-4	256.8	24.97	10.28
P168R'-5	269.6	25.33	10.65

สถาบันวิทยบริการ
จุฬาลงกรณ์มหาวิทยาลัย

Table 3.5 The activity of crude enzyme from *E. coli* JM109 containing G38E, L101E or A231E mutant plasmid

Crude extract	Total activity (unit)	Total protein (mg)	Specific activity (unit/mg protein)
AlaDH wild type	312.2	27.42	11.39
G38E-1	306.2	34.45	8.88
G38E-2	-	22.36	-
G38E-3	289.3	26.49	10.92
G38E-4	164.8	24.89	6.62
L101E-1	247.9	26.50	9.35
L101E-2	264.6	27.79	9.52
L101E-3	246.5	24.38	10.11
A231E-1	321.0	30.70	10.46
A231E-2	310.3	26.6	11.65

Table 3.6 .The activities of crude AlaDHs in *E. coli* JM109 cultured in 500 ml LB medium

Crude extract	Total activity (unit)	Total protein (mg)	Specific activity (unit/mg protein)
AlaDH wild type	1,179.6	101.15	11.66
G38E	954.9	132.58	11.72
L58R	791.0	135.78	5.83
L101E	1,186.3	165.53	11.72
P168R	954.9	98.58	9.69
A231E	1,497.0	152.99	9.78

3.5 Nucleotide sequencing

The *alaDH* gene from each type of mutant was sequenced by using universal primers, M13 forward primer and M13 reverse primer, as described in section 2.9. The whole sequences of all mutant genes were not different from their wild type gene except the mutated site as shown in Appendix G. This result indicated that no error occurred during PCR amplification.

3.6 Thermostability of crude enzyme

Crude enzyme of each mutant was preincubated at various temperatures for 10 minutes before its activity was assayed as described in section 2.13.3. The activity of non-preincubated enzyme was defined as 100% relative activity. The result of crude enzyme from mutants compared with wild type is shown in Figure 3.7. The crude enzyme of L101E and A231E showed higher thermostability than crude enzyme of wild type. In addition, crude enzyme of G38R showed almost the same thermostability as that of wild type, whereas those from L58R and P168R were lower.

3.7 Double site-directed mutagenesis

Since replacement of Leu 101 and Ala 231 residues with Glu could enhance thermostability of the enzyme, these two residues were selected for double mutation. The mutant plasmid A231E and L101E primers were used as DNA template and mutagenic primers for QuikChange site-directed mutagenesis, respectively. The mutation was confirmed by nucleotide sequencing as the result shown in Appendix G. AlaDH activity of crude extract of double mutant clones was equal to that of wild type (Table 3.7).

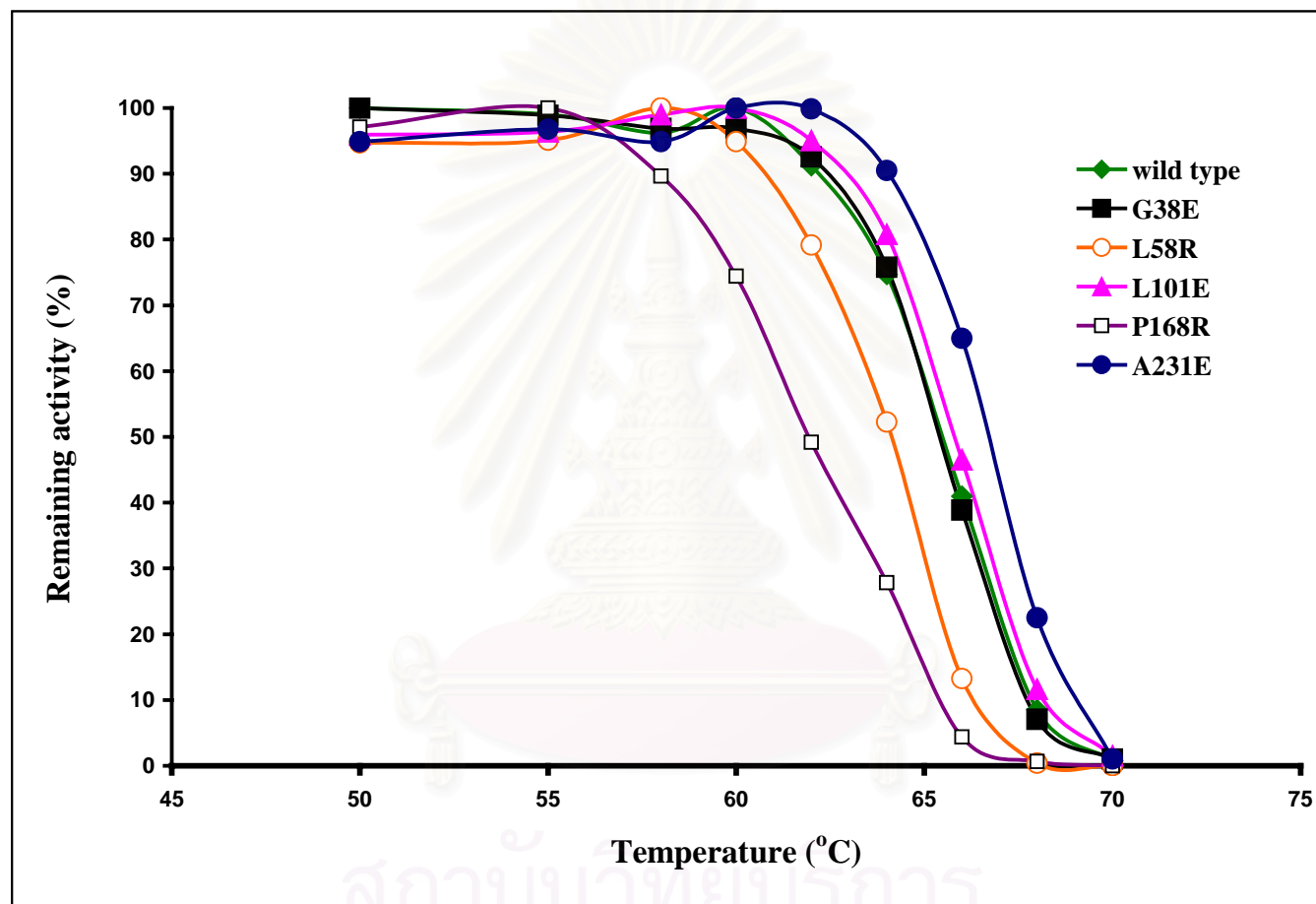


Figure 3.7 Thermostability of crude AlaDH from wild type and mutants.

After crude enzyme was treated at various temperatures for 10 min and chilled on ice. The relative activity was assayed for the oxidative deamination of L-alanine at 30°C. (◆) AlaDH wild type; (■) G38E; (○) L58R; (▲) L101E; (□) P168R; (●) A231E

Table 3.7 The activity of crude enzyme from *E. coli* JM109 containing L101E/A231E mutant plasmid

Crude extract	Total activity (unit)	Total protein (mg)	Specific activity (unit/mg protein)
AlaDH wild type	384.0	42.58	9.02
L101E/A231E-1	406.6	43.60	9.33
L101E/A231E-2	356.0	47.80	7.45
L101E/A231E-3	359.5	38.35	9.37
L101E/A231E-4	408.3	48.13	8.48
L101E/A231E-5	373.9	15.14	8.28
L101E/A231E-6	386.0	38.74	10.13
L101E/A231E-7	350.9	37.61	9.33
L101E/A231E-8	371.0	39.37	9.42
L101E/A231E-9	378.3	34.18	11.07

L101E/A231E mutant enzyme was further purified and characterized to compare some properties, especially thermostability, with wild type, L101E and A231E mutants.

3.8 Purification of alanine dehydrogenase

3.8.1 Preparation of crude enzyme

Crude enzyme solution was prepared from 17 g wet weight of cell which was cultivated from 6 liters of LB medium supplement with 100 µg/ml ampicillin and 75 µg/ml IPTG, as described in section 2.11.1 and 2.11.2. The crude enzyme of wild type and mutants contained total activity of AlaDH in range of 14×10^3 - 17×10^3 units, total protein 2.2 – 2.4 mg and specific activity 5.9 - 7.6 unit/mg protein as shown in Table 3.8

3.8.2 Ammonium sulfate precipitation

Crude enzymes were further purified by ammonium sulfate precipitation as mentioned in section 2.11.3.1. The enzymes were precipitated in the range of 20 - 40% saturated ammonium sulfate. The precipitated proteins were then dissolved with 10 mM KPBS, pH 7.4 and dialyzed against the same buffer. In this step, the enzymes were purified 1.63 to 2.17 fold with 60 - 77% recovery.

3.8.3 DEAE-Toyopearl column chromatography

The enzymes from section 3.8.2 were applied into DEAE-Toyopearl column as described in section 2.11.3.2. The chromatographic profile of wild type AlaDH and mutant AlaDHs were similar. Thus, only the profile of wild type is shown in Figure 3.8. The unbound proteins were eluted from DEAE-Toyopearl column with working buffer. The bound proteins were then eluted with linear salt gradient of 0 to 1 M

potassium chloride solution. The enzyme was eluted at 0.1 M potassium chloride solution as indicated in the profile. The fractions with AlaDH activity were pooled and dialyzed against working buffer. The wild type and mutants enzymes were purified about 2.2 - 3.8 fold with 39 - 55% recovery compared with crude enzyme (Table 3.8).

3.8.4 Blue Sepharose column chromatography

The pooled active fractions from DEAE-Toyopearl column were further purified by Blue Sepharose column as described in section 2.11.3.3. The enzyme solutions were then loaded into Blue Sepharose column and eluted with 0 - 2 M potassium chloride solution in KPB buffer, pH 7.4 as indicated in Figure 3.9. The fractions with AlaDH activity were pooled and dialyzed against working buffer. This operation obtained the enzymes with 126 - 327 mg protein and 3,000 - 6,400 activity units. The specific activity of enzymes from this last step was in the range of 18 - 32 unit/mg protein. The enzymes were purified about 3-4 fold about 23 - 40% recovery compared with crude enzyme as showed in Table 3.8. The purified enzymes from this step were kept as aliquot at 4°C for characterization experiments.

3.9 Determination of enzyme purity and protein pattern on polyacrylamide gel electrophoresis

3.9.1 Non-denaturing polyacrylamide gel electrophoresis

The enzymes of wild type and mutants (L101E, A231E and L101E/A231E) from Blue Sepharose column step of purification were analyzed for purity and protein pattern by non-denaturing polyacrylamide gel electrophoresis as described in section

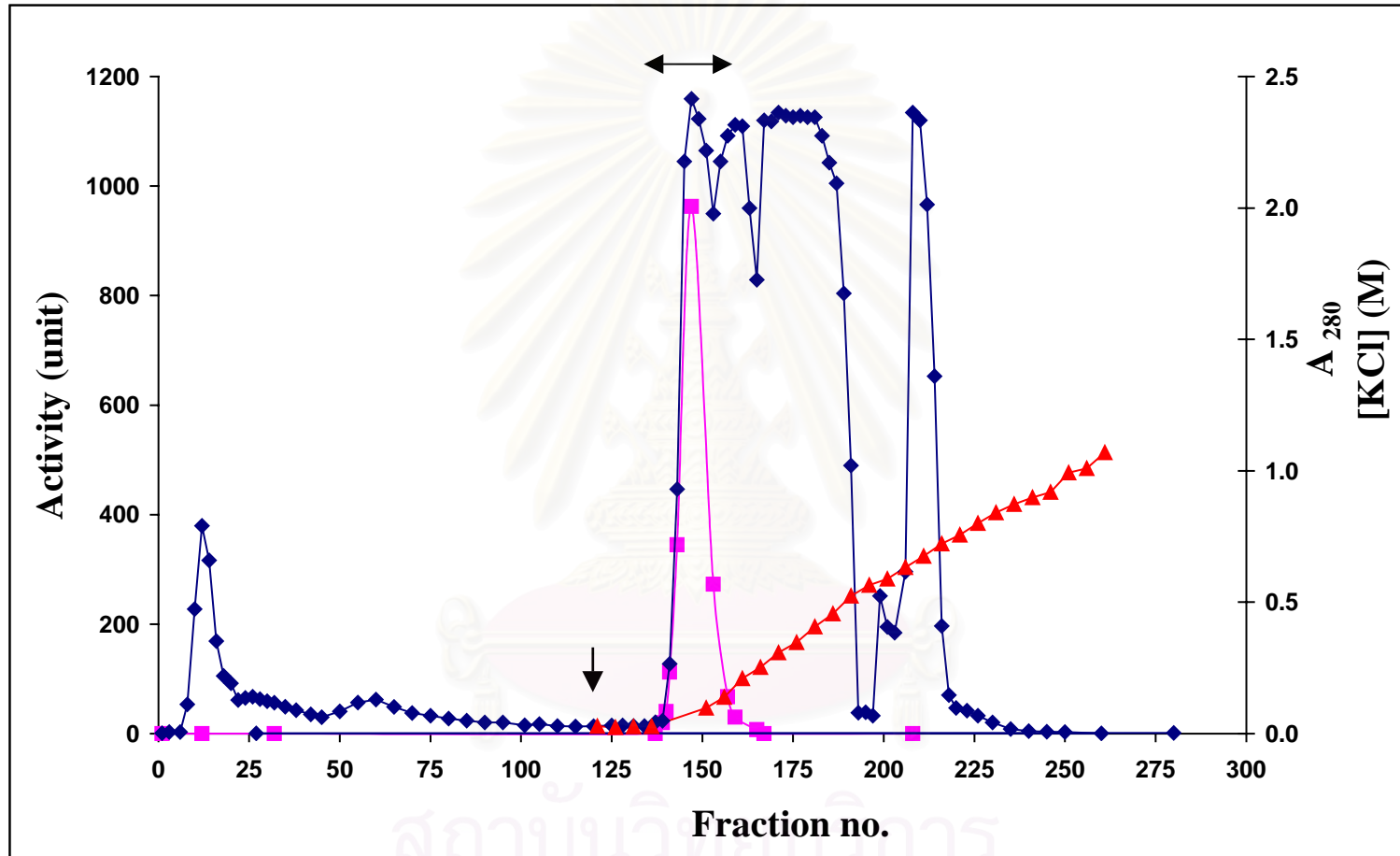


Figure 3.8 Purification of alanine dehydrogenase by DEAE-Toyopearl column

The enzyme solution was applied to DEAE-Toyopearl column and washed with 10 KPB buffer, pH 7.4 until A_{280} decreased to base line. Gradient elution of bound proteins was made by 0 - 1 M KCl in the same buffer at the flow rate of 1 ml/min.

◆ A₂₈₀ ■ AlaDH activity ▲ [KCl] ↓ gradient started ↔ the pool fraction (fraction no. 140 - 159)

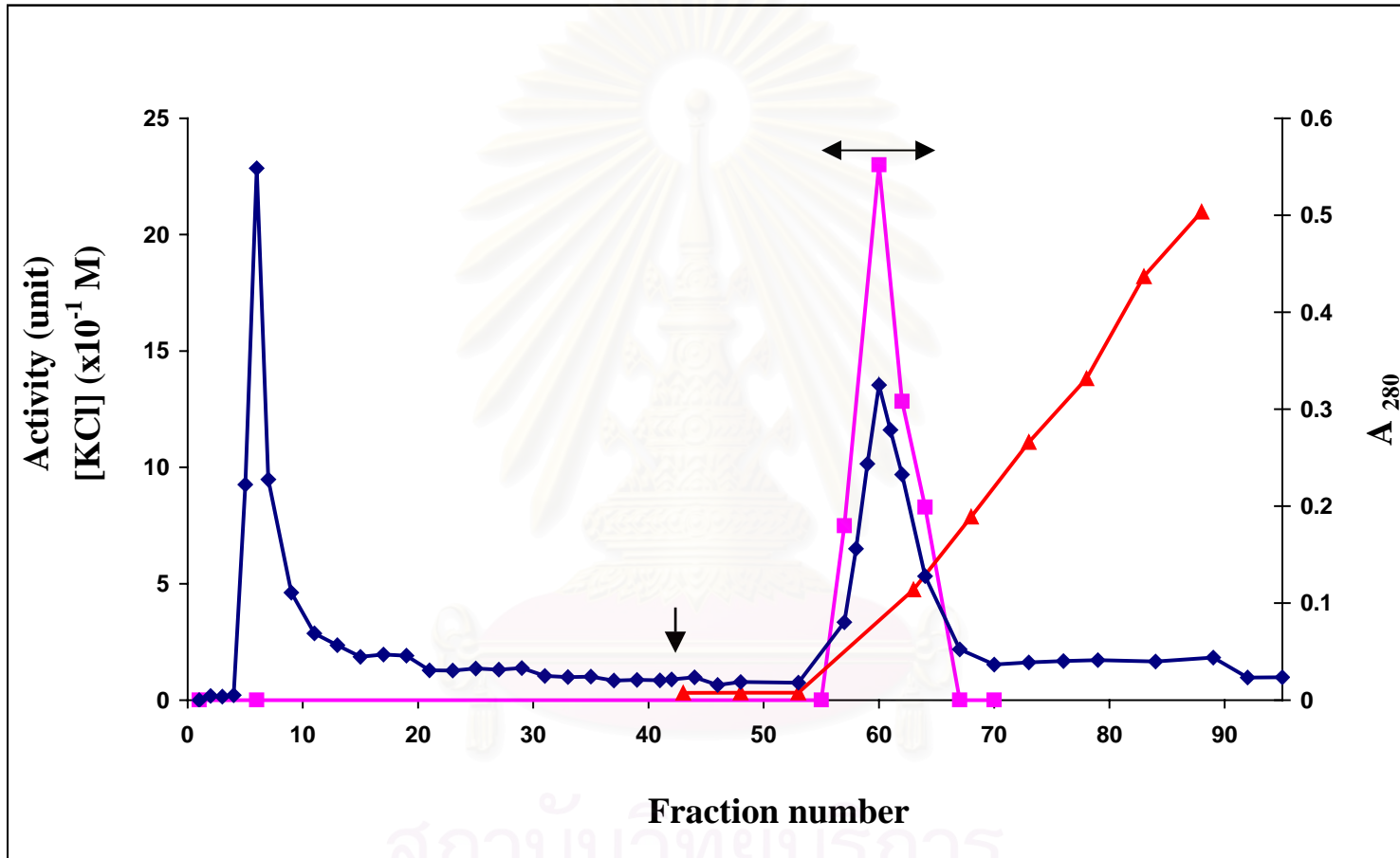


Figure 3.9 Purification of alanine dehydrogenase by Blue Sepharose column

The enzyme solution was applied to Blue Sepharose column and washed with 10 KPB buffer, pH 7.4 until A_{280} decreased to base line. Gradient elution of bound proteins was made by 0 - 2 M KCl in the same buffer at the flow rate of 1 ml/min.

◆ A_{280} ■ AlaDH activity ▲ [KCl] ↓ gradient started ↔ the pool fraction (fraction no. 55 - 67)

Table 3.8 Purification table of AlaDHs

AlaDH	Purification step	Total activity (unit)	Total protein (mg)	Specific activity (unit/mg protein)	% Recovery	Purification fold
wild type	Crude enzyme	16.3×10 ³	2,237	7.28	100.0	1.0
	20-40% Ammonium sulfate precipitation	11.2×10 ³	944	11.88	68.8	1.6
	DEAE-Toyopearl column	9.0×10 ³	555	16.27	55.5	2.2
	Blue Sepharose column	4.0×10 ³	155	25.75	24.5	3.5
L101E	Crude enzyme	17.0×10 ³	2,232	7.63	100.0	1.0
	20-40% Ammonium sulfate precipitation	13.2×10 ³	890	14.82	77.4	1.9
	DEAE-Toyopearl column	6.8×10 ³	233	28.91	39.6	3.8
	Blue Sepharose column	4.1×10 ³	126	32.05	23.8	4.0
A231E	Crude enzyme	16.3×10 ³	2,375	6.85	100.0	1.0
	20-40% Ammonium sulfate precipitation	9.8×10 ³	716	13.76	60.5	2.0
	DEAE-Toyopearl column	7.3×10 ³	449	16.27	44.9	2.4
	Blue Sepharose column	6.4×10 ³	327	19.55	39.3	2.9
L101E/A231E	Crude enzyme	14.1×10 ³	2,375	5.92	100.0	1.0
	20-40% Ammonium sulfate precipitation	9.8×10 ³	763	12.84	69.7	2.2
	DEAE-Toyopearl column	6.3×10 ³	450	15.50	44.6	2.6
	Blue Sepharose column	3.2×10 ³	173	18.36	22.7	3.1

2.12.1. The activity staining was performed to compare with protein staining. The result is shown in Figure 3.10. All of purified AlaDH showed a single protein band which corresponded with their activity staining. Single mutant enzyme, L101E and A231E, moved faster than wild type enzyme, while double mutant enzyme, L101E/A231E moved fastest. This evidence reflected the net charge on enzyme.

3.9.2 SDS polyacrylamide gel electrophoresis (SDS-PAGE)

The enzyme from each step of purification was analyzed for purity and protein pattern by SDS-PAGE as described in section 2.12.2. The protein staining was performed to compare between wild type AlaDH and its mutants as exhibited in Figure 3.11. The purity of enzymes increased in each step. The enzymes from final step, Blue Sepharose column, had purity higher than 90%. Thus, these purified enzymes were suitable for characterization of their properties. The mobility of all mutant enzymes was similar to their wild type with estimated molecular weight of 40,000 Dalton.

3.10 Characterization of AlaDH wild type and mutants

3.10.1 Effect of temperature on AlaDH activity

The optimum temperature of AlaDH wild type and mutants was assayed by the method described in section 2.13.1 at various temperatures (30°C - 65°C). The highest temperature observed from each source of enzyme was set as 100% relative activity. AlaDH wild type showed the highest activity at 50°C, whereas the optimum temperature of all mutants was 52.5°C (Figure 3.12).

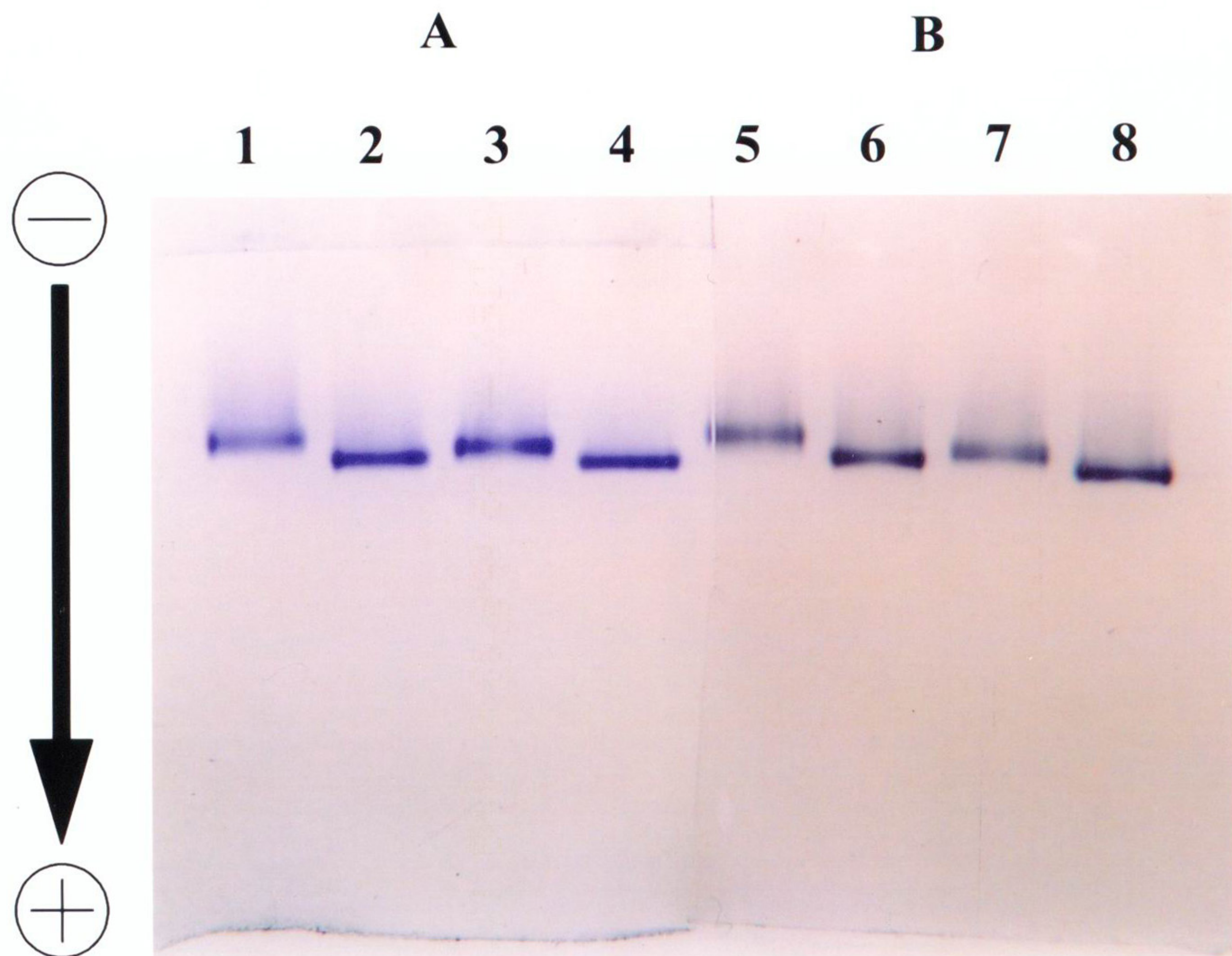


Figure 3.10 Non-denaturing PAGE of alanine dehydrogenases from Blue Sepharose column

A. Protein staining

Lane 1	wild type
Lane 2	L101E
Lane 3	A231E
Lane 4	L101E/A231E

B. Activity staining

Lane 5	wild type
Lane 6	L101E
Lane 7	A231E
Lane 8	L101E/A231E

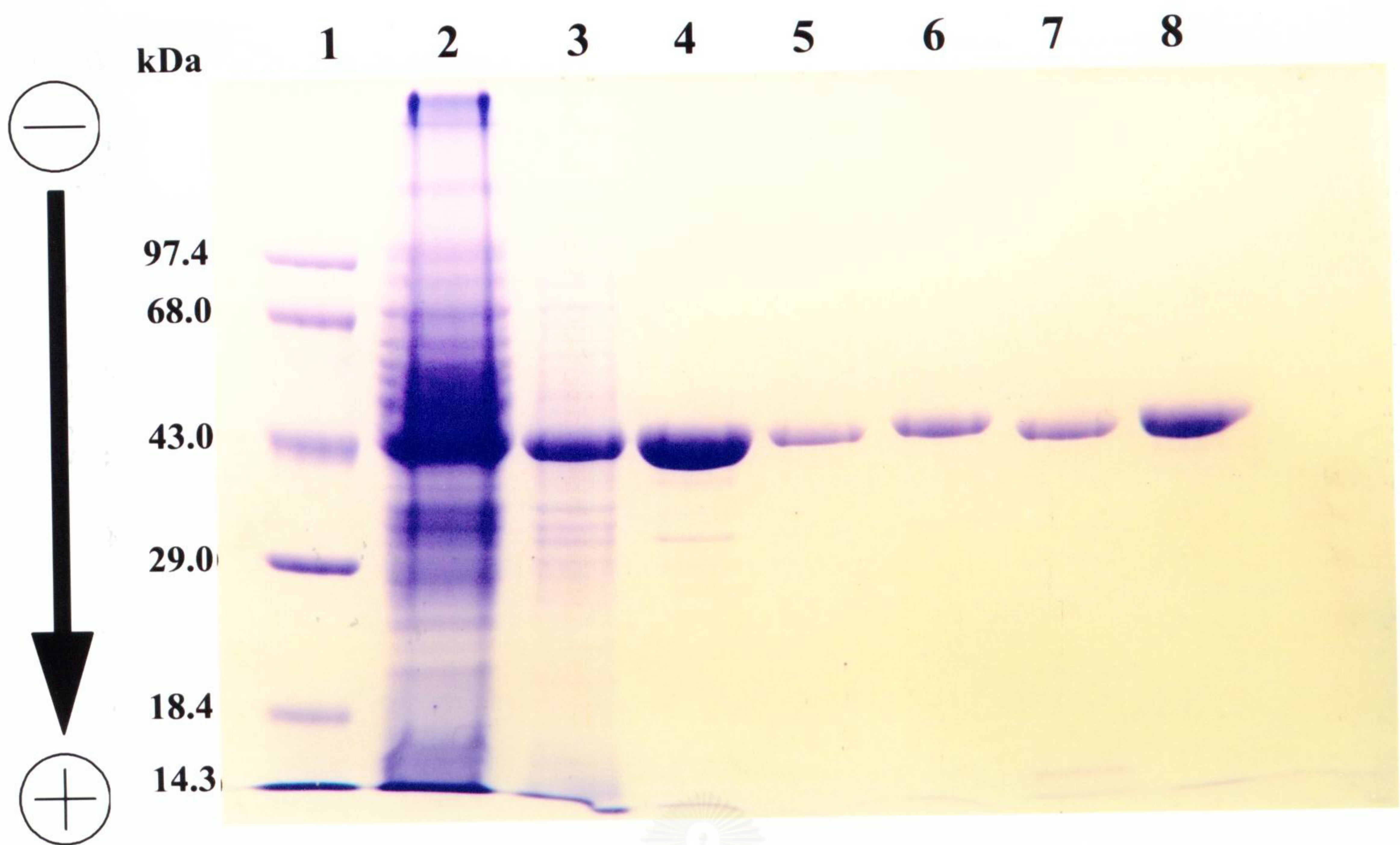


Figure 3.11 SDS-polyacrylamide gel electrophoresis of alanine dehydrogenase

- Lane 1 low molecular weight marker protein
- Lane 2 crude enzyme/ wild type
- Lane 3 20-40% ammonium sulfate precipitation/ wild type
- Lane 4 DEAE-Toyopearl column/ wild type
- Lane 5 Blue Sepharose column/ wild type
- Lane 6 Blue Sepharose column/ L101E
- Lane 7 Blue Sepharose column/ A231E
- Lane 8 Blue Sepharose column/ L101E/A231E

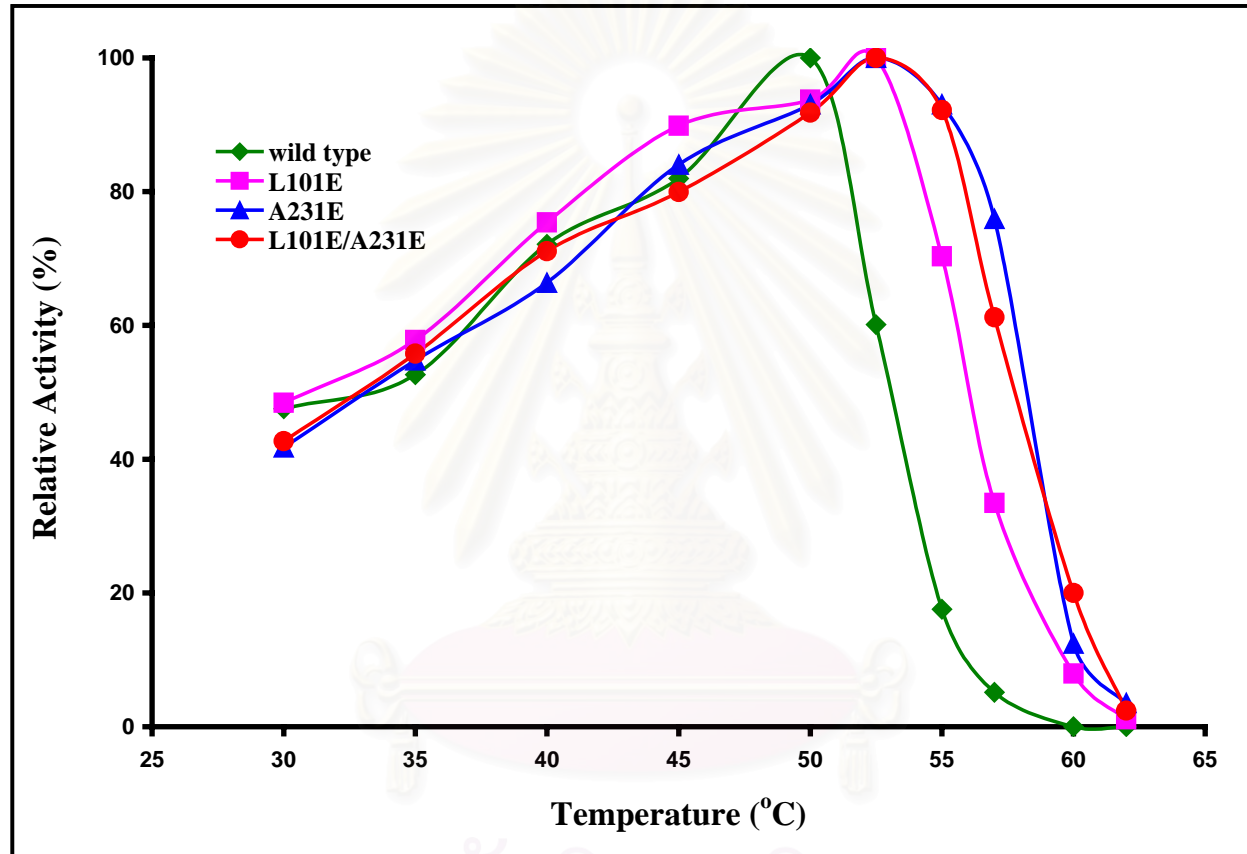


Figure 3.12 Effect of temperature on AlaDH activity

(◆) wild type; (■) L101E; (▲) A231E; (●) L101E/A231E

3.10.2 Effect of pH on AlaDH activity

The optimum pH of enzyme was performed as the method described in section 2.13.2. The pH of each reaction mixture was measured at room temperature after the reaction. All AlaDHs showed maximum activity in the pH range of 10.4 - 10.6 as shown in Figure 3.13.

3.10.3 Effect of temperature on AlaDH stability

Thermostability of AlaDHs was determined as described in section 2.13.3. The enzyme activity of non-preincubated enzyme was defined as 100% relative activity. The result is shown in Figure 3.14. The wild type enzyme retained almost its full activity up to 50°C. When incubating temperatures were higher than 50°C, the enzyme activities rapidly declined. Single mutant enzyme from L101E and A231E could retain their full activities up to 55°C whereas double mutant enzyme was stable up to 57°C. The temperature at which 50% relative activity was obtained (T_m) of wild type, L101E, A231E and L101E/A231E enzyme were 58, 60, 60 and 61°C, respectively.

3.10.4 Substrate specificity of alanine dehydrogenase

Substrate specificity of AlaDHs in the direction of oxidative deamination was investigated as mentioned in section 2.13.4. All enzymes in this test showed similar result as illustrated in Table 3.9. The highest activity observed with L-alanine as substrate was defined as 100% relative activity. No activity was observed with D-alanine, D-aspartate, L-aspartate, L-phenylalanine, L-leucine, D-leucine, L-methionine, L-Threonine, L-isoleucine, D-tryptophan, L-valine, glycine, L-glutamate, L-cysteine,

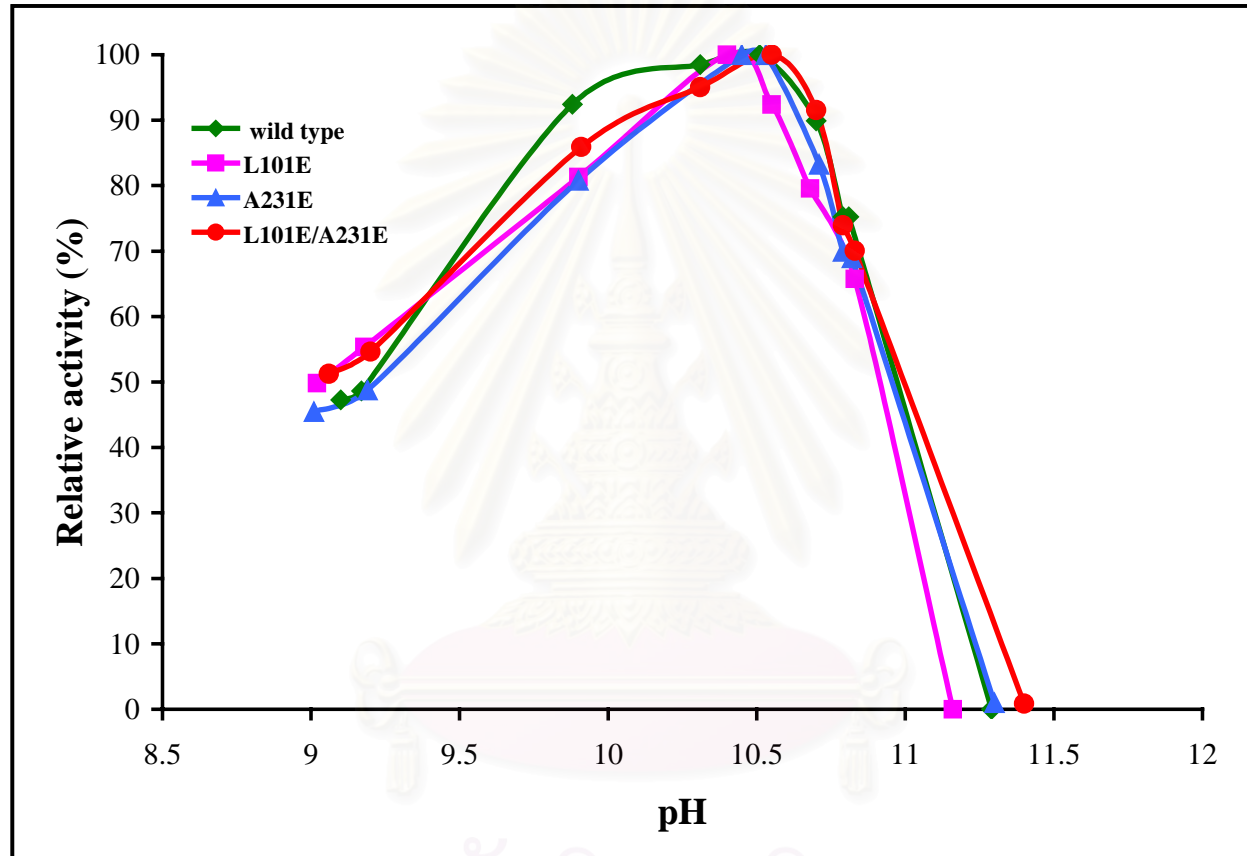


Figure 3.13 Effect of pH on AlaDH activity

(◆) wild type; (■) L101E; (▲) A231E; (●) L101E/A231E

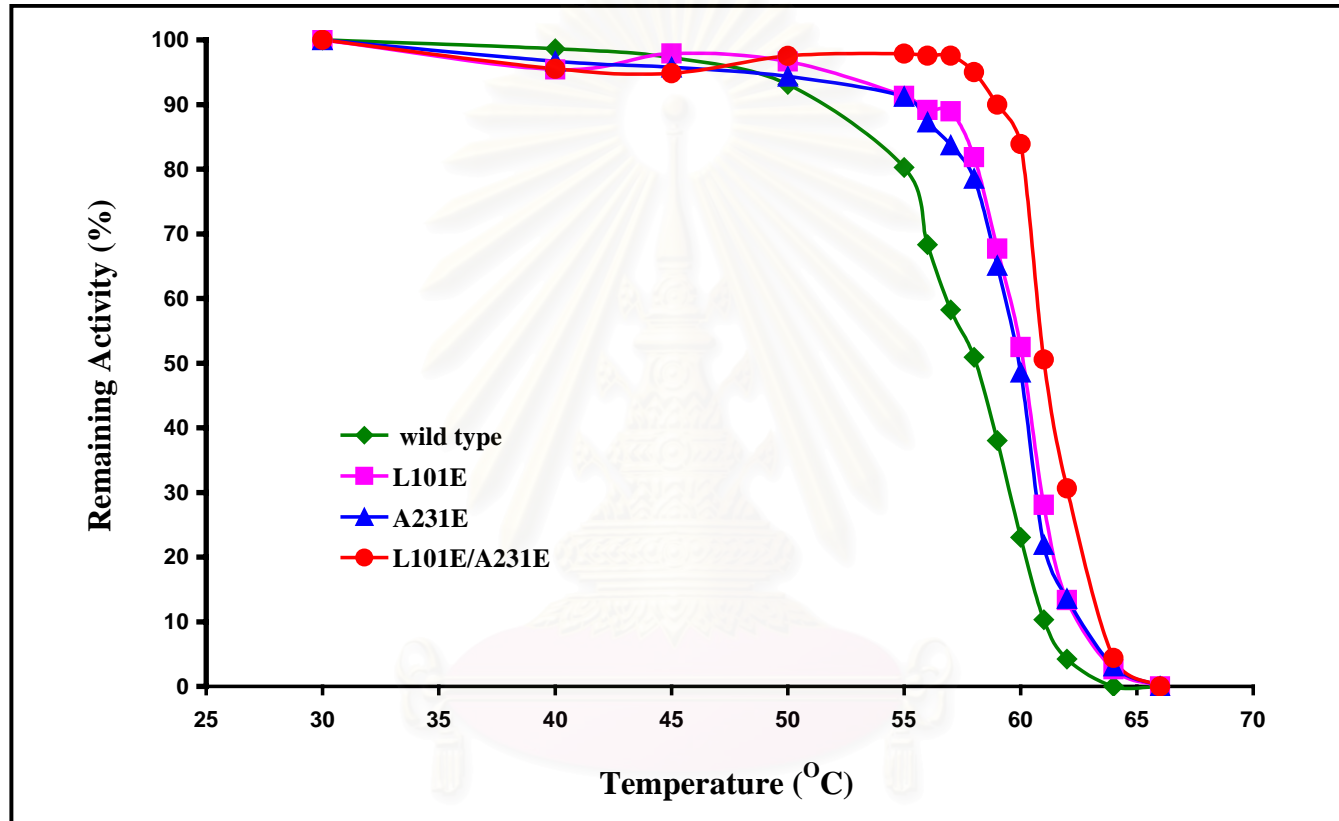


Figure 3.14 Effect of temperature of AlaDH thermostability

(◆) wild type; (■) L101E; (▲) A231E; (●) L101E/A231E

Table 3.9 Substrate specificity of AlaDHs

Substrates ^a	Relative activity ^b (%)			
	AlaDH wild type	L101E	A231E	L101E/A231E
L-alanine	100	100	100	100
L-serine	1.50	1.29	1.98	1.36
L- α -amino-butyric acid	1.89	1.92	2.67	1.89

^a Final concentration of each substrate was 20 mM. The following were inert: D-alanine, L-asparagine, D-aspartic acid, L-aspartic acid, L-cysteine, L-glutamic acid, glycine, L-isoleucine, D-leucine, L-leucine, L-lysine, L-methionine, L-phenylalanine, D-serine, L-threonine, D-tryptophan and L-valine

^b For oxidative deamination

L- asparagine, L-lysine, and D-serine, whereas L-serine and L- α -amino-*N*-butyrate gave activity in the range of 1.29 - 1.98 and 1.89 - 2.67% relative activity, respectively.

3.11 Kinetic parameter of alanine dehydrogenase

Steady state kinetic analysis was carried out to investigate the K_m values on L-alanine and NAD^+ of AlaDH wild type and mutant enzymes. First, studies for oxidative deamination were performed with L-alanine as variable substrate in the presence of several fixed concentrations of NAD^+ . The data from the experiments were then used for double reciprocal plots of initial velocities versus L-alanine concentrations. The apparent K_m values for L-alanine were calculated to be 6.41, 7.24, 6.67 and 6.67 mM for wild type, L101E, A231E and L101E/A231E enzyme, respectively as shown in Figure 1.15A and 1.16B, 1.17A and 1.18B, 1.19A and 1.20B as well as 1.21A and 1.22B. The secondary plot of the intercepts at the ordinate versus reciprocal concentrations of NAD^+ was used to calculate K_m value of NAD^+ . As shown in Figure 1.15B and 1.16A, 1.17B and 1.18A, 1.19B and 1.20A, as well as 1.21B and 1.22A, the apparent K_m values of wild type, L101E, A231E and L101E/A231E enzyme were 0.15, 0.15, 0.20 and 0.18 mM, respectively. All K_m values for L-alanine and NAD^+ are summarized in Table 3.10.

The all properties of wild type and mutants in this experiment are shown in Table 3.11.

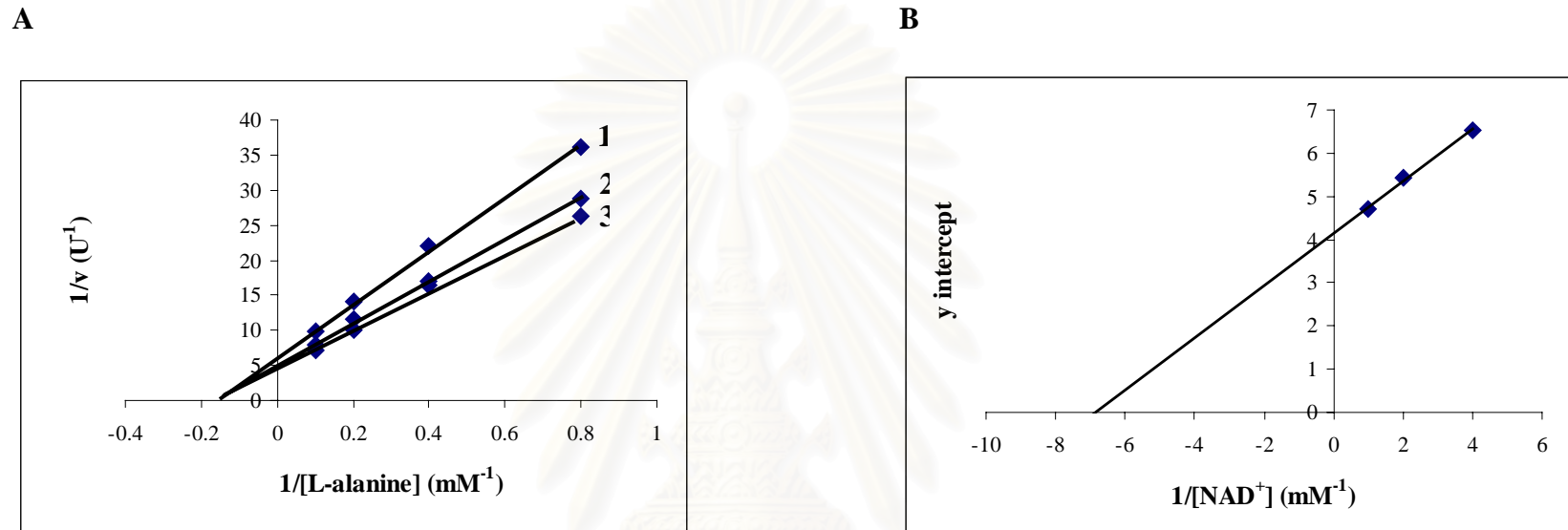


Figure 3.15 Initial velocity patterns for oxidative deamination of wild type enzyme when varied L-alanine

A. Double-reciprocal plots of initial velocities versus L-alanine concentrations at series of fixed concentrations of NAD^+

Concentrations of NAD^+ were: 0.25 mM (line 1), 0.5 mM (line 2) and 1.0 mM (line 3)

Concentrations of L-alanine were: 1.25, 2.5, 5.0 and 10.0 mM

B. Secondary plots of y intercept versus reciprocal concentrations of NAD^+

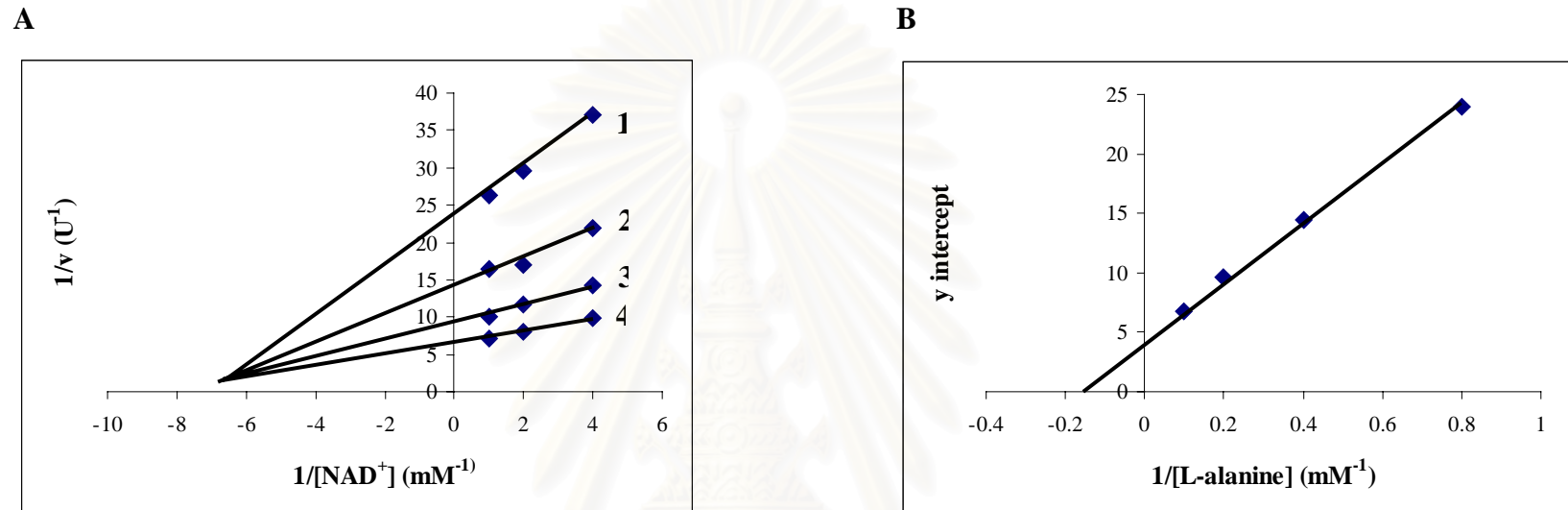


Figure 3.16 Initial velocity patterns for oxidative deamination of wild type enzyme when varied NAD^+

A. Double-reciprocal plots of initial velocities versus NAD^+ concentrations at series of fixed concentrations of L-alanine

Concentrations of L-alanine were: 1.25 mM (line 1), 2.5 mM (line 2), 5.0 mM (line 3) and 10.0 mM (line 4)

Concentrations of NAD^+ were: 0.25, 0.5 and 1.0 mM

B. Secondary plots of y intercept versus reciprocal concentrations of L-alanine

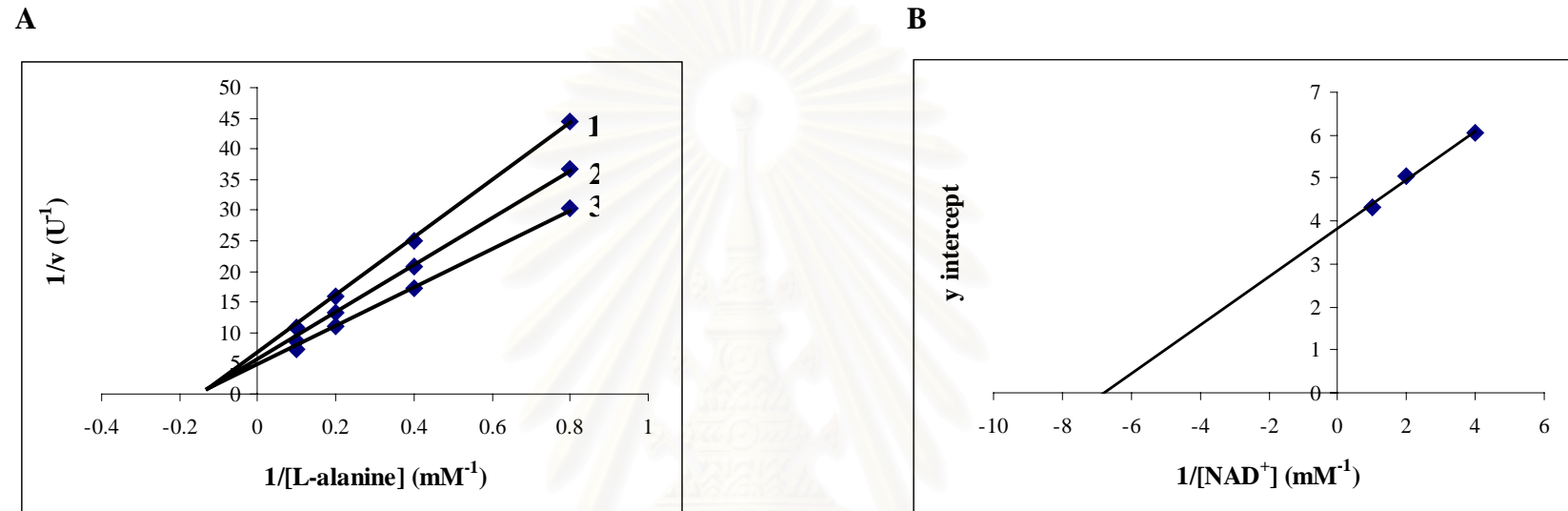


Figure 3.17 Initial velocity patterns for oxidative deamination of L101E enzyme when varied L-alanine

A. Double-reciprocal plots of initial velocities versus L-alanine concentrations at series of fixed concentration of NAD⁺

Concentrations of NAD⁺ were: 0.25 mM (line 1), 0.5 mM (line 2) and 1.0 mM (line 3)

Concentrations of L-alanine were: 1.25, 2.5, 5.0 and 10.0 mM

B. Secondary plots of y intercept versus reciprocal concentrations of NAD⁺

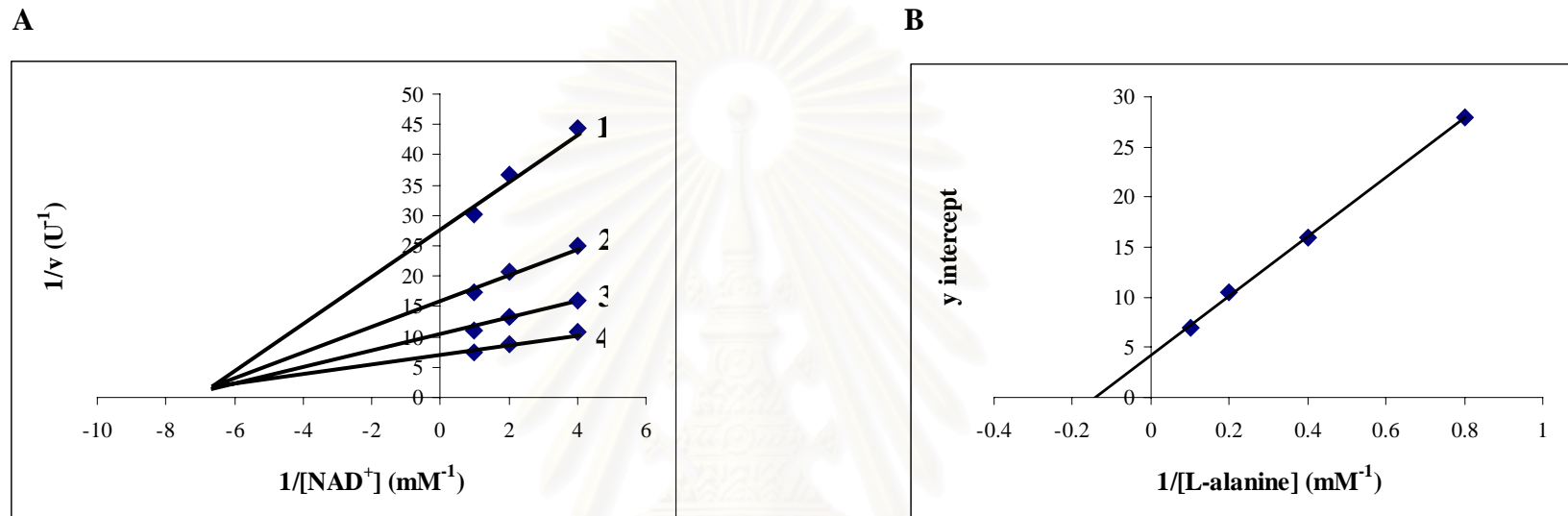


Figure 3.18 Initial velocity patterns for oxidative deamination of L101E enzyme when varied NAD^+

A. Double-reciprocal plots of initial velocities versus NAD^+ concentration at series of fixed concentration of L-alanine

Concentrations of L-alanine were: 1.25 mM (line 1), 2.5 mM (line 2), 5.0 mM (line 3) and 10.0 mM (line 4)

Concentrations of NAD^+ were: 0.25, 0.5 and 1.0 mM

B. Secondary plots of y intercept versus reciprocal concentrations of L-alanine

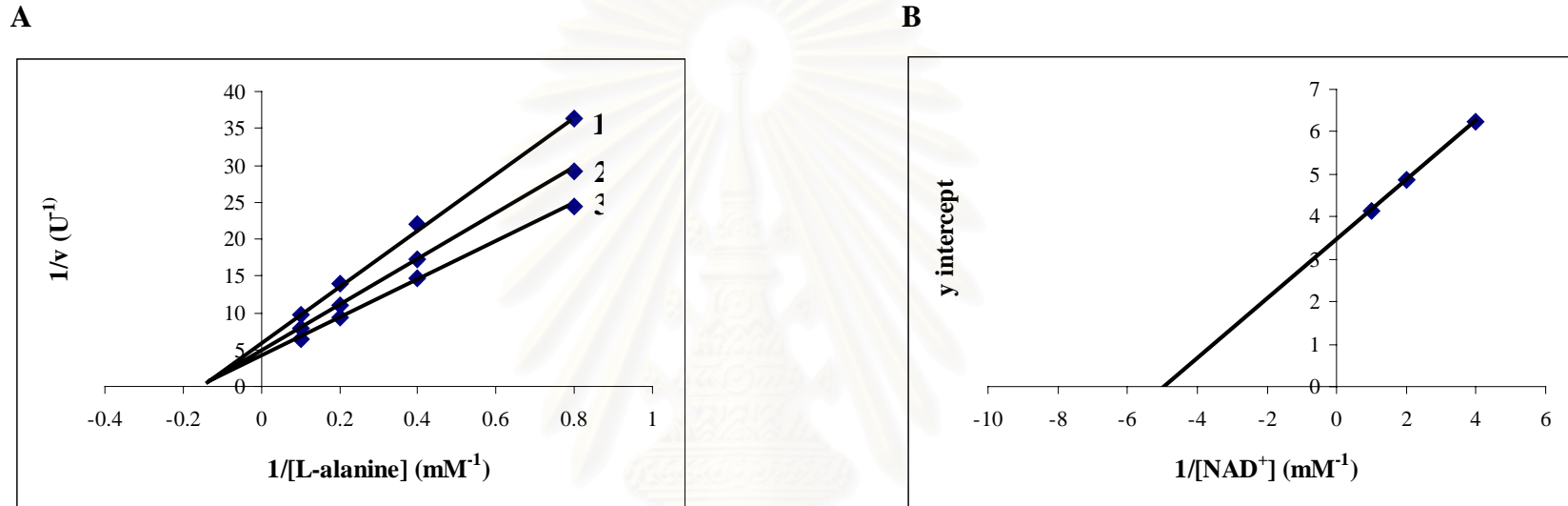


Figure 3.19 Initial velocity patterns for oxidative deamination of A231E enzyme when varied L-alanine

A. Double-reciprocal plots of initial velocities versus L-alanine concentrations at series of fixed concentration of NAD^+

Concentrations of NAD^+ were: 0.25 mM (line 1), 0.5 mM (line 2) and 1.0 mM (line 3)

Concentrations of L-alanine were: 1.25, 2.5, 5.0 and 10.0 mM

B. Secondary plots of y intercept versus reciprocal concentrations of NAD^+

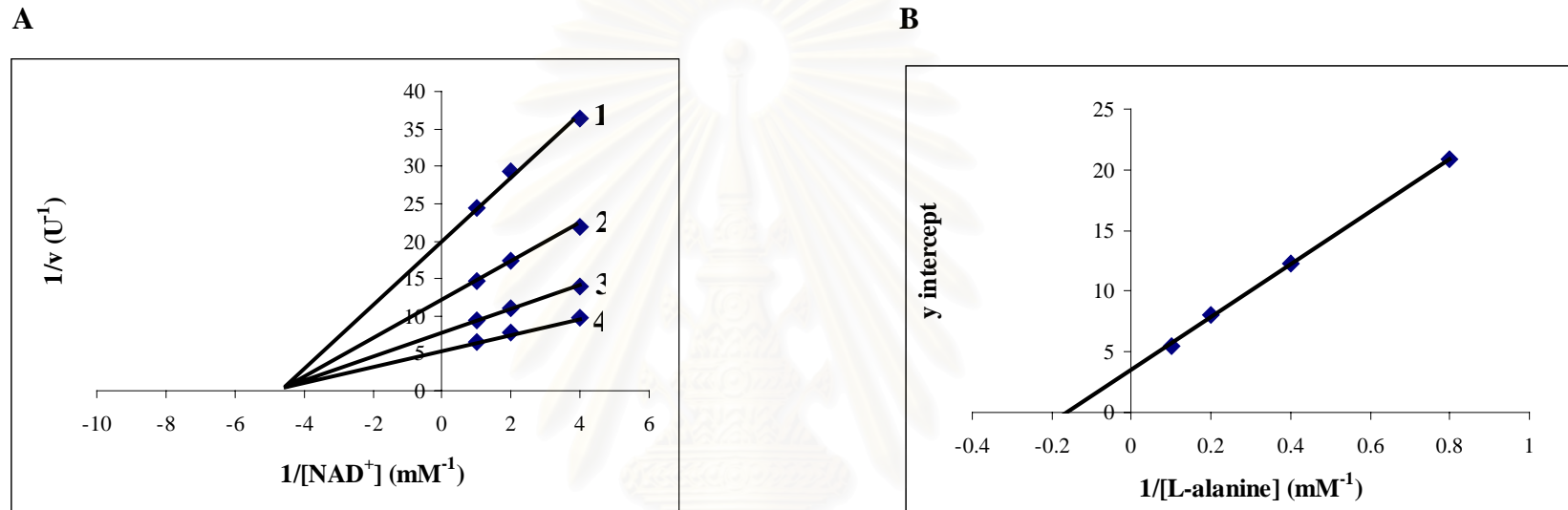


Figure 3.20 Initial velocity patterns for oxidative deamination of A231E enzyme when varied NAD^+

A. Double-reciprocal plots of initial velocities versus NAD^+ concentrations at series of fixed concentration of L-alanine
 Concentrations of L-alanine were: 1.25 mM (line 1), 2.5 mM (line 2), 5.0 mM (line 3) and 10.0 mM (line 4)

Concentrations of NAD^+ were: 0.25, 0.5 and 1.0 mM

B. Secondary plots of y intercept versus reciprocal concentrations of L-alanine

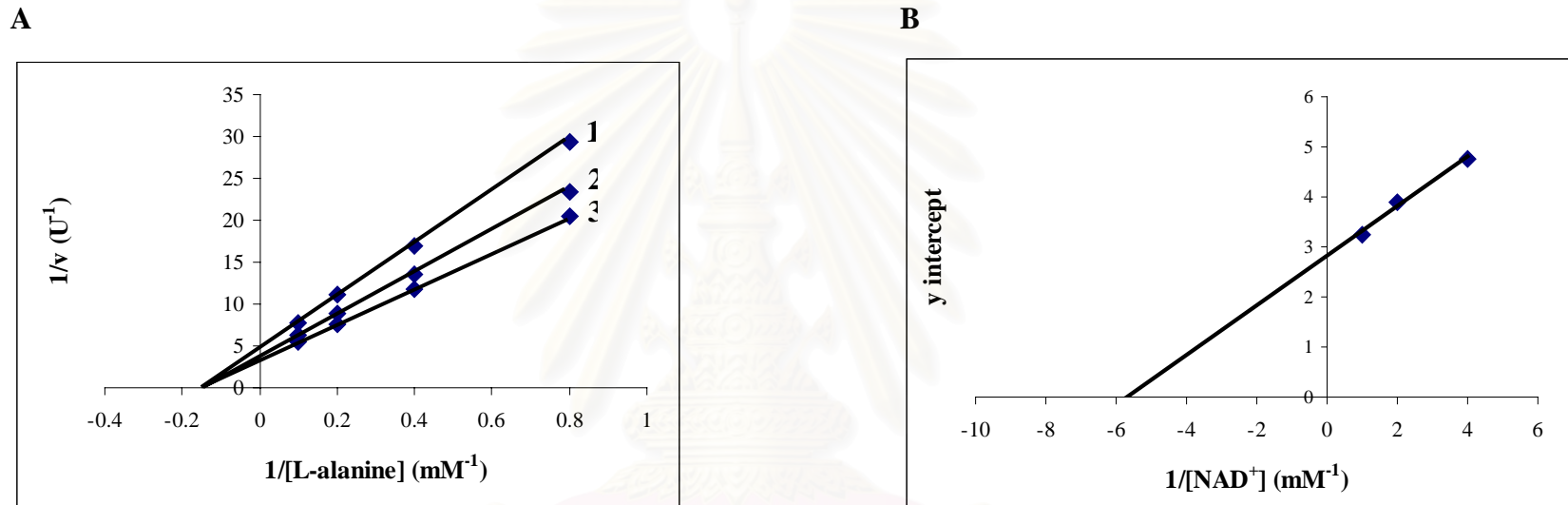


Figure 3.21 Initial velocity patterns for oxidative deamination of L101/A231E enzyme when varied L-alanine

A. Double-reciprocal plots of initial velocities versus L-alanine concentrations at series of fixed concentration of NAD^+

Concentrations of NAD^+ were: 0.25 mM (line 1), 0.5 mM (line 2) and 1.0 mM (line 3)

Concentrations of L-alanine were: 1.25, 2.5, 5.0 and 10.0 mM

B. Secondary plots of y intercept versus reciprocal concentrations of NAD^+

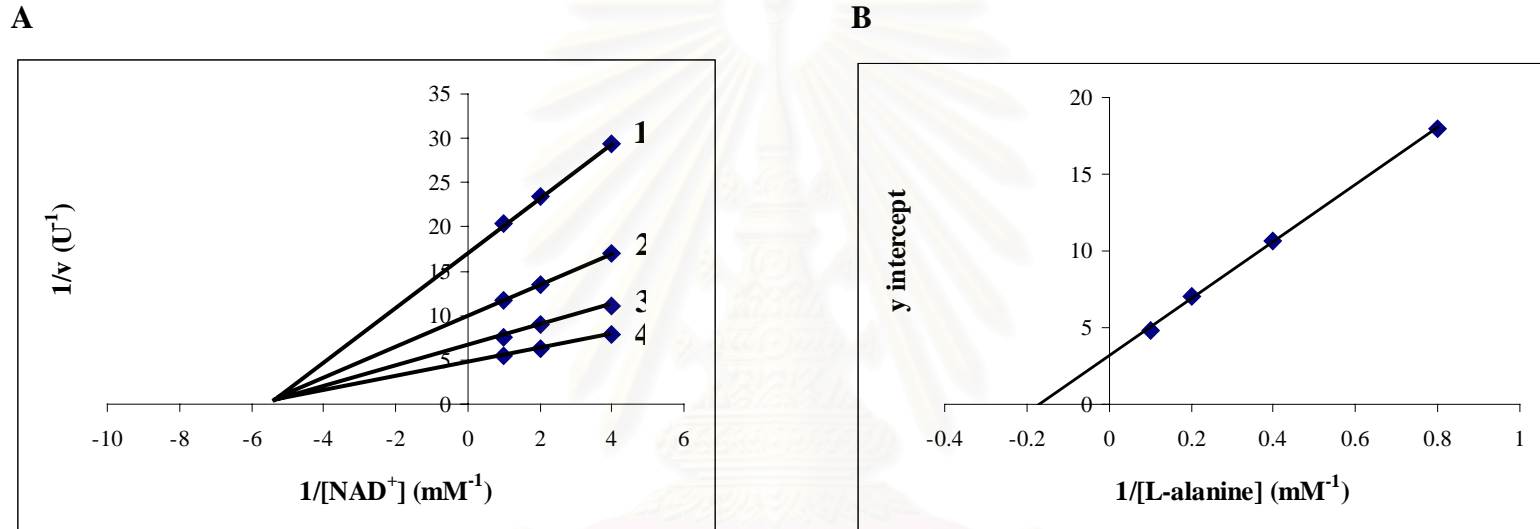


Figure 3.22 Initial velocity patterns for oxidative deamination of L101E/A231E enzyme when varied NAD^+

A. Double-reciprocal plots of initial velocities versus NAD^+ concentrations at series of fixed concentration of L-alanine
 Concentrations of L-alanine were: 1.25 mM (line 1), 2.5 mM (line 2), 5.0 mM (line 3) and 10.0 mM (line 4)

Concentrations of NAD^+ were: 0.25, 0.5 and 1.0 mM

B. Secondary plots of y intercept versus reciprocal concentrations of L-alanine

Table 3.10 The apparent K_m values of AlaDHs

K_m (mM)	wild type	L101E	A231E	L101E/A231E
L-alanine	6.41	7.27	6.67	6.67
NAD ⁺	0.15	0.15	0.20	0.18

สถาบันวิทยบริการ
จุฬาลงกรณ์มหาวิทยาลัย

Table 3.11 Properties of AlaDHs

Properties	wild type	L101E	A231E	L101E/A231E
Thermostability (°C)	58	60	60	61
Optimum temperature (°C)	50.0	52.5	52.5	52.5
Optimum pH	10.51	10.57	10.53	10.55
Substrate specificity (% relative activity)				
L-serine	1.50	1.29	1.98	1.36
L-α-amino-butyric acid	1.89	1.92	2.67	1.89
K_m (mM)				
L-alanine	6.41	7.27	6.67	6.67
NAD⁺	0.15	0.15	0.20	0.18

CHAPTER IV

DISCUSSION

Amino acid dehydrogenases play important roles in all life. In bacteria, amino acid can be metabolized as the energy sources by these enzymes. They have the advantages of producing the amino group in of free ammonium form and other important metabolize molecules such as pyruvate and α -ketoglutarate. Several amino acid dehydrogenases were used as biocatalysts in industrial and clinical proposes.

To extend the use of amino acid dehydrogenase, a more abundant and cheaper supply of stable amino acid dehydrogenase was required. The thermostable amino acid dehydrogenases have practical advantages in amino acid production and analytical uses compared with their thermolabile counterparts from mesophiles. There are 2 possible ways to obtain the thermostable enzymes: 1) to isolate directly from a variety of thermophiles and 2) to improve the property of thermolabiles through genetic engineering based on DNA sequence and structure of their thermostable counterparts.

Alanine dehydrogenase is used for producing L-alanine and pyruvate which are of industrial importance. *Aeromonas hydrophila* isolated from soil in Bangkok was found to have high alanine dehydrogenase activity (Phungsangthum, 1997). Moreover, the *alaDH* gene was cloned and expressed in *E. coli* (Poomipark, 2000). Although catalytic properties of *A. hydrophila* enzyme are suitable for application such as L-alanine production or clinical diagnosis, its thermostability is not so high enough. Thus, improvement of AlaDH was performed in this work.

4.1 Rational design and selection of amino acid residues

To improve thermostability of protein, rational design principle is to compare amino acid sequence and three-dimensional structure of protein counterparts from mesophilic and (hyper) thermophilic organisms for identification of residues related to thermostability. In this experiment, amino acid sequence and protein structure of AlaDH from *Aeromonas hydrophila*, a mesophilic organism, was compared with thermophilic AlaDH from *Bacillus stearothermophilus*. However, reports on structure are not available. Thus, computational methods play a crucial role in this experiment. Comparative of protein modeling is of great assistance during the rational design for mutagenesis.

In this part, structures of both AlaDHs were constructed from amino acid sequence using SWISS-MODEL. X-ray crystallography of AlaDH from *Phormidium lapideum* was used as template for construction of model structures. Characteristics of model structure depend on alignment of protein with template. Schwede *et al.*, (2000) compared protein structures generated by SWISS-MODEL with their 3D-structure from X-ray crystallography or nuclear magnetic resonance (NMR). They found that 79% of the sequences sharing 50 - 59% identity with their templates yielded a SWISS-MODEL deviating by less than 3 Å from their control structure. Since amino acid sequence alignment of both AlaDHs showed over 50% identity to template (53.10% in *A. hydrophila* and 54.03% in *B. stearothermophilus*), their model structures were reliable. The three-dimensional structures of AlaDHs exhibited high similarity in protein core when they were compared with template. Furthermore, formation of α -helix and β -sheet were displayed in the same location. At different amino acid sequence position, possible side chain conformations were selected from a backbone dependent rotamer library,

which has been constructed carefully taking into account the quality of the source structure.

Although, both model structures of AlaDH were similar, their thermostability was different. Galkin *et al.*, (1999) exhibited that salt bridge in protein has an important role in thermostability of AlaDH. Moreover, Lebbink *et al.*, (1998) showed that cooperative charge-charge interactions in an ion-pair network are important in glutamate dehydrogenase. Hence, electrostatic interaction in both models of AlaDH was calculated.

Amino acid residues, at which difference in electrostatic interaction were found, were considered for site-directed mutagenesis. Performance of two residues mutation per one interaction should be avoided. Moreover, mutated residues must not locate in an active site of the enzyme. Five residues expected to form electrostatic interaction; G38E, L58R, L101E, P168R and A231E were calculated for distance between opposite side-chain. L58R, L101E and A231E could form salt bridge and/or long-range pattern of electrostatic interaction while G38E and P168R showed only long-range pattern.

4.2 Site-directed mutagenesis

The QuikChange site-directed mutagenesis based on PCR strategy is used for construction *alaDH* mutant gene. Both of mutagenic primers contain the desired mutation and anneal to the same sequence on opposite strands of the plasmid. Instruction manual of this method recommended the small amount of starting DNA template, the high fidelity of the *Pfu* Turbo DNA polymerase, and low numbers of thermal cycles for high mutation efficiency and decreased potential for generating random mutagenesis during the reaction. Thus, PCR product could not be visualized in agarose electrophoresis. The reaction was treated with *DpnI* endonuclease which is used to digest the methylated or

hemimethylate DNA template and to select for mutation-containing synthesized DNA. DNA isolated from most *E. coli* strains except strains JM110 and SCS110 are dam⁻ methylated and therefore susceptible to *DpnI* digestion. Consequently, the nick plasmid was transformed into *E. coli* XL1-Blue supercompetent (from mutagenesis kit). In this experiment, the mutagenesis efficiency, expected by number of blue colony appeared in the transformation of pWhitescript control mutagenesis reaction, was in the range of 85 - 89%. The mutagenesis efficiency of control was used to anticipate the efficiency of AlaDH mutagenesis. Wang and Malcolm (1999) used QuikChange site-directed mutagenesis for multiple mutations. They obtained a few number of mutants, about 50-80 clones, because of low amount of DNA used in the experiment. The low transformation efficiency was improved by Shubeita and Rohwer (2000) by adding *Tag* DNA ligase into PCR reaction step to join nick plasmid DNA.

4.3 Enzyme assay and thermostability of crude enzyme

The AlaDH activities of mutant enzymes in *E. coli* XL1-Blue were markedly lowers than activity of wild type *E. coli* JM109 (Table 3.2 – 3.3). This result is caused by property variation in both stains such as polylytic deficiency and solubilization of recombinant protein. *E. coli* XL1-Blue is mainly used for transformation and propagation of plasmid while *E. coli* JM109 is used for gene expression. For example, cloning and expression of gene encoding a protein obtained from earthworm secretion used *E. coli* XL1-Blue as host cell for cDNA library construction and used *E. coli* JM109 for expression (Liu *et al.*, 1997). Furthermore, SIGMA-ALDRICH Company recommended *E. coli* JM109 as compatible host of plasmid pUC 18 for high level expression.

Therefore, mutant plasmids were extracted from *E. coli* XL1-Blue and transformed into *E. coli* JM109 for higher expression. Specific activity of crude AlaDH from G38E, L101E, P168R and A231E were close to that of wild type while specific activity from L58R was lower (Table 3.4 – 3.5). Since Leu 58 locates on domain I which contains substrate binding site and most of its neighbor residues such as Leu 51, Ile 57, Ala 59 and Ala 61 are hydrophobic, the formation of electrostatic interaction in this position might destabilize the correct folding of protein that leads to the reduction of activity.

The thermostability of the AlaDH was determined from crude enzyme. A231E and L101E showed higher stability than wild type. Increasing thermostability should result from electrostatic interaction of the constructed Glu residue which could stabilize protein structure. Even though G38E was expected to or electrostatic interaction, G38E showed similar thermostability to its wild type. This can be explained that the interaction between Glu 38 and Lys 7 were long-length which is the weakest electrostatic interaction so it could not promote thermostability. Correspondingly, Dao-pin *et al.*, (1991) determined the contribution of long-range electrostatic interaction which involved in the stability of bacteriophage T4 lysozyme protein and found that the thermostability of all 13 variant proteins were fairly similar with wild type. The contrary results were observed with L58R and P168R. Both mutant enzymes showed less stable than wild type although they could form electrostatic interaction in molecular model. In the L58R, substitution of arginine into hydrophobic region altered overall structure of the enzyme which affected both enzyme thermostability and activity. For P168R, the constructed Arg 168 could form electrostatic interaction with Asp 193 which is closed to hydrophobic bounded turn

at interface of dimer so Arg 168 might decrease dimer formation of AlaDH subunit at high temperature.

4.4 Purification of alanine dehydrogenase

In this experiment, AlaDH from wild type and three mutants (L101E, A231E and L101E/A231E) were purified for comparison of their properties. The purification consisted of 3 steps: 20 - 40% ammonium sulfate precipitation, DEAE-Toyoperal and Blue Sepharose column chromatography. All enzymes showed similar purification pattern with about 24 - 40% yield, 3 - 4 purification fold with specific activity 18 - 32 unit/mg protein and total activity 14×10^3 - 17×10^3 unit/17 g of cell wet weight. Phungsangthum (1997) purified AlaDH from *Aeromonas hydrophila* using 5 steps: 30 - 40% ammonium sulfate precipitation, DEAE-cellulose, Hydroxyapatite column, Blue Sepharose column and Sephadex G-200 column chromatography. Overall purification achieved from 30 g wet weight was 100 fold, 18% yield with total activity 168.3 units and specific activity 23.0 unit/mg protein. Since, AlaDH production in *E. coli* JM109 clones which contained *lac* promoter on pUC18 vector could be induced by IPTG, AlaDH became the major protein in crude extract. Hence, the purification of clone enzymes was easier than the enzyme from original strain.

Ammonium sulfate was the salt of choice and used in this work because it combined many useful features such as salting out effect, pH versatility, high solubility, low heat of solution and low price (Bollag *et al.*, 1996). In this experiment, 20 - 40% ammonium sulfate was used whereas purification from *A. hydrophila* used 30 - 40% ammonium sulfate which might be due to different surrounding proteins in the crude extracts. This step is very effective for impurity removal. About half of proteins were

removed but about one thirds of the enzyme activity was lost. The lost of enzyme activity might be caused by the removal of some factors important for stabilizing the enzyme activity.

DEAE-Toyopearl is an anion exchanger, widely used in the purification of amino acid dehydrogenase. Its popularity stems from the possibility of high resolving power, versatility, reproducibility and ease performance. This column contributed greatly to the purification procedures, with less loss of AlaDH activity compared to the amount of protein removed. Subsequently, the enzyme was purified by Blue Sepharose chromatography which is affinity chromatography for selection of NAD^+ -dependent enzymes. Blue Sepharose column contains dye (Cibacron Blue F3G-A) as a ligand which covalently attached to agarose. The enzyme can bind with Cibacron Blue because the dye has similar structure with NAD^+ and NAD(P)^+ . AlaDHs were purified by Blue Sepharose column with its high effectiveness. The purity of purified enzymes was higher than 90% which was acceptable for enzyme characterization.

When using non-denaturing polyacrylamide gel electrophoresis, the relative mobility of native proteins from wild type was less than all mutant enzymes because uncharged residues were substituted with negatively charged residue (Glu) in mutants. However, L101E moved faster than A231E though one residue was substituted in both mutants. Thus, Glu in 101 might promote charge better than in A231E. L101E/A231E had the highest mobility with two Glu residues substituted. However, SDS-PAGE showed no difference in mobility among wild type and mutants who suggests that the change in amino acid residue(s) as performed did not affect molecular size and shape of the enzyme AlaDH.

4.5 Characterization of AlaDH wild type and mutant enzymes

4.5.1 Effect of temperature on AlaDH activity and thermostability

The optimum temperature of AlaDH wild type from *E. coli* JM109 for oxidative deamination was 50°C whereas those of all mutants shifted to 52.5°C. Temperature affects the rate of an enzyme-catalyzed reaction by increasing the thermal energy of the substrate and enzyme molecules. Moreover, increasing thermal energy of molecules which make up the protein structure will increase the chance of breaking the multiple weak noncovalent interactions holding the three-dimensional structure (Hames, 1998). AlaDH lost absolute functions at 60°C for wild type and 62.5°C for all mutants. Difference of optimum temperature between wild type and mutants should be the result of adding electrostatic interactions on molecule of mutants. This evidence was confirmed in an engineering of electrostatic interactions to improve thermostability of malate dehydrogenase (Trejo *et al.*, 2001). The constructed salt bridge could not enhance stability but it resulted in a 15°C shift in optimum temperature.

The temperature at the mid point of process is known as the protein's melting temperature T_m , in analogy with the melting of a solid (Voet, 1995). T_m value is the best descriptor and widely used as an appropriate represent for thermostability of proteins (Kumn *et al.*, 2000). The T_m of AlaDH wild type was 58°C while single mutated enzymes (L101E and A231E) were 60°C and T_m value of double mutated enzyme (L101E/A231E) was 3°C higher than wild type. Improvement of thermostability of glutamate dehydrogenase by induced salt bridge also raised T_m by 2.5 °C (Vetriani *et al.*, 1998). Ala 231 of *A. hydrophila* AlaDH is coincident with Glu 230 *Phormidium lapideum* AlaDH (Figure 4.1) which locates in hydrophilic part at interface center of dimer. Thus, increasing of hydrophilic character in the interface region of dimmer was likely to be a

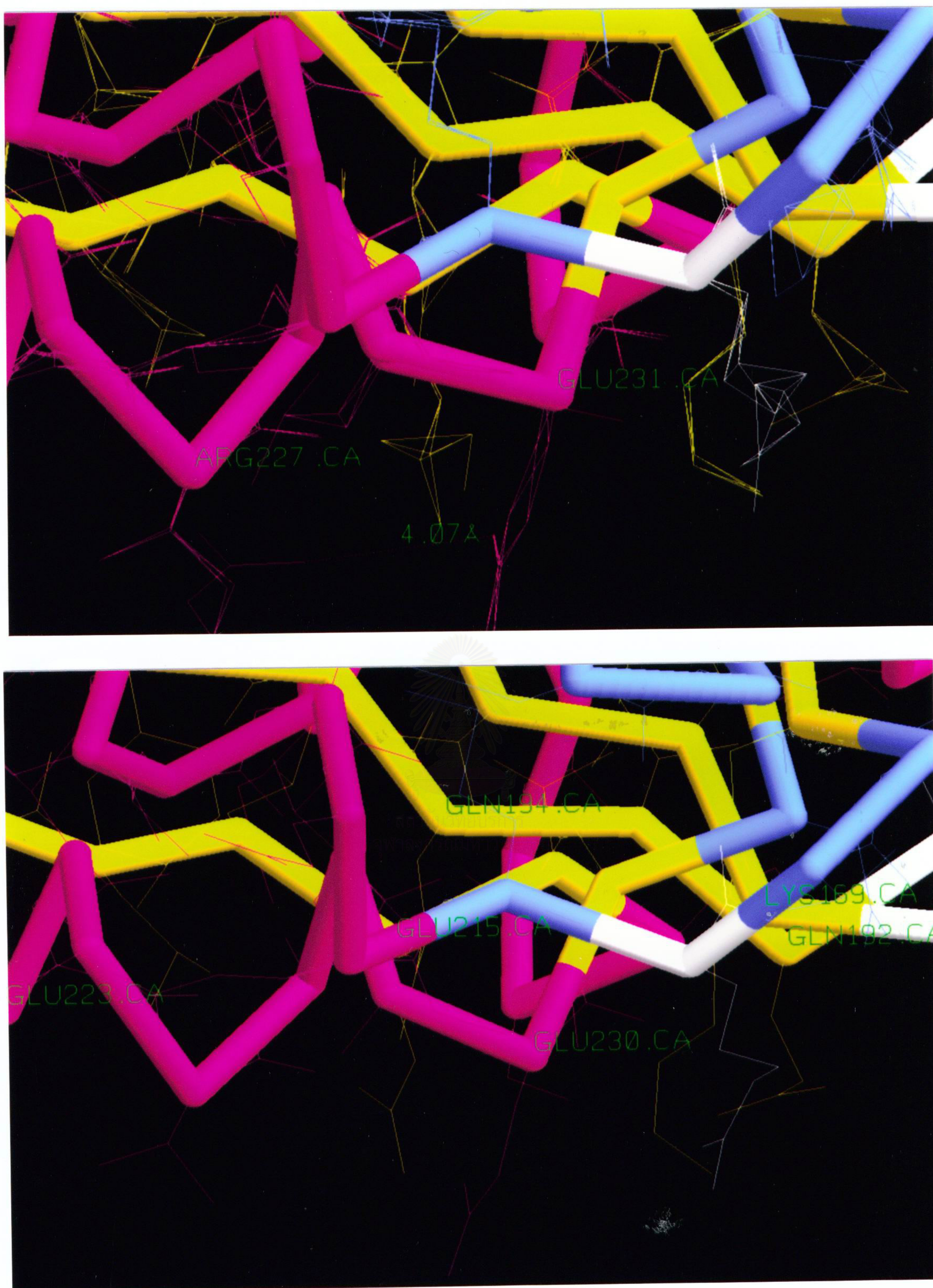


Figure 4.1 Glu 231 of *A. hydrophila* (upper) coincided with Glu 230 of *P. lapideum* (lower)

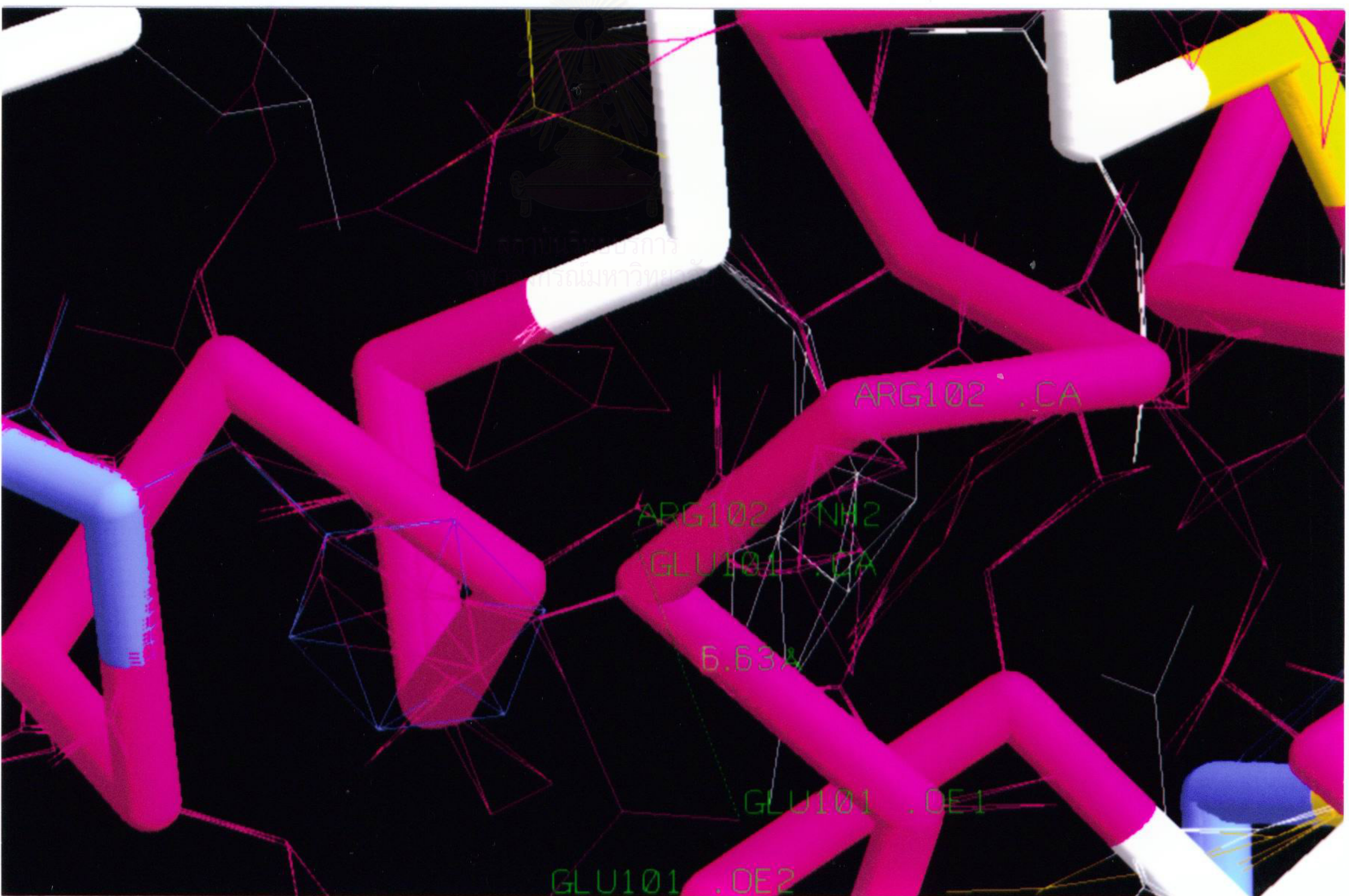
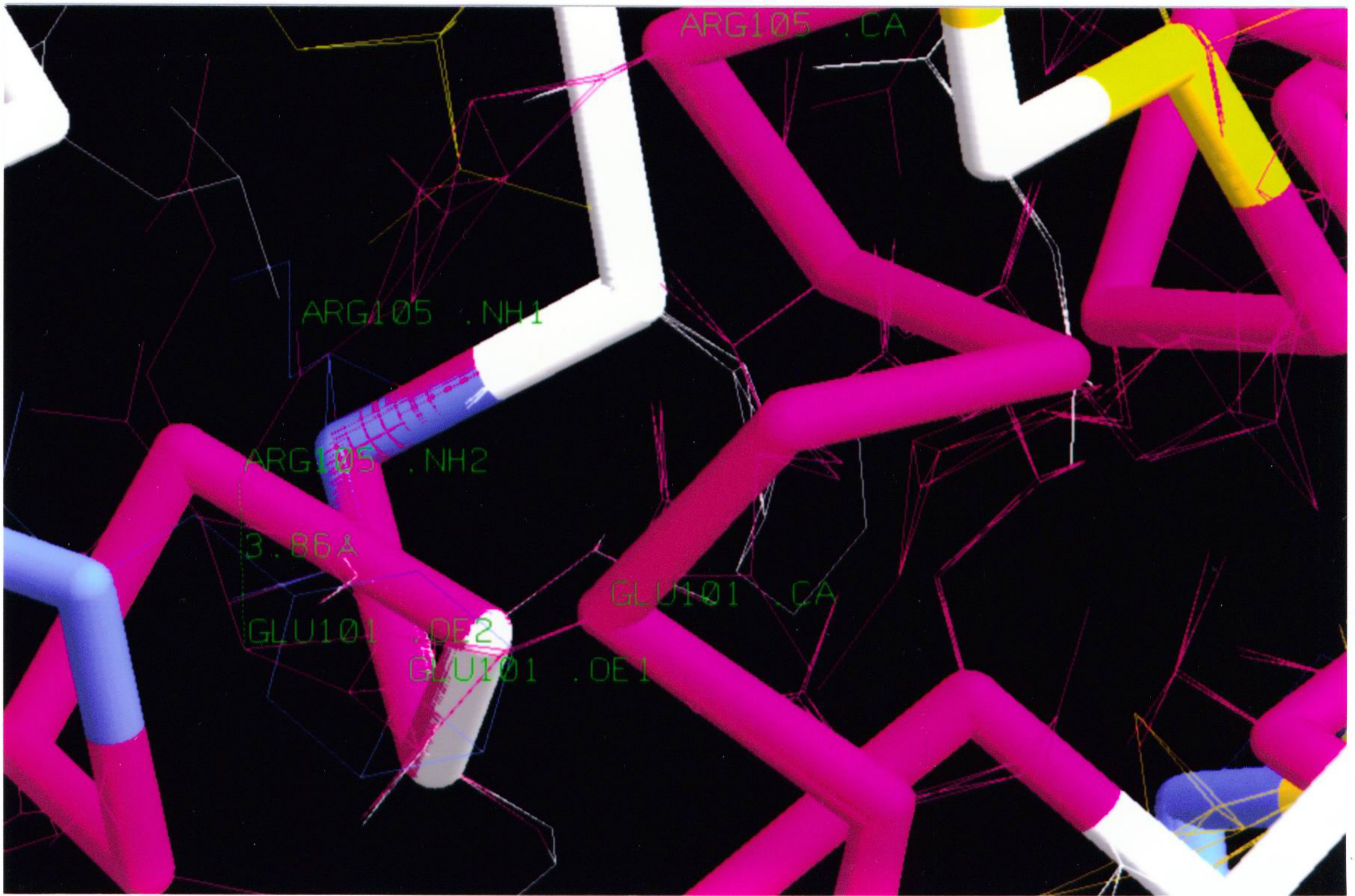


Figure 4.2 Glu 101 and Arg 105 formation in *A. hydrophila* AlaDH (upper) and Glu 101 and Arg 102 formation in *B. stearrowthermophilus* AlaDH (lower)

factor help in promoting the enzyme thermostability. By the way, substituted Glu 101 residue might form an interaction with Arg 105 (Figure 4.2) whereas Glu 101 in *B. stearothermophilus* interacts with Arg 102 (Figure 4.2) So, formation of electrostatic interaction at these two residues is important for thermostability of AlaDH.

4.5.2 Effect of pH on AlaDH activity

All tested AlaDHs showed similar optimum pH for oxidative determination, approximately 10.5, with the AlaDH from *A. hydrophila* (Phungsangthum, 1997). This suggested that all point mutations did not affect the ionization of amino acid residues in an active site.

4.5.3 Substrate specificity of AlaDH

Substrate specificity of AlaDH wild type from *E. coli* JM109 and mutants was not different from the property of AlaDH extracted from *A. hydrophila* (Phungsangthum, 1997). Therefore, this experiment confirmed that the active site of all mutants was not altered by mutation.

4.5.4 Kinetic studies of AlaDH

The K_m for alanine of wild type and mutant enzymes exhibited no significant difference. On the other hand, K_m for NAD^+ of A231E and L101E/A231E differed slightly from the wild type. This appearance should not be the effect of structure alteration. Thus, replacement of Leu 101 and Ala 231 with Glu can form electrostatic interaction which contributed to thermostability without change in catalytic activity of AlaDH. In contrast, improvement of hydrophobic interaction in alanine racemase could

elevate thermostability with a markedly lower K_m value than wild type (Yodoigawa *et al.*, 2003)

In the case of enzyme engineering, several kinds of interactions were suggested to contribute in enhancement of thermostability. The comparison of structure and sequence of homologous protein from thermophilic and mesophilic organisms can provide the important clues to stabilize protein. Electrostatic interaction is one factor involved in thermostability between protein counterparts. In this work, thermostability of AlaDH from *Aeromonas hydrophila* was improved through site directed mutagenesis based on different electrostatic interactions from its counterpart thermophilic AlaDH. Since few publications about alanine dehydrogenase are available, this is the first report on improvement of the AlaDH property by site-directed mutagenesis. The constructed enzyme is more useful than wild type in industrial and medical application.



สถาบันวิทยบริการ
จุฬาลงกรณ์มหาวิทยาลัย

CHAPTER V

CONCLUSIONS

1. To improve thermostability of alanine dehydrogenase from *Aeromonas hydrophila*, G38E, L58R, L101E, P168R, A231E and L101E/A231E mutants were constructed by QuikChange site-directed mutagenesis.
2. Crude enzymes from L101E and A231E showed higher thermostability than that of wild type while the stability from L58R and P168R enzymes were lower.
3. Alanine dehydrogenases from wild type and L101E, A231E as well as L101E/A231E mutants were purified to high purity (>90% purity) with 20 - 40% yield and 3 - 4 purification folds.
4. Purified L101E/A231E AlaDH exhibited higher T_m than wild type by 3°C while L101E and A231E showed 2°C higher.
5. Optimum temperature of L101E, A231E and L101E/A231E enzymes shifted up 2.5°C when compared with that of wild type.
6. From the studies of optimum pH, substrate specificity and K_m value, the activity of AlaDH from L101E, A231E and L101E/A231E mutants were not altered.

REFERENCES

- Baker, P., Sawa, Y., Shibata, H., Sedelnikova, S., and Rice, D. 1998. Analysis of the structure and substrate binding of *Phormidium lapideum* alanine dehydrogenase. *Nat Struct Biol* 5: 561-567.
- Bojan, O., Bologa, M., Niac, G., Palibroda, N., Vargha, E., and Barzu, O. 1980. Simple enzymatic procedure for preparation of ¹⁵N-labeled L-glutamic acid. *Anal Biochem* 101: 23-25.
- Bollag, D.M., Rozycki, M.D., and Edelstein, S.J. 1996. *Protein methods* 2nd ed: Wiley-Liss, Inc.
- Brunhuber, N.M., and Blanchard, J.S. 1994. The biochemistry and enzymology of amino acid dehydrogenases. *Crit Rev Biochem Mol Biol* 29: 415-467.
- Calton, and L., G. 1992. The enzymatic preparation of L-alanine. In *Biocatalytic Production of Amino Acids and Derivatives*; Rozzell, J. D., Wagner, F., Eds.; Hanser: New York. 59-74.
- Cambillau, C., and Claverie, J.-M. 2000. Structural and genomic correlates of Hyperthermostability. *J. Biol. Chem.* 275: 32383-32386.
- Chakravarty, S., and Varadarajan, R. 2000. Elucidation of determinants of protein stability through genome sequence analysis. *FEBS Letters* 470: 65-69.
- Chowdhury, E.K., Saitoh, T., Nagata, S., Ashiuchi, M., and Misono, H. 1998. Alanine dehydrogenase from *Enterobacter aerogenes*: purification, characterization, and primary structure. *Biosci Biotechnol Biochem* 62: 2357-2363.
- Dao-pin, S., Soderlind, E., Baase, W.A., Wozniak, J.A., Sauer, U., and Matthews, B.W. 1991. Cumulative site-directed charge-change replacements in bacteriophage T₄

lysozyme suggest that long-range electrostatic interactions contribute little to protein stability. *Journal of Molecular Biology* 221: 873-887.

Delforge, D., Devreese, B., Dieu, M., Delaive, E., Van Beeumen, J., and Remacle, J. 1997. Identification of lysine 74 in the pyruvate binding site of alanine dehydrogenase from *Bacillus subtilis*. *J. Biol. Chem.* 272: 2276-2284.

Dower, W.J., Miller, J.F., and Ragsdale, C.W. 1988. High efficiency transformation of *E. coli* by high voltage electroporation. *Nucleic Acids Res* 16: 6127-6145.

Galkin, A., Kulakova, L., Ashida, H., Sawa, Y., and Esaki, N. 1999. Cold-adapted alanine dehydrogenases from two antarctic bacterial strains: Gene cloning, protein characterization, and comparison with mesophilic and thermophilic counterparts. *Appl. Envir. Microbiol.* 65: 4014-4020.

Giver, L., Gershenson, A., Freskgard, P.O., and Arnold, F.H. 1998. Directed evolution of a thermostable esterase. *Proc Natl Acad Sci U S A* 95: 12809-12813.

Jaenicke, R. and Bohm, G 1998. The stability of protein in extreme environment. *Curr. Opin. Struct. Biol.* 8: 738-748

Jareonpanich, J. 2001. Nucleotide sequencing and cloning of the phenylalanine dehydrogenase gene from thermotolerant *Bacillus badius*. Master's Thesis, Department of Biochemistry, Faculty of Science, Chulalongkorn University.

Kumar, S., and Nussinov, R. 2002. Relationship between ion pair geometries and electrostatic strengths in proteins. *Biophys. J.* 83: 1595-1612.

Kunkel, T.A. 1985. Rapid and efficient site-specific mutagenesis without phenotypic selection. *Proc Natl Acad Sci U S A* 82: 488-492.

Kuroda, S., Tanizawa, K., Sakamoto, Y., Tanaka, H., and Soda, K. 1990. Alanine dehydrogenases from two *Bacillus* species with distinct thermostabilities:

molecular cloning, DNA and protein sequence determination, and structural comparison with other NAD(P)⁽⁺⁾-dependent dehydrogenases. *Biochemistry* 29: 1009-1015.

Lebbink, J.H.G., Knapp, S., van der Oost, J., Rice, D., Ladenstein, R., and de Vos, W.M. 1998. Engineering activity and stability of *Thermotoga maritima* glutamate dehydrogenase. Introduction of a six-residue ion-pair network in the hinge region1. *Journal of Molecular Biology* 280: 287-296.

Lehmann, M., and Wyss, M. 2001. Engineering proteins for thermostability: the use of sequence alignments versus rational design and directed evolution. *Curr Opin Biotechnol* 12: 371-375.

Leksakorn, A. 2001. Purification and characterization of phenylalanine dehydrogenase from thermotolerant *Bacillus* sp. BC1. Master's Thesis, Department of Biochemistry, Faculty of Science, Chulalongkorn University.

Lowrey, O. H., Rosibrough, N. J., Farr, A. L., and Randall, R. J. 1951. Protein measurement with Folin phenol reagent. *J. Biol. Chem.* 193: 265-275.

Lui, W. Wang, D., Chen, P. and Halpern, M. 1997. Cloning and expression of gene encoding a protein obtain from earthworm secretion that is a chemoattractant for garter snakes. *J. Biol. Chem.* 272: 27378-27381.

Makhatadze, G., Loladze, V., Ermolenko, D., Chen, X., and Thomas, S. 2003. Contribution of surface salt bridges to protein stability: Guidelines for protein engineering. *J Mol Biol* 327: 1135-1148.

Mocanu, A., Niac, G., Ivanof, A., Gorun, V., Palibroda, N., Vargha, E., Bologa, M., and Barzu, O. 1982. Preparation of ¹⁵N-labeled L-alanine by coupling the alanine dehydrogenase and alcohol dehydrogenase reactions. *FEBS Lett* 143: 153-156.

- Mrabet, N., Van den Broeck, A., Van den brande, I., Stanssens, P., Laroche, Y., Lambeir, A., Matthijssens, G., Jenkins, J., Chiadmi, M., and van Tilbeurgh, H. 1992. Arginine residues as stabilizing elements in proteins. *Biochemistry* 31: 2239-2253.
- Ohshima, T., and Soda, K. 1990. Biochemistry and biotechnology of amino acid dehydrogenases. *Adv Biochem Eng Biotechnol* 42: 187-209.
- Ohshima, T., and Soda, K. 2000. Stereoselective biocatalysis, amino acid dehydrogenase, and their applications; in: Ramesh N. Patel, *Stereoselective Biocatalysis*. New York: Marcel Dekker, Inc. pp. 877-902.
- Perl, D., Mueller, U., Heinemann, U., and Schmid, F.X. 2000. Two exposed amino acid residues confer thermostability on a cold shock protein. *Nat Struct Biol* 7: 380-383.
- Phungsangthum, P. 1997. Screening of pyridine nucleotide-dependent L-alanine dehydrogenase production of the enzyme. Master's Thesis, Department of Biochemistry, Faculty of Science, Chulalongkorn University.
- Poomipark, N. 2000. Nucleotide sequencing and cloning of alanine dehydrogenase gene from *Aeromonas hydrophila*. Master's Thesis, Department of Biochemistry, Faculty of Science, Chulalongkorn University.
- Reinhhold, D., Uthe, T., and Abramson, N.L. 1987. Process for L-dopa. NJ.4716246.
- Sakamoto, Y., Nagata, S., Esaki, N., Tanaka, H., and Soda, K. 1990. Gene cloning, purification and characterization of thermostable alanine dehydrogenase of *Bacillus stearothermophilus*. *Journal of Fermentation and Bioengineering* 69: 154-158.
- Sawa, Y., Tani, M., Murata, K., Shibata, H., and Ochiai, H. 1994. Purification and characterization of alanine dehydrogenase from a cyanobacterium, *Phormidium lapideum*. *J Biochem (Tokyo)* 116: 995-1000.

- Sawano, A., and Miyawaki, A. 2000. Directed evolution of green fluorescent protein by a new versatile PCR strategy for site-directed and semi-random mutagenesis. *Nucl. Acids. Res.* 28: e78-.
- Schwede, T., Diemand, A., Guex, N., and Peitsch, M.C. 2000. Protein structure computing in the genomic era. *Res Microbiol* 151: 107-112.
- Schwede, T., Kopp, J., Guex, N., and Peitsch, M.C. 2003. SWISS-MODEL: an automated protein homology-modeling server. *Nucl. Acids. Res.* 31: 3381-3385.
- Shubeita, S. and Rohwer, F. 2002. Site-directed mutagenesis. *Biochemistry, Cell & molecular biology laboratory II*. Available from: <http://www.sci.sdsu.edu/classes/chemistry/chem4671/mardahl/html>
- Siranosian, K., Ireton, K., and Grossman, A. 1993. Alanine dehydrogenase (ald) is required for normal sporulation in *Bacillus subtilis*. *J. Bacteriol.* 175: 6789-6796.
- Strop, P., and Mayo, S.L. 2000. Contribution of surface salt bridges to protein stability. *Biochemistry* 39: 1251-1255.
- Suye, S.I., Kawagee, M., and Inuta, S. 1992. Enzymatic production of L-alanine from malic acid with malic enzyme and alanine dehydrogenase with coenzyme regeneration. *Can. J. Chem. Eng.* 70: 306-312.
- Szilagyi, A., and Zavodszky, P. 2000. Structural differences between mesophilic, moderately thermophilic and extremely thermophilic protein subunits: results of a comprehensive survey. *Structure with Folding & Design* 8: 493-504.
- Takahashi, T., Kondo, T., Ohno, H., Minato, S., Ohshima, T., Mikuni, S., Soda, K., and Taniguchi, N. 1987. A spectrophotometric method for the determination of gamma-glutamyl cyclotransferase with alanine dehydrogenase in the presence of anthglutin. *Biochem Med Metab Biol* 38: 311-316.

- Takamiya, S., Ohshima, T., Tanizawa, K., and Soda, K. 1983. A spectrophotometric method for the determination of aminopeptidase activity with leucine dehydrogenase. *Anal Biochem* 130: 266-270.
- Takano, K., Tsuchimori, K., Yamagata, Y., and Yutani, K. 2000. Contribution of salt bridges near the surface of a protein to the conformational stability. *Biochemistry* 39: 12375-12381.
- Thompson, M.J., and Eisenberg, D. 1999. Transproteomic evidence of a loop-deletion mechanism for enhancing protein thermostability. *J Mol Biol* 290: 595-604.
- Trejo, F., Gelpi, J.L., Ferrer, A., Boronat, A., Busquets, M., and Cortes, A. 2001. Contribution of engineered electrostatic interactions to the stability of cytosolic malate dehydrogenase. *Protein Eng* 14: 911-917.
- Vadas, A., Schroder, I., and Monbouquette, H. 2002. Room-temperature synthesis of L-alanine using the alanine dehydrogenase of the hyperthermophilic archaeon *Archaeoglobus fulgidus*. *Biotechnol Prog* 18: 909-911.
- Vali, Z., Kilar, F., Lakatos, S., Venyaminov, S.A., and Zavodszky, P. 1980. L-alanine dehydrogenase from *Thermus thermophilus*. *Biochim Biophys Acta* 615: 34-47.
- Vetriani, C., Maeder, D.L., Tolliday, N., Yip, K.S.-P., Stillman, T.J., Britton, K.L., Rice, D.W., Klump, H.H., and Robb, F.T. 1998. Protein thermostability above 100°C: A key role for ionic interactions. *PNAS* 95: 12300-12305.
- Voet, D and Voet, J. G. 1995. Biochemistry. Second edition. John Wiley & Sons, Inc. New York.
- Wada, M., Uchiumi, T., Ichiba, T., and Hachimori, A. 2001. Enhancement of the thermostability of thermophilic bacterium PS-3 PPase on substitution of Ser-89 with carboxylic amino acids. *J Biochem (Tokyo)* 129: 955-961.

- Wandrey, C., Fiolitakis, E., Wichmann, U., and Kula, M.R. 1984. L-amino acids from a racemic mixture of alpha-hydroxy acids. *Ann N Y Acad Sci* 434: 91-94.
- Wang, W., and Malcolm, B.A. 1999. Two-stage PCR protocol allowing introduction of multiple mutations, deletions and insertions using QuikChange Site-Directed Mutagenesis. *Biotechniques* 26: 680-682.
- Yamamoto, K., Tosa, T., and Chibata, I. 1980. Continuous production of L-alanine using *Pseudomonas dacungae* immobilized in carrageenan. *Biotech. Bioeng.*22: 2045-2054.
- Yip, K., Britton, K., Stillman, T., Lebbink, J., de Vos, W., Robb, F., Vetriani, C., Maeder D., and Rice, D. 1998. Insights into the molecular basis of thermal stability from the analysis of ion-pair network in the glutamate dehydrogenase family. *Eur J Biochem.* 255:336-346.
- Yokoigawa, K., Okubo, Y., Soda, K. and Misono, H. 2003. Improvement in thermostability and psychrophilicity of psychrophilic alanine reemase by site-directed mutagenesis. *Journal of Molecular Catalysis B: Enzymatic.* 23: 389-395.
- Yoshida, A., and Freese, E. 1964. Purification and chemical characterization of alanine dehydrogenase of *Bacillus subtilis*. *Biochimica et Biophysica Acta (BBA) – Specialized Section on Enzymological Subjects.* 92: 33-43.

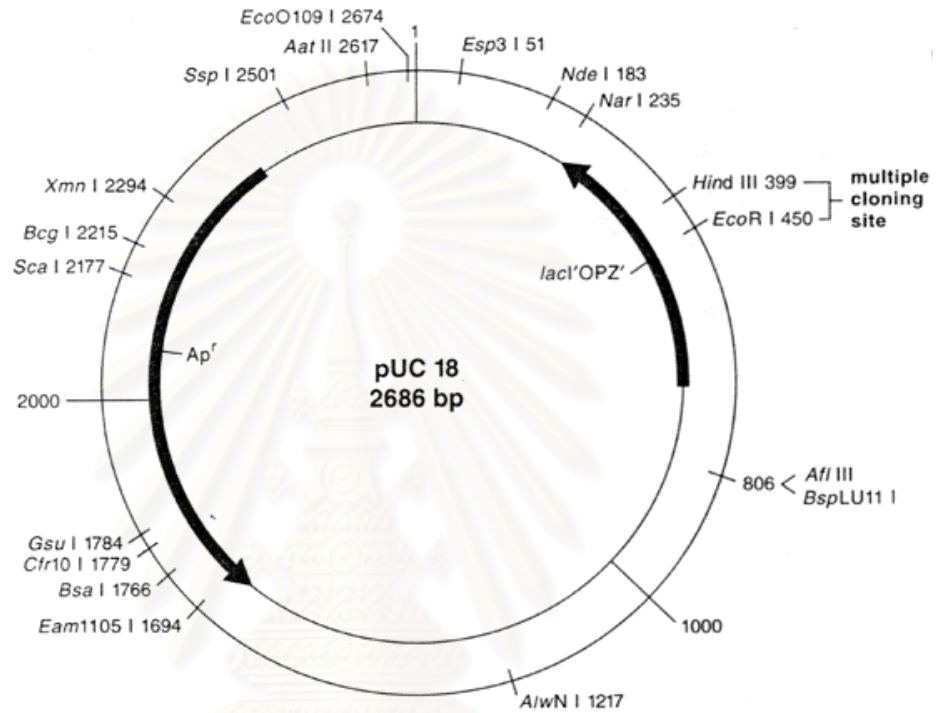


APPENDICES

สถาบันวิทยบริการ
จุฬาลงกรณ์มหาวิทยาลัย

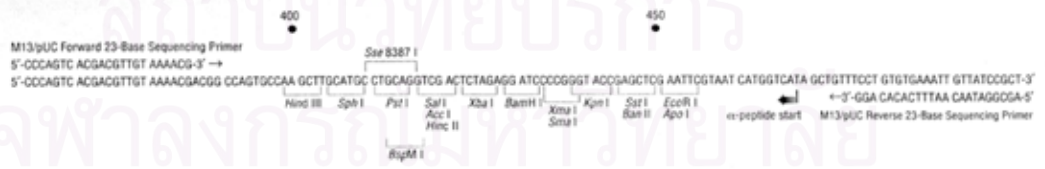
APPENDIX A

Restriction map of pUC18

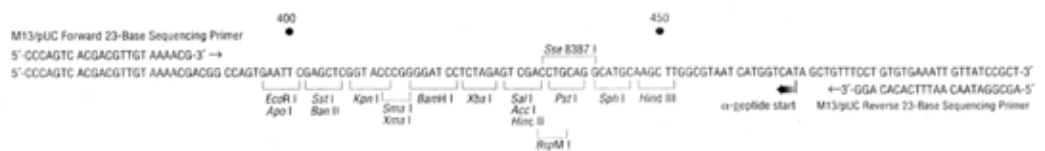


The sequence has not been confirmed by sequence analysis. It was assembled from the known sequence of fragments used to construct the vector.

pUC18 multiple cloning site and primer binding regions: 364-500



pUC19 multiple cloning site and primer binding regions: 364-500



APPENDIX B

QuikChange Site-Directed Mutagenesis Control

The pWhitescript™ 4.5-kb control plasmid is used to test the efficiency of mutant plasmid generation using the QuikChange site-directed mutagenesis kit. The pWhitescript 4.5-kb control plasmid contains stop codon (TAA) at the position where a glutamate codon (CAA) would normally appear in the β-galactosidase gene of the pBluescript® II SK(-) phagemid (corresponding to amino acid 9 of the protein). *E. coli* XL1-Blue supercompetent cells transformed with this control plasmid appear white on LB-ampicillin agar plate, containing IPTG and X-gal, because β-galactosidase activity has been obligated. The oligonucleotide control primers create a point mutation on the pWhitescript 4.5-kb control plasmid that revert T residue of the stop codon (TAA) at amino acid 9 of the β-galactosidase gene to a C residue, to produce the glutamine codon (CAA) found in the wild type sequence. Following transformation, colonies can be screened for the β-galactosidase (β-gal⁺, blue) phenotype.

Expected result for the control transformations

The expected colony number from the transformation of the pWhitescript control mutagenesis reaction is between 50 and 800 colonies. Greater than 80% of the colonies should contain the mutation and appear as blue colonies on agar plates containing IPTG and X-gal.

The mutagenesis efficiency (ME) for the pWhitescript 4.5-kb control plasmid is calculated by the following formula:

$$ME = \frac{\text{Number of blue colony forming units (cfu)}}{\text{Total number of colony forming units (cfu)}} \times 100$$

APPENDIX C

NZY⁺ Broth (per liter)

10 g of NZ amine (casein hydrolysate)

5 g of yeast extract

5 g of NaCl

Add deionized H₂O to a final volume of 1 liter

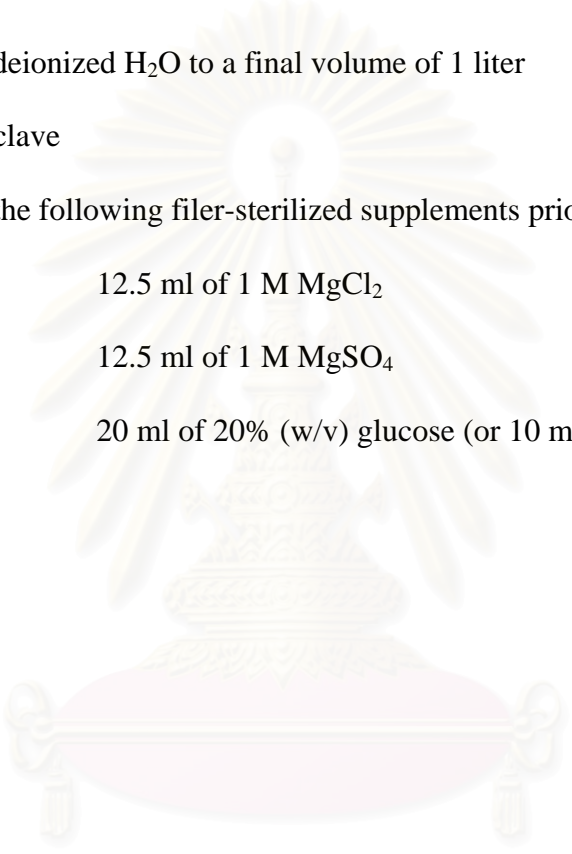
Autoclave

Add the following filter-sterilized supplements prior to use:

12.5 ml of 1 M MgCl₂

12.5 ml of 1 M MgSO₄

20 ml of 20% (w/v) glucose (or 10 ml of 2 glucose)



สถาบันวิทยบริการ
จุฬาลงกรณ์มหาวิทยาลัย

APPENDIX D

Preparation for protein determination

Reagent for determination of protein concentration (modified from Lowry *et al.*, 1951)

Solution A (0.5% copper sulfate, 1% potassium tartate, pH 7.0)

Potassium tartate	1.0	g
Copper sulfate	0.5	g
Adjust pH to 7.0 and adjust the solution volume to 100 ml		

Solution B (2% sodium carbonate, 1N sodium hydroxide)

Sodium carbonate	20.0	g
Sodium hydroxide	4.0	g
Dissolved in distilled water to 1 liter.		

Solution C (phenol reagent)

Sodium tungstate	50.0	g
Sodium molybdate	12.5	g
85% phosphoric acid	25.0	g
Distilled water	350	ml
Concentrated hydrochloric acid	50	ml
Reflex for 10 hour		
Lithium sulphate	75.0	g
Distilled water	25	ml
Bromine solution	2-3	drops

Boil the solution to reduce excess bromine for 15 minutes, then adjust volume to 500 ml with distilled water and store at 4 °C. Dilute the stock solution with distilled water in ratio 1: (V/V) before using.

APPENDIX E

Preparation of *E. coli* competent cells for electroporation (Dower, 1988)

1. A fresh overnight culture of *E. coli* JM 109 was inoculated into 1 liter of LB broth with 1 volume of overnight culture to 100 volume of LB broth.
2. Cells were grown to log phase at 37°C with vigorous shaking. The OD₆₀₀ was about 0.5 to 0.8.
3. To harvest, the culture was chilled on ice for 15 to 30 minutes, and then centrifuged at 8,000 x g for 15 minutes at 4°C.
4. The cells were washed with 1 liter of cold water, were spun down and washed again with 0.5 liter of cold water.
5. After the centrifugation, cells were resuspended in approximately 20 ml of 10% glycerol in distilled water and centrifuged at 8,000 x g for 15 minutes at 4°C.
6. The cell pellets were resuspended to a final volume of 2 to 3 ml in 10 % glycerol. This suspension was stored at -70°C until used.

APPENDIX F

Salt bridges of *Aeromonas hydrophila*

The list of salt bridges:

Date= 2003-02-27 17:58:58

1	8	GLU	(8)	OE1	-	73	LYS	(73)	NZ	3.23
2	8	GLU	(8)	OE2	-	73	LYS	(73)	NZ	3.24
3	13	GLU	(13)	OE1	-	15	ARG	(15)	NH1	5.23
4	13	GLU	(13)	OE1	-	15	ARG	(15)	NH2	3.19
5	13	GLU	(13)	OE2	-	15	ARG	(15)	NH1	5.11
6	13	GLU	(13)	OE2	-	15	ARG	(15)	NH2	3.80
7	13	GLU	(13)	OE1	-	75	LYS	(75)	NZ	5.57
8	25	GLU	(25)	OE1	-	24	ARG	(24)	NH1	6.56
9	25	GLU	(25)	OE1	-	24	ARG	(24)	NH2	5.87
10	63	ASP	(63)	OD1	-	86	ARG	(86)	NH2	6.65
11	69	GLU	(69)	OE2	-	86	ARG	(86)	NH1	5.54
12	69	GLU	(69)	OE2	-	86	ARG	(86)	NH2	6.14
13	76	GLU	(76)	OE1	-	10	LYS	(10)	NZ	4.13
14	76	GLU	(76)	OE2	-	10	LYS	(10)	NZ	2.81
15	76	GLU	(76)	OE1	-	75	LYS	(75)	NZ	4.61
16	76	GLU	(76)	OE2	-	75	LYS	(75)	NZ	6.30
17	76	GLU	(76)	OE1	-	96	HIS	(96)	ND1	5.49
18	81	GLU	(81)	OE1	-	73	LYS	(73)	NZ	4.15
19	81	GLU	(81)	OE2	-	73	LYS	(73)	NZ	4.06
20	106	GLU	(106)	OE1	-	82	ARG	(82)	NH1	3.93
21	106	GLU	(106)	OE1	-	82	ARG	(82)	NH2	5.51
22	106	GLU	(106)	OE2	-	82	ARG	(82)	NH1	5.11
23	106	GLU	(106)	OE2	-	82	ARG	(82)	NH2	6.77
24	118	GLU	(118)	OE1	-	96	HIS	(96)	ND1	4.42
25	118	GLU	(118)	OE1	-	96	HIS	(96)	NE2	5.21
26	118	GLU	(118)	OE2	-	96	HIS	(96)	ND1	4.15
27	118	GLU	(118)	OE2	-	96	HIS	(96)	NE2	5.00
28	122	ASP	(122)	OD2	-	124	ARG	(124)	NH1	5.99
39	122	ASP	(122)	OD2	-	124	ARG	(124)	NH2	6.67
30	122	ASP	(122)	OD1	-	338	HIS	(338)	NE2	5.16
31	122	ASP	(122)	OD2	-	338	HIS	(338)	NE2	5.16
32	135	GLU	(135)	OE1	-	139	ARG	(139)	NH1	4.38
33	135	GLU	(135)	OE1	-	139	ARG	(139)	NH2	4.21
34	135	GLU	(135)	OE2	-	139	ARG	(139)	NH1	3.84
35	135	GLU	(135)	OE2	-	139	ARG	(139)	NH2	4.14
36	135	GLU	(135)	OE1	-	185	ARG	(185)	NH1	5.32
37	135	GLU	(135)	OE2	-	185	ARG	(185)	NH1	5.98
38	150	GLU	(150)	OE1	-	153	ARG	(153)	NH1	6.29
39	167	GLU	(167)	OE1	-	170	LYS	(170)	NZ	6.90
40	167	GLU	(167)	OE2	-	170	LYS	(170)	NZ	4.84
41	193	ASP	(193)	OD2	-	170	LYS	(170)	NZ	5.52
42	208	ASP	(208)	OD2	-	205	ARG	(205)	NH1	6.19
43	210	GLU	(210)	OE1	-	185	ARG	(185)	NH2	6.18
44	210	GLU	(210)	OE2	-	185	ARG	(185)	NH1	5.75
45	210	GLU	(210)	OE2	-	185	ARG	(185)	NH2	4.00
46	210	GLU	(210)	OE1	-	206	ARG	(206)	NH1	6.37
47	210	GLU	(210)	OE2	-	206	ARG	(206)	NH1	5.76
48	226	GLU	(226)	OE2	-	222	ARG	(222)	NH2	5.65
49	226	GLU	(226)	OE1	-	254	HIS	(254)	ND1	4.96
50	226	GLU	(226)	OE1	-	254	HIS	(254)	NE2	5.64

51	226	GLU	(226)	OE2	-	254	HIS	(254)	ND1	3.63
52	226	GLU	(226)	OE2	-	254	HIS	(254)	NE2	3.64
53	226	GLU	(226)	OE1	-	257	ARG	(257)	NH1	3.52
54	226	GLU	(226)	OE1	-	257	ARG	(257)	NH2	5.13
55	226	GLU	(226)	OE2	-	257	ARG	(257)	NH1	3.53
56	226	GLU	(226)	OE2	-	257	ARG	(257)	NH2	4.45
57	233	ASP	(233)	OD2	-	170	LYS	(170)	NZ	5.80
58	233	ASP	(233)	OD1	-	259	LYS	(259)	NZ	4.34
59	233	ASP	(233)	OD2	-	259	LYS	(259)	NZ	5.01
60	253	ASP	(253)	OD1	-	252	ARG	(252)	NH1	3.95
61	253	ASP	(253)	OD1	-	252	ARG	(252)	NH2	3.84
62	253	ASP	(253)	OD2	-	252	ARG	(252)	NH1	5.44
63	253	ASP	(253)	OD2	-	252	ARG	(252)	NH2	4.57
64	253	ASP	(253)	OD2	-	254	HIS	(254)	NE2	6.46
65	253	ASP	(253)	OD1	-	257	ARG	(257)	NH2	5.92
66	253	ASP	(253)	OD2	-	257	ARG	(257)	NH2	5.94
67	270	ASP	(270)	OD2	-	96	HIS	(96)	NE2	5.95
68	276	GLU	(276)	OE2	-	248	LYS	(248)	NZ	6.88
69	276	GLU	(276)	OE1	-	252	ARG	(252)	NH1	6.84
70	276	GLU	(276)	OE1	-	252	ARG	(252)	NH2	6.00
71	284	GLU	(284)	OE1	-	12	HIS	(12)	ND1	6.69
72	284	GLU	(284)	OE1	-	12	HIS	(12)	NE2	6.15
73	291	ASP	(291)	OD1	-	252	ARG	(252)	NH1	6.27
74	291	ASP	(291)	OD2	-	252	ARG	(252)	NH1	5.87
75	291	ASP	(291)	OD2	-	295	HIS	(295)	NE2	6.89
76	326	GLU	(326)	OE2	-	29	ARG	(29)	NH1	6.19
77	326	GLU	(326)	OE2	-	29	ARG	(29)	NH2	5.34
78	326	GLU	(326)	OE1	-	31	HIS	(31)	ND1	4.15
79	326	GLU	(326)	OE1	-	31	HIS	(31)	NE2	2.71
80	326	GLU	(326)	OE2	-	31	HIS	(31)	ND1	5.84
81	326	GLU	(326)	OE2	-	31	HIS	(31)	NE2	4.82
82	336	ASP	(336)	OD1	-	323	LYS	(323)	NZ	4.76
83	336	ASP	(336)	OD2	-	323	LYS	(323)	NZ	2.79
84	336	ASP	(336)	OD1	-	338	HIS	(338)	ND1	3.53
85	336	ASP	(336)	OD1	-	338	HIS	(338)	NE2	5.54
86	336	ASP	(336)	OD2	-	338	HIS	(338)	ND1	4.28
87	336	ASP	(336)	OD2	-	338	HIS	(338)	NE2	6.39

Salt bridges of *Bacillus stearothermophilus*

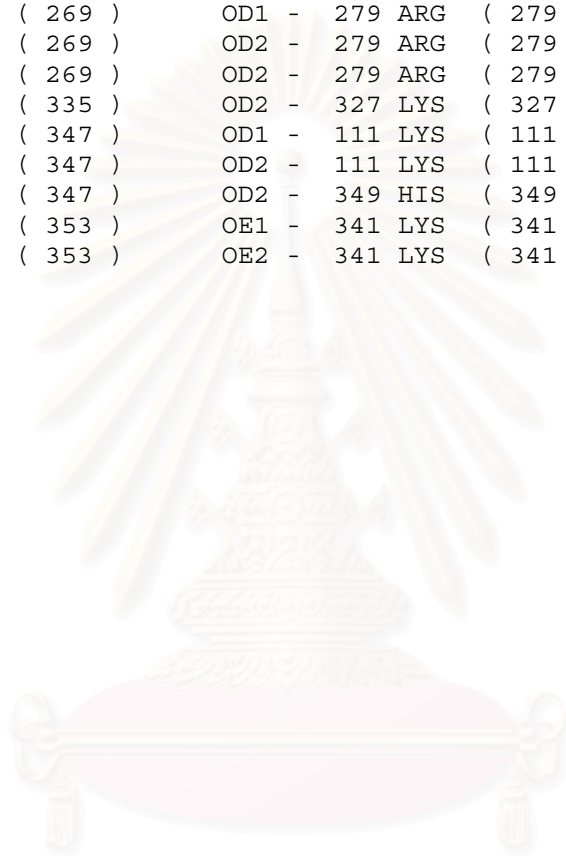
The list of salt bridges:

Date= 2003-02-25 08:22:36

1	8	GLU	(8)	OE1	-	73	LYS	(73)	NZ	3.24
2	8	GLU	(8)	OE2	-	73	LYS	(73)	NZ	3.24
3	13	GLU	(13)	OE1	-	15	ARG	(15)	NH1	5.24
4	13	GLU	(13)	OE1	-	15	ARG	(15)	NH2	3.19
5	13	GLU	(13)	OE2	-	15	ARG	(15)	NH1	5.10
6	13	GLU	(13)	OE2	-	15	ARG	(15)	NH2	3.79
7	13	GLU	(13)	OE1	-	75	LYS	(75)	NZ	5.57
8	32	GLU	(32)	OE1	-	2	LYS	(2)	NZ	5.99
9	38	GLU	(38)	OE2	-	7	LYS	(7)	NZ	6.66
10	49	GLU	(49)	OE1	-	52	LYS	(52)	NZ	4.15
11	49	GLU	(49)	OE2	-	52	LYS	(52)	NZ	5.97
12	64	ASP	(64)	OD1	-	58	ARG	(58)	NH1	4.91
13	64	ASP	(64)	OD1	-	58	ARG	(58)	NH2	3.84
14	64	ASP	(64)	OD2	-	58	ARG	(58)	NH1	6.24

15	64	ASP	(64)	OD2	-	58	ARG	(58)	NH2	5.46
16	64	ASP	(64)	OD2	-	60	ARG	(60)	NH1	6.30
17	64	ASP	(64)	OD2	-	60	ARG	(60)	NH2	6.97
18	64	ASP	(64)	OD1	-	63	ARG	(63)	NH1	4.53
19	64	ASP	(64)	OD1	-	63	ARG	(63)	NH2	3.05
20	64	ASP	(64)	OD2	-	63	ARG	(63)	NH1	6.34
21	64	ASP	(64)	OD2	-	63	ARG	(63)	NH2	4.65
22	69	GLU	(69)	OE1	-	2	LYS	(2)	NZ	6.60
23	69	GLU	(69)	OE2	-	2	LYS	(2)	NZ	4.75
24	69	GLU	(69)	OE1	-	86	ARG	(86)	NH2	6.37
25	76	GLU	(76)	OE1	-	10	LYS	(10)	NZ	4.14
26	76	GLU	(76)	OE2	-	10	LYS	(10)	NZ	2.81
27	76	GLU	(76)	OE1	-	75	LYS	(75)	NZ	4.61
28	76	GLU	(76)	OE2	-	75	LYS	(75)	NZ	6.29
29	76	GLU	(76)	OE1	-	96	HIS	(96)	ND1	5.49
30	81	GLU	(81)	OE1	-	73	LYS	(73)	NZ	4.14
31	81	GLU	(81)	OE2	-	73	LYS	(73)	NZ	4.06
32	101	GLU	(101)	OE1	-	359	HIS	(359)	ND1	6.93
33	101	GLU	(101)	OE1	-	359	HIS	(359)	NE2	6.44
34	101	GLU	(101)	OE2	-	359	HIS	(359)	ND1	6.44
35	101	GLU	(101)	OE2	-	359	HIS	(359)	NE2	6.35
36	118	GLU	(118)	OE1	-	96	HIS	(96)	ND1	4.42
37	118	GLU	(118)	OE1	-	96	HIS	(96)	NE2	5.21
38	118	GLU	(118)	OE2	-	96	HIS	(96)	ND1	4.14
39	118	GLU	(118)	OE2	-	96	HIS	(96)	NE2	4.98
40	135	GLU	(135)	OE1	-	139	ARG	(139)	NH1	4.38
41	135	GLU	(135)	OE1	-	139	ARG	(139)	NH2	4.21
42	135	GLU	(135)	OE2	-	139	ARG	(139)	NH1	3.83
43	135	GLU	(135)	OE2	-	139	ARG	(139)	NH2	4.13
44	135	GLU	(135)	OE1	-	185	LYS	(185)	NZ	6.57
45	150	GLU	(150)	OE1	-	153	HIS	(153)	ND1	4.69
46	150	GLU	(150)	OE1	-	153	HIS	(153)	NE2	2.79
47	150	GLU	(150)	OE2	-	153	HIS	(153)	ND1	5.64
48	150	GLU	(150)	OE2	-	153	HIS	(153)	NE2	4.16
49	193	ASP	(193)	OD2	-	167	ARG	(167)	NH2	6.69
50	193	ASP	(193)	OD1	-	168	ARG	(168)	NH1	5.05
51	193	ASP	(193)	OD1	-	168	ARG	(168)	NH2	6.45
52	193	ASP	(193)	OD2	-	168	ARG	(168)	NH1	6.07
53	193	ASP	(193)	OD2	-	170	LYS	(170)	NZ	5.68
54	193	ASP	(193)	OD1	-	214	HIS	(214)	NE2	6.70
55	206	GLU	(206)	OE1	-	203	ARG	(203)	NH1	6.19
56	208	ASP	(208)	OD2	-	205	ARG	(205)	NH1	6.22
57	227	GLU	(227)	OE1	-	230	ARG	(230)	NH1	5.95
58	227	GLU	(227)	OE1	-	230	ARG	(230)	NH2	4.19
59	227	GLU	(227)	OE2	-	230	ARG	(230)	NH1	6.26
60	227	GLU	(227)	OE2	-	230	ARG	(230)	NH2	4.06
61	231	GLU	(231)	OE1	-	170	LYS	(170)	NZ	4.97
62	231	GLU	(231)	OE2	-	170	LYS	(170)	NZ	5.87
63	231	GLU	(231)	OE1	-	230	ARG	(230)	NH1	6.04
64	231	GLU	(231)	OE1	-	230	ARG	(230)	NH2	5.20
65	231	GLU	(231)	OE2	-	230	ARG	(230)	NH1	4.57
66	231	GLU	(231)	OE2	-	230	ARG	(230)	NH2	3.71
67	233	ASP	(233)	OD1	-	156	LYS	(156)	NZ	5.39
68	233	ASP	(233)	OD2	-	170	LYS	(170)	NZ	5.80
69	251	GLU	(251)	OE1	-	255	ARG	(255)	NH1	5.00
70	251	GLU	(251)	OE1	-	255	ARG	(255)	NH2	6.09
71	251	GLU	(251)	OE2	-	255	ARG	(255)	NH1	4.46
72	251	GLU	(251)	OE2	-	255	ARG	(255)	NH2	6.04
73	251	GLU	(251)	OE1	-	290	LYS	(290)	NZ	5.26

74	251	GLU	(251)	OE2	-	290	LYS	(290)	NZ	4.65
75	251	GLU	(251)	OE1	-	291	HIS	(291)	ND1	4.13
75	251	GLU	(251)	OE1	-	291	HIS	(291)	NE2	2.64
77	251	GLU	(251)	OE2	-	291	HIS	(291)	ND1	5.07
78	251	GLU	(251)	OE2	-	291	HIS	(291)	NE2	3.47
79	252	GLU	(252)	OE1	-	255	ARG	(255)	NH1	3.05
80	252	GLU	(252)	OE1	-	255	ARG	(255)	NH2	2.99
81	252	GLU	(252)	OE2	-	255	ARG	(255)	NH1	4.19
82	252	GLU	(252)	OE2	-	255	ARG	(255)	NH2	2.86
83	252	GLU	(252)	OE1	-	291	HIS	(291)	NE2	6.48
84	269	ASP	(269)	OD2	-	96	HIS	(96)	NE2	5.95
85	269	ASP	(269)	OD1	-	279	ARG	(279)	NH2	6.05
86	269	ASP	(269)	OD2	-	279	ARG	(279)	NH1	6.69
87	269	ASP	(269)	OD2	-	279	ARG	(279)	NH2	5.39
88	335	ASP	(335)	OD2	-	327	LYS	(327)	NZ	6.32
89	347	ASP	(347)	OD1	-	111	LYS	(111)	NZ	2.88
90	347	ASP	(347)	OD2	-	111	LYS	(111)	NZ	4.10
91	347	ASP	(347)	OD2	-	349	HIS	(349)	NE2	6.70
92	353	GLU	(353)	OE1	-	341	LYS	(341)	NZ	6.73
93	353	GLU	(353)	OE2	-	341	LYS	(341)	NZ	5.63



สถาบันวิทยบริการ
จุฬาลงกรณ์มหาวิทยาลัย

APPENDIX G

The DNA sequencing profile of the *alaDH* gene fragment

- (a) **AlaDH wild type using M13 Forward primer**
- (b) **AlaDH wild type using M13 Reverse primer**
- (c) **G388R using M13 Reverse primer**
- (d) **L58R using M13 Reverse primer**
- (e) **L101E using M13 Reverse primer**
- (f) **P168 using M13 Reverse primer**
- (g) **A231E using M13 Forward primer**
- (h) **L101E/A231E using M13 Forward primer**
- (i) **L101E/A231E using M13 Reverse primer**

Note: mutant sequences are boxed



Model 377
Version 3.7
Basecaller-377.bcp
BC 1.3.0.0

19L58R J-1-M13Forward primer.ab1
L58R J-1-M13Forward primer
Cap 19

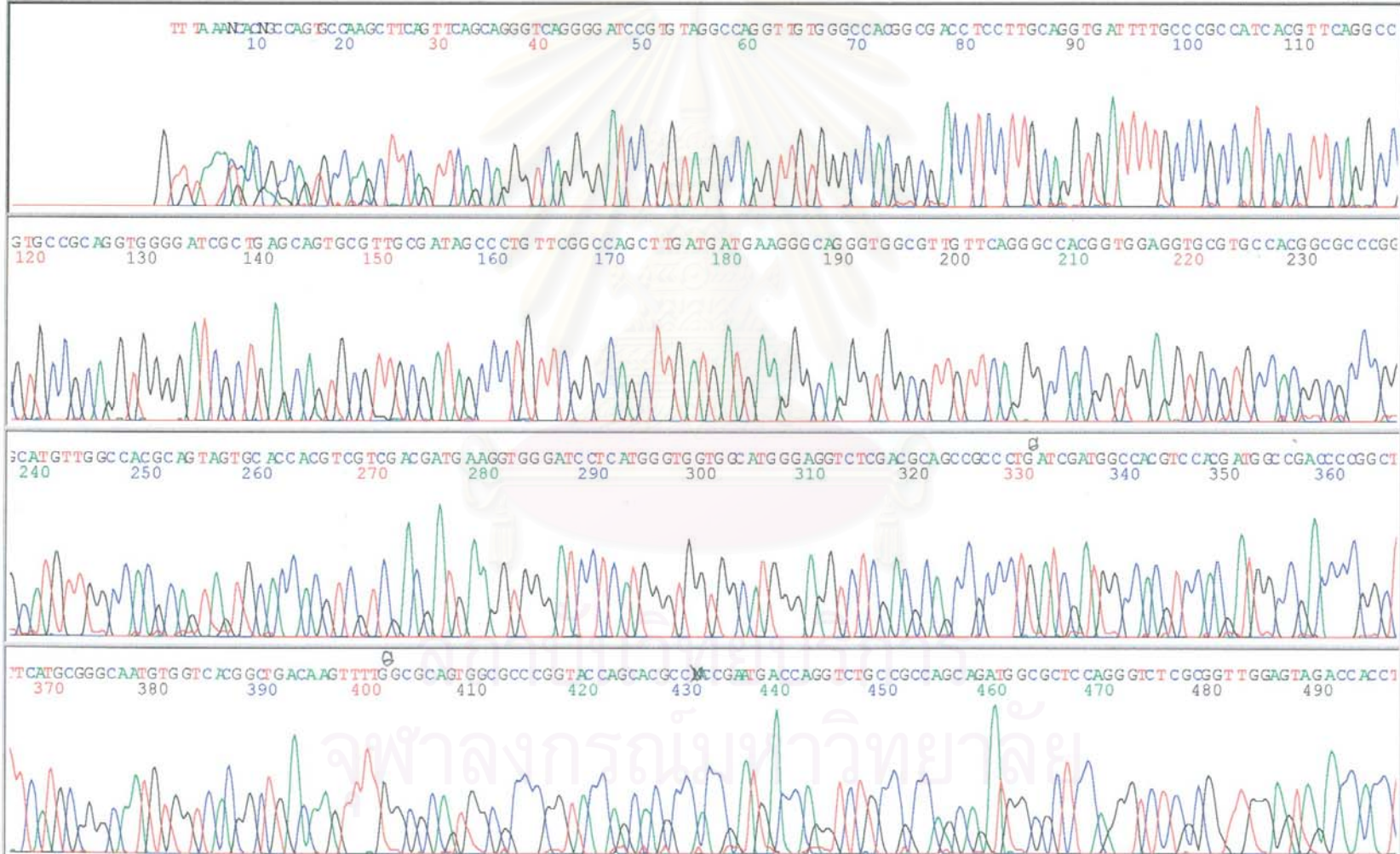
SQ...14358

Signal G:1093 A:355 T:257 C:730
DT377{BDv3}v1.mob
BD_MatrixV3.mtx
Points 1000 to 10616 Pk 1 Loc: 1000

Page 2 of 3

Page 1 of 3
Wed, May 21, 2003 3:03 PM
Tue, May 20, 2003 4:39 PM
Spacing: 10.36{10.36}

(a)





Model 377
Version 3.7
Basecaller-377.bcp
BC 1.3.0.0

19L58R J-1-M13Forward primer.ab1
L58R J-1-M13Forward primer
Cap 19

SQ.....14358.....

Signal G:1093 A:355 T:257 C:730
DT377(BDv3)v1.mob
BD_MatrixV3.mtx
Points 1000 to 10616 Pk 1 Loc: 1000

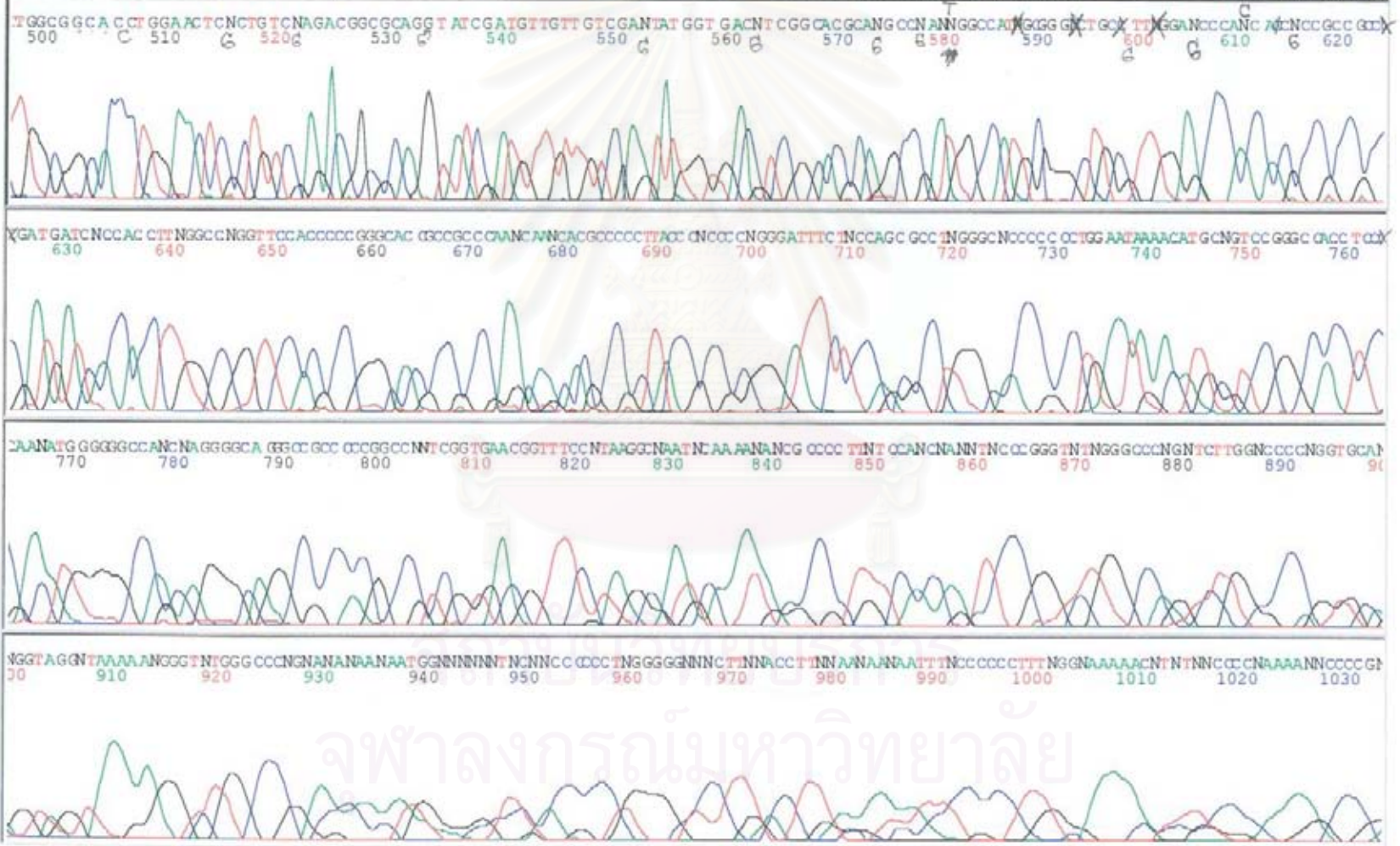
Page 3 of 3

Page 2 of 3

Wed, May 21, 2003 3:03 PM

Tue, May 20, 2003 4:39 PM

Spacing: 10.36(10.36)



(a) continued



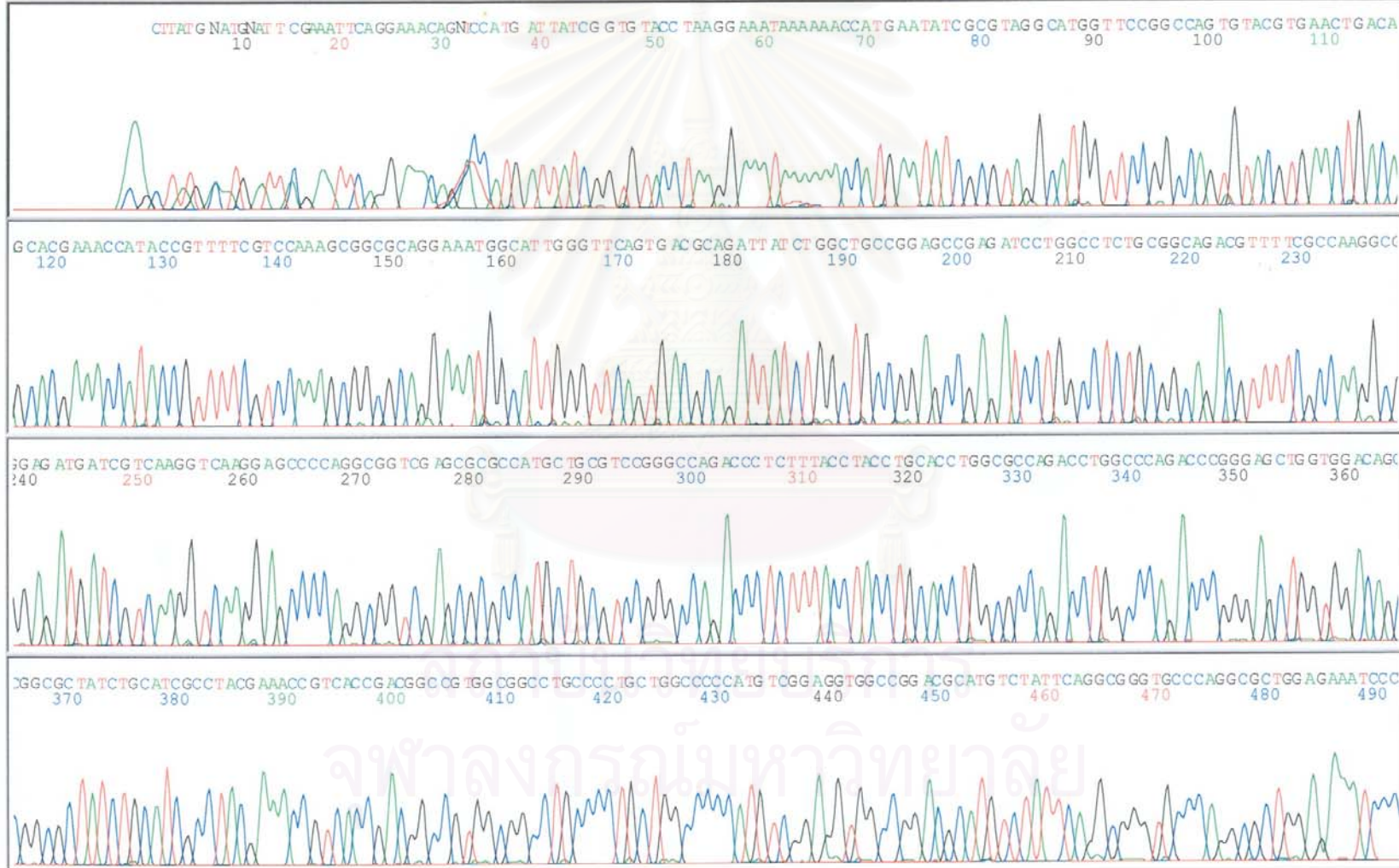
Model 3100
Version 3.7
Basecaller-3100SR.bcp L58RNo.9-M13Reverse
BC 1.3.0.0 Cap 16

H10_L58RNo.9-M13Reverse_16.ab1

SQ..... 1000

Signal G:2607 A:1394 T:1355 C:1310
DT3100POP6(BDv3)v1.mob
3100_GA
Points 500 to 10106 Pk 1 Loc: 500

Page.....of..... Page 1 of 3
Fri, Nov 01, 2002 7:52 AM
Thu, Oct 31, 2002 12:08 AM
Spacing: 10.56{10.56}



(b)

จุฬาลงกรณ์มหาวิทยาลัย



Model 3100
Version 3.7
Basecaller-3100SR.bcp L58RNo.9-M13Reverse
BC 1.3.0.0 Cap 16

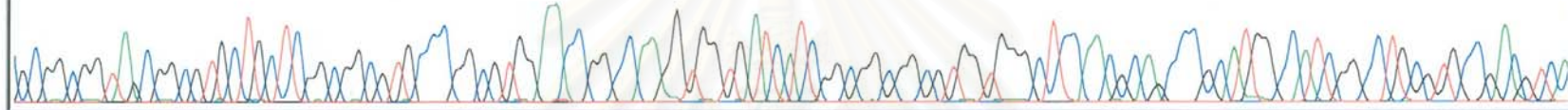
H10_L58RNo.9-M13Reverse_16.ab1

SQ.....

Signal G:2607 A:1394 T:1355 C:1310
DT3100POP6(BDv3)v1.mob
3100_GA
Points 500 to 10106 Pk 1 Loc: 500

Page 2 of 3
Fri, Nov 01, 2002 7:52 AM
Thu, Oct 31, 2002 12:08 AM
Spacing: 10.56(10.56)

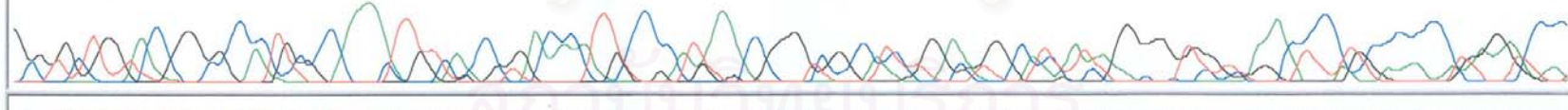
GCGGCGG TAGCGGCG TGC TGC TCG GCGGCG TGCCCG GCG TGG AACCGGCCAAGG TGG TG ATCATCG GCGGCGGCG TGG TGGGC TCCAACGCAGCCC GC ATGG CCATCG GCGT GCG TGCCG ACG TCA
500 510 520 530 540 550 560 570 580 590 600 610



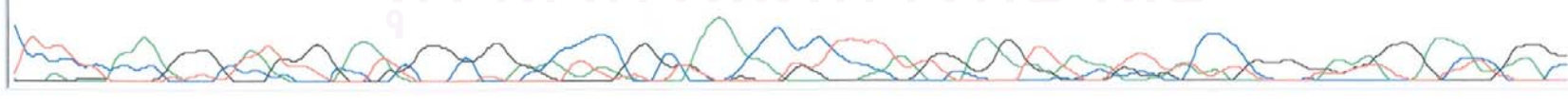
CC ATACTCG ACAACAACATCG ATACCC TG CGCG TC TCGACGCG AGI TCCAGG GTGCCGCCNANGNGGTC TAC TCCAACCGCG AGANC TGG AGCGCCAT CTGC TGGCGGCAGACCTGGT CATCNG NG
620 630 640 650 660 670 680 690 700 710 720 730 740



GCGGTC TGGTACCGGG CGCCAC TCGCCAAAATT NTNNCCGNG A CACAT TGCCCNAT NAAACCGGG TCGGCCAT CN GSN NGT GG CATNAAAANG GNG GNGGG TNNAACCTCC TNCNCCCCNGANGATCCC
750 760 770 780 790 800 810 820 830 840 850 860 870 880

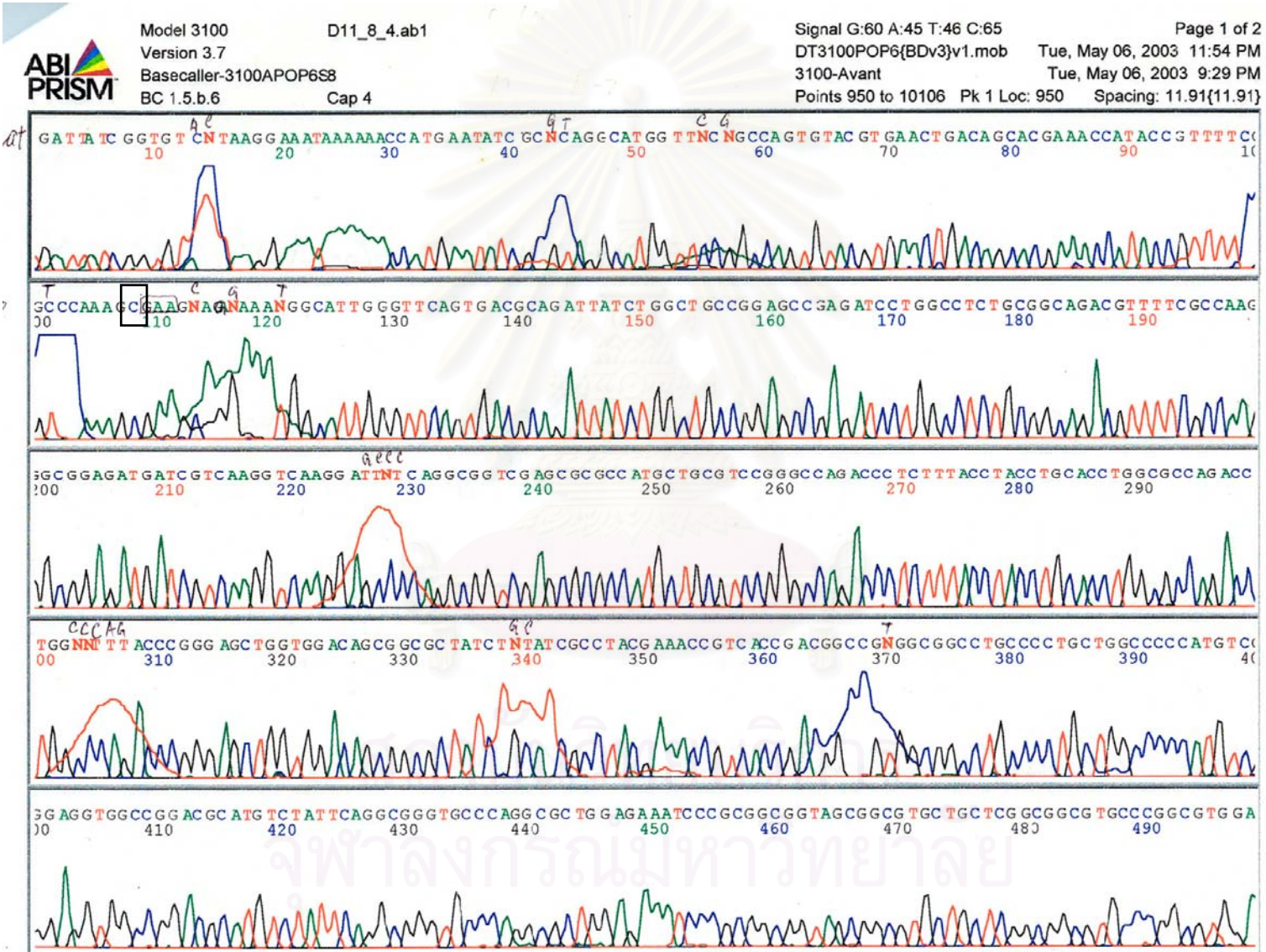


TTTT NTCCANA NA GGG GAC TNINGGCG AAATNNGGG CGGG GAAACCCC CGGG CNAAAACCTNC TTNIT TANNGGAAAGN TTNANNNT TNAACCNC GGGGGNAANA GGGGAAANIN AGGGGN
890 900 910 920 930 940 950 960 970 980 990 1000 1010



(b) continued

จุฬาลงกรณ์มหาวิทยาลัย



(c)



Model 377
Version 3.7
Basecaller-377.bcp
BC 1.3.0.0

22L58R No.10-M13Reverse primer.ab1
L58R No.10-M13Reverse primer
Cap 22

SQ.....¹³⁷⁶⁴

Signal G:1624 A:745 T:457 C:1221
DT377{BDv3}v1.mob
BD_MatrixV3.mtx
Points 1200 to 10616 Pk 1 Loc: 1200

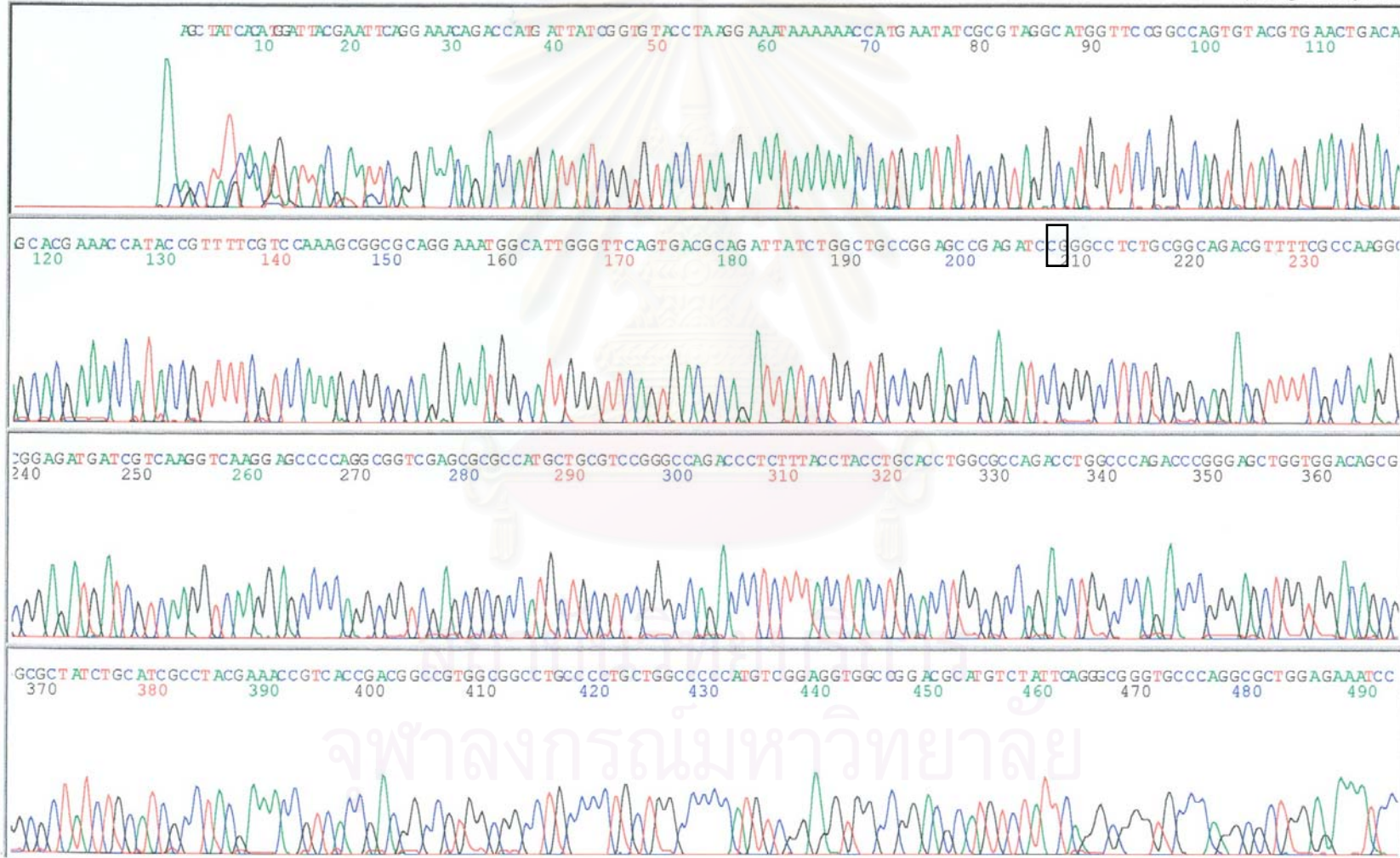
Page 2 of 3

Page 1 of 2

Tue, Mar 18, 2003 9:04 AM

Mon, Mar 17, 2003 9:32 AM

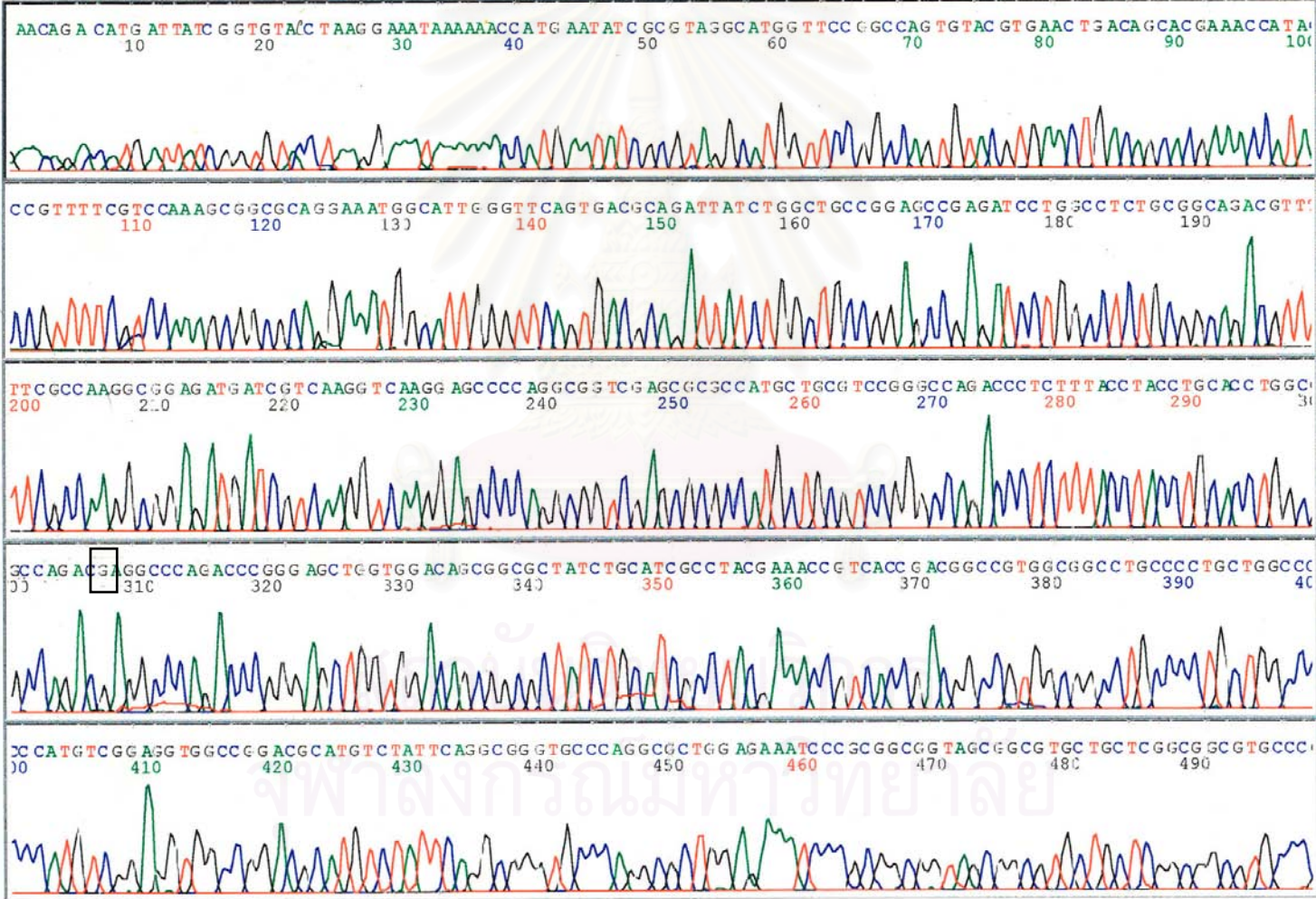
Spacing: 10.71{10.71}



(p)

จุฬาลงกรณ์มหาวิทยาลัย

ABI PRISM Model 3100 A01_1_.ab1 Signal G:108 A:70 T:58 C:95 Page 1 of 2
Version 3.7 DT3100POF6{3Dv3}v1.mob Thu, May 15, 2003 10:57 PM
Basecaller-310CAPOP6S1 3100-Avant Thu, May 15, 2003 8:27 PM
BC 1.5.b.6 Cap 1 Points 847 to 10106 Pk 1 Loc: 847 Spacing: 12.05(12.05)



(a)



Model 377
Version 3.7
Basecaller-377.bcp
BC 1.3.0.0

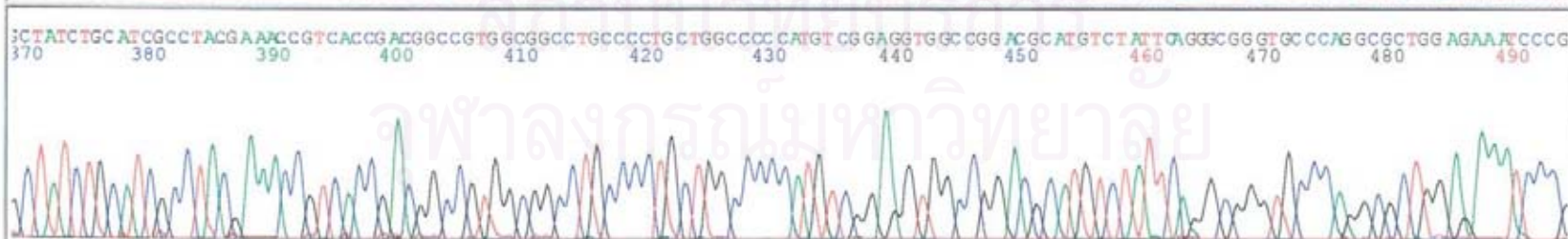
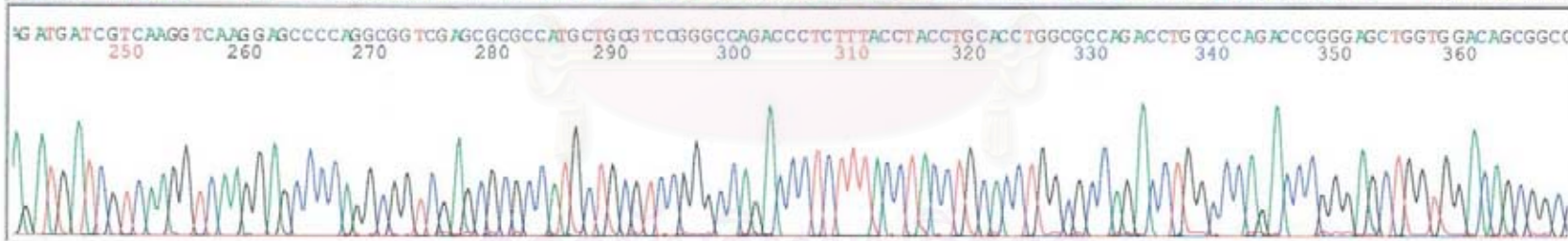
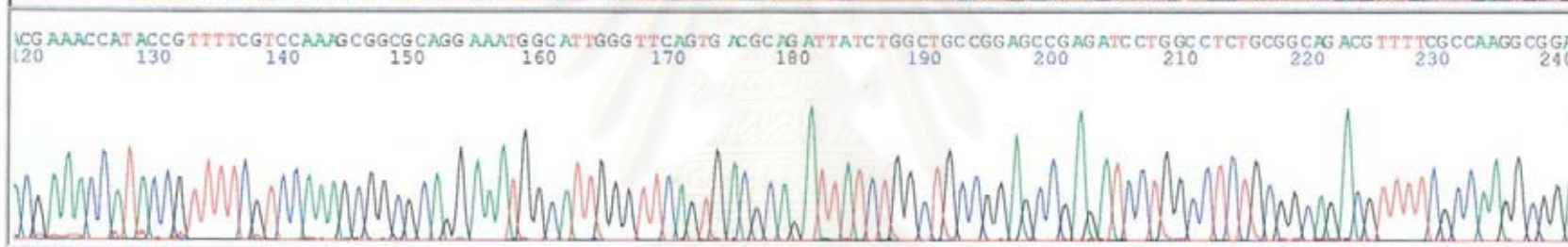
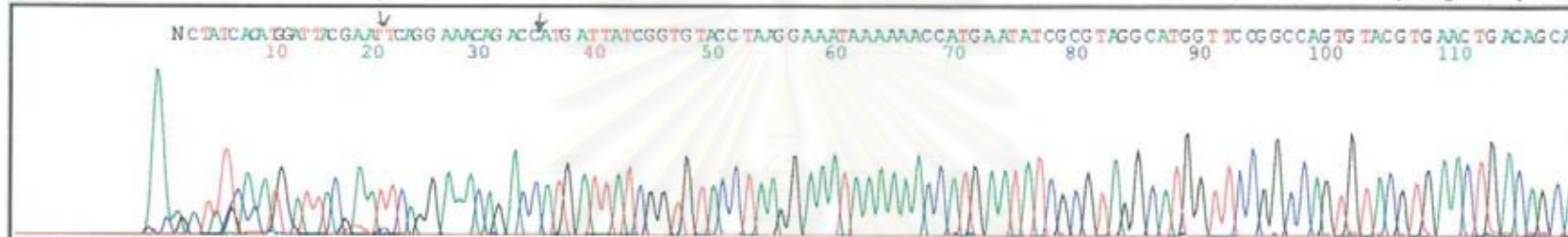
12P168R No.13-M13Reverse primer.ab1
P168R No.13-M13Reverse primer
Cap 12

SQ.....of.....
17269

Signal G:1516 A:554 T:368 C:980
DT377(BDv3)v1.mob
BD_MatrixV3.mtx
Points 1150 to 10616 Pk 1 Loc: 1150

Page 1 of 2
Thu, Feb 13, 2003 8:35 AM
Wed, Feb 12, 2003 9:58 AM
Spacing: 10.79(10.79)

(f)



จุฬาลงกรณ์มหาวิทยาลัย



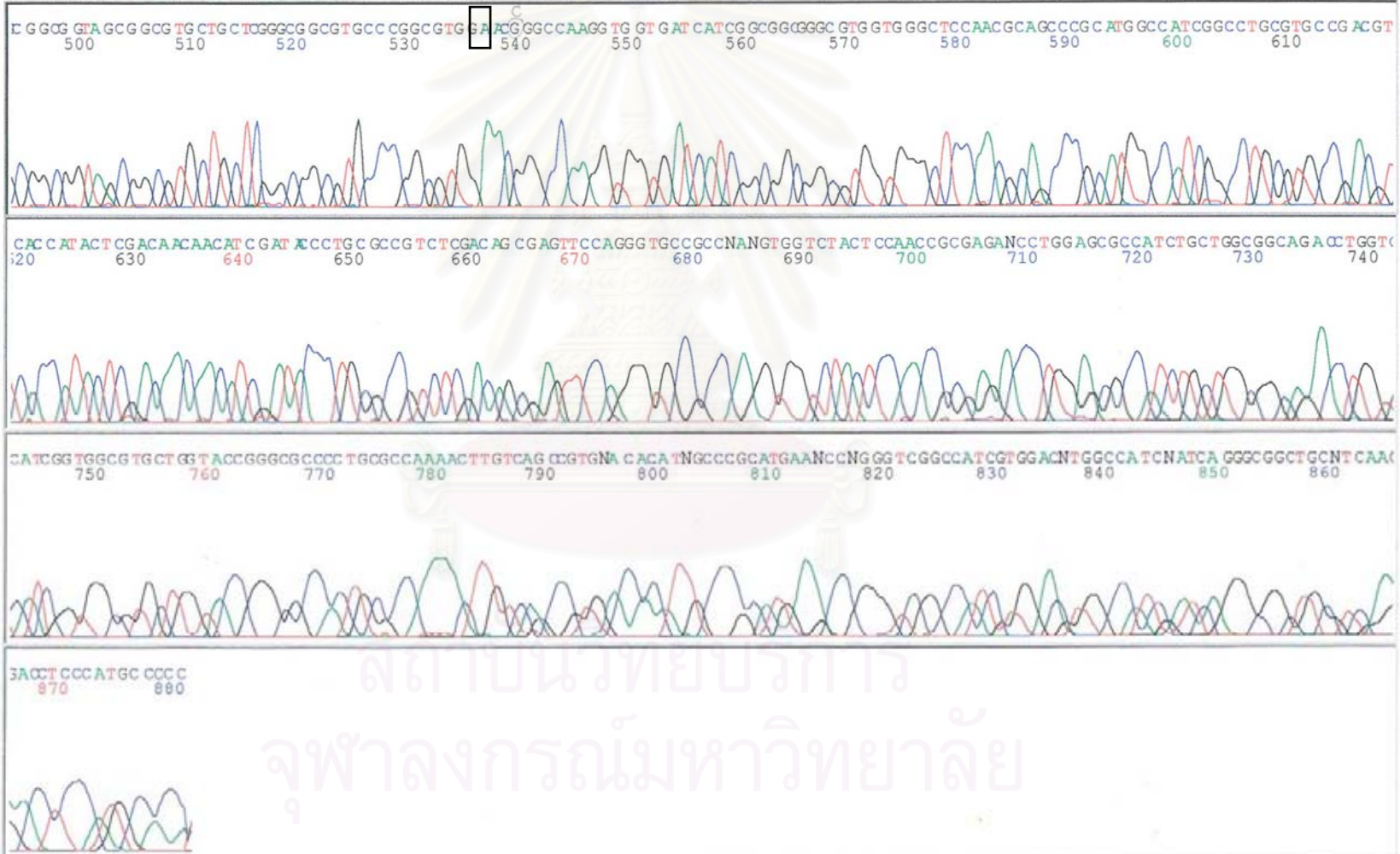
Model 377
Version 3.7
Basecaller-377.bcp
BC 1.3.0.0

12P168R No.13-M13Reverse primer, ab1
P168R No.13-M13Reverse primer
Cap 12

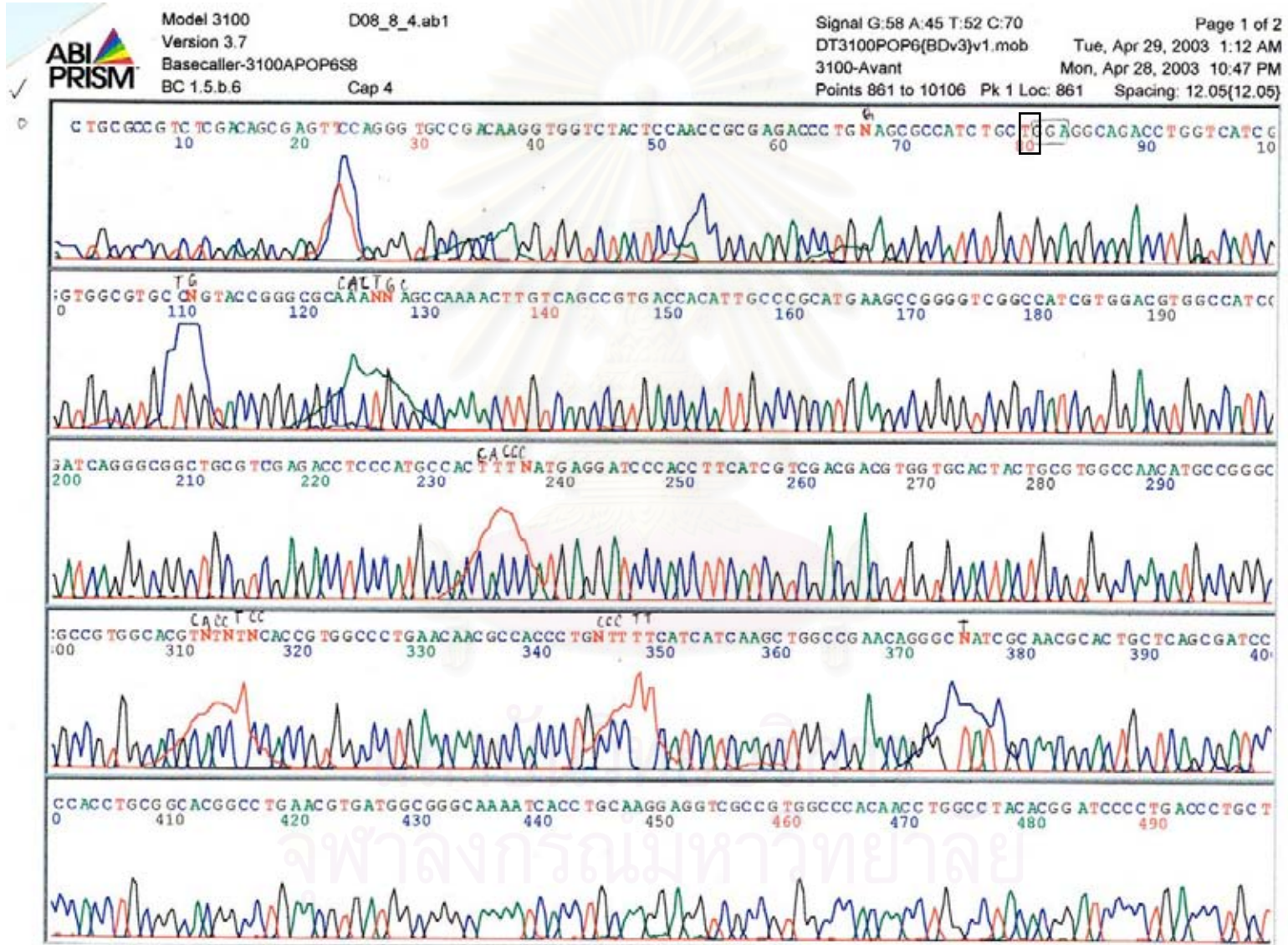
SQ.....h 269

Signal G:1516 A:554 T:368 C:980
DT377(BDv3)v1.mob
BD_MatrixV3.mtx
Points 1150 to 10616 Pk 1 Loc: 1150

Page.....of..... Page 2 of 2
Thu, Feb 13, 2003 8:35 AM
Wed, Feb 12, 2003 9:58 AM
Spacing: 10.79(10.79)



(f) continued



(8)

จุฬาลงกรณ์มหาวิทยาลัย



Model 377
Version 3.7
Basecaller-377.bcp
BC 1.3.0.0

08L101E,A231EXLNo.2-M13Forward.ab1
L101E,A231EXLNo.2-M13Forward
Cap 8

SQ.....1524

Signal G:1638 A:584 T:438 C:1242
DT377{BDv3}v1.mob
BD_MatrixV3.mtx
Points 1120 to 10616 Pk 1 Loc: 1120

Page.....01.....

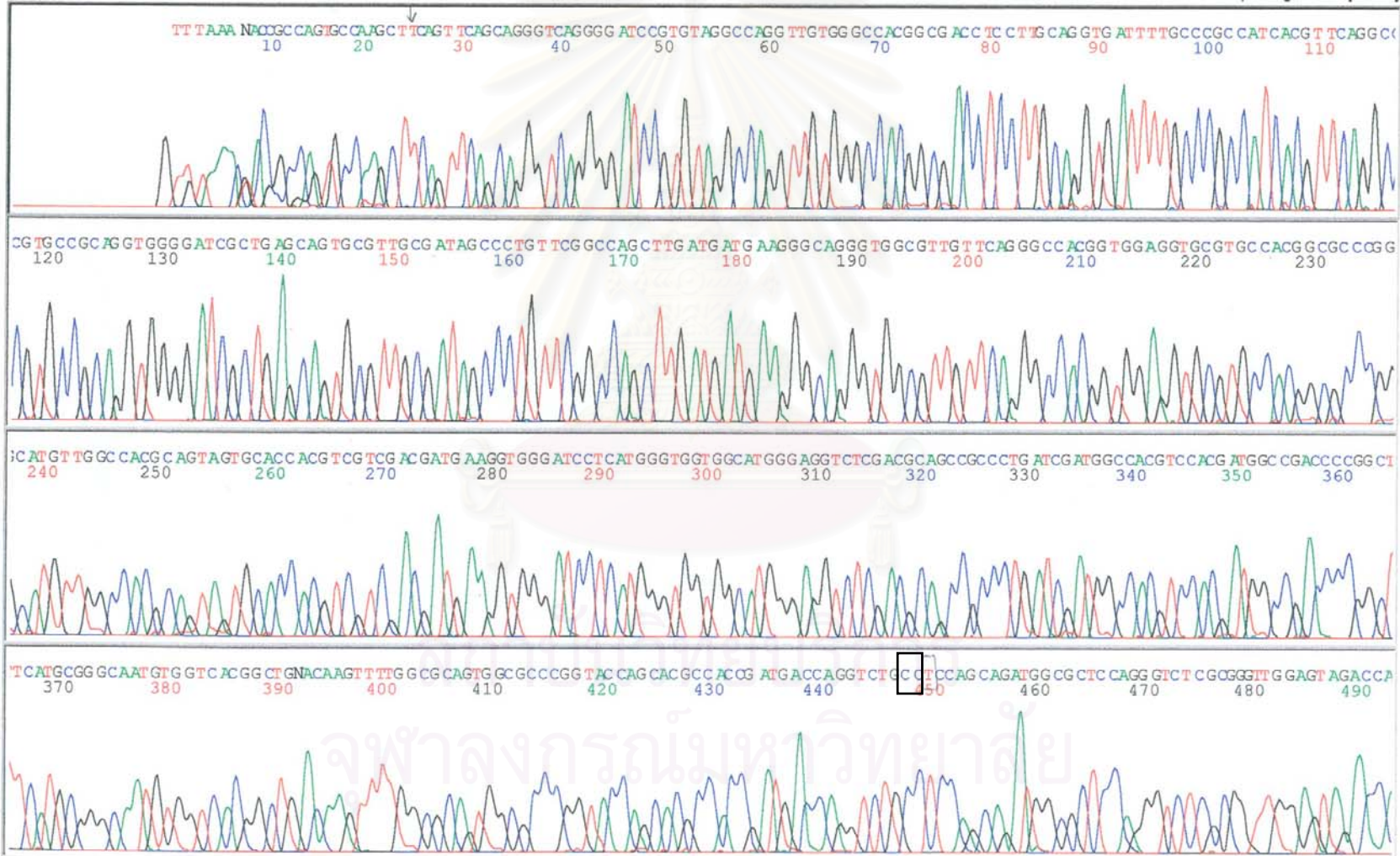
Page 1 of 2

Fri, Jul 11, 2003 8:01 AM

Thu, Jul 10, 2003 7:54 AM

Spacing: 10.04{10.04}

(h)





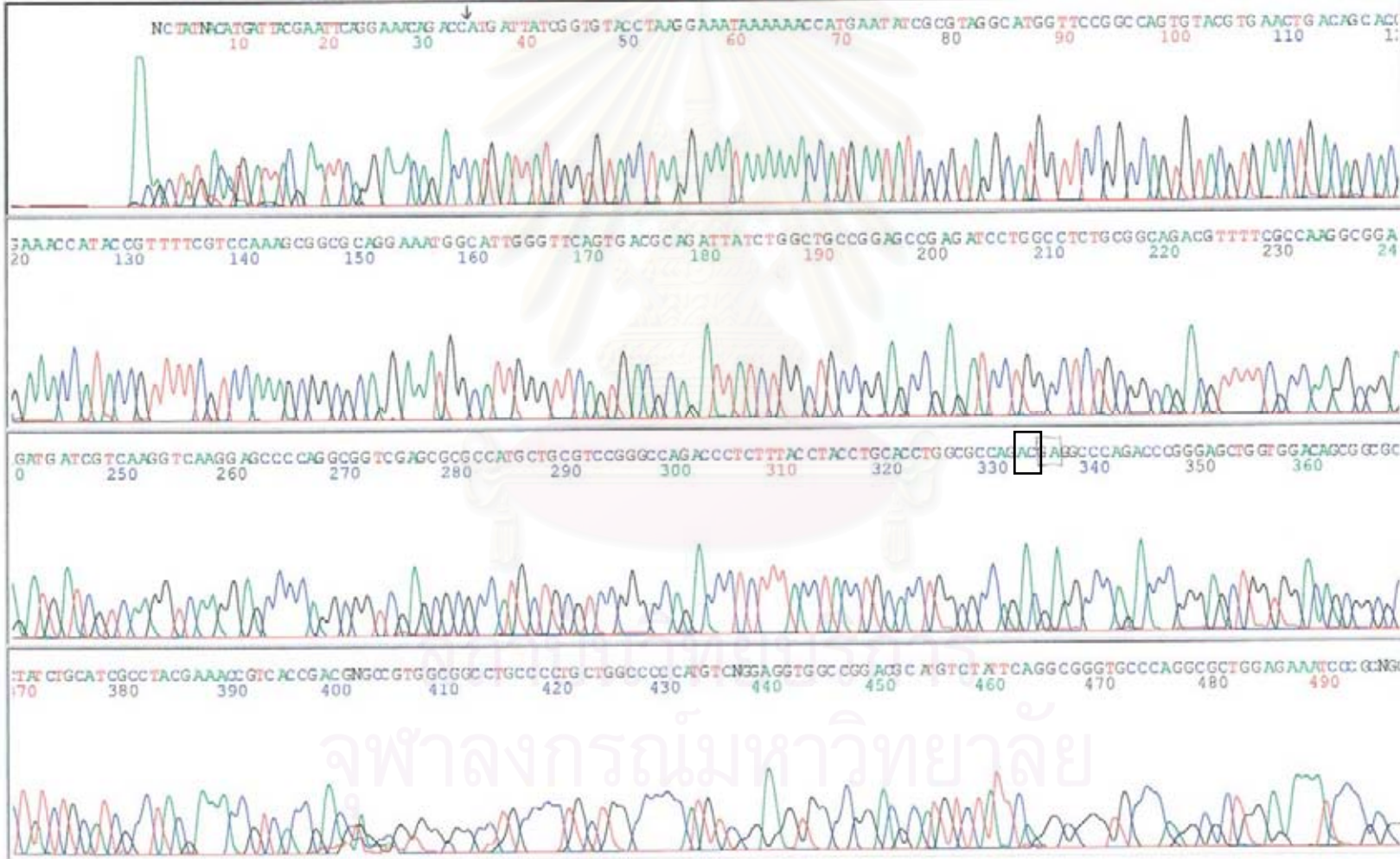
Model 377
Version 3.7
Basecaller-377.bcp
BC 1.3.0.0

09L101E,A231EXLNo.2-M13Reverse.ab1
L101E,A231EXLNo.2-M13Reverse
Cap 9

SQ.....18242

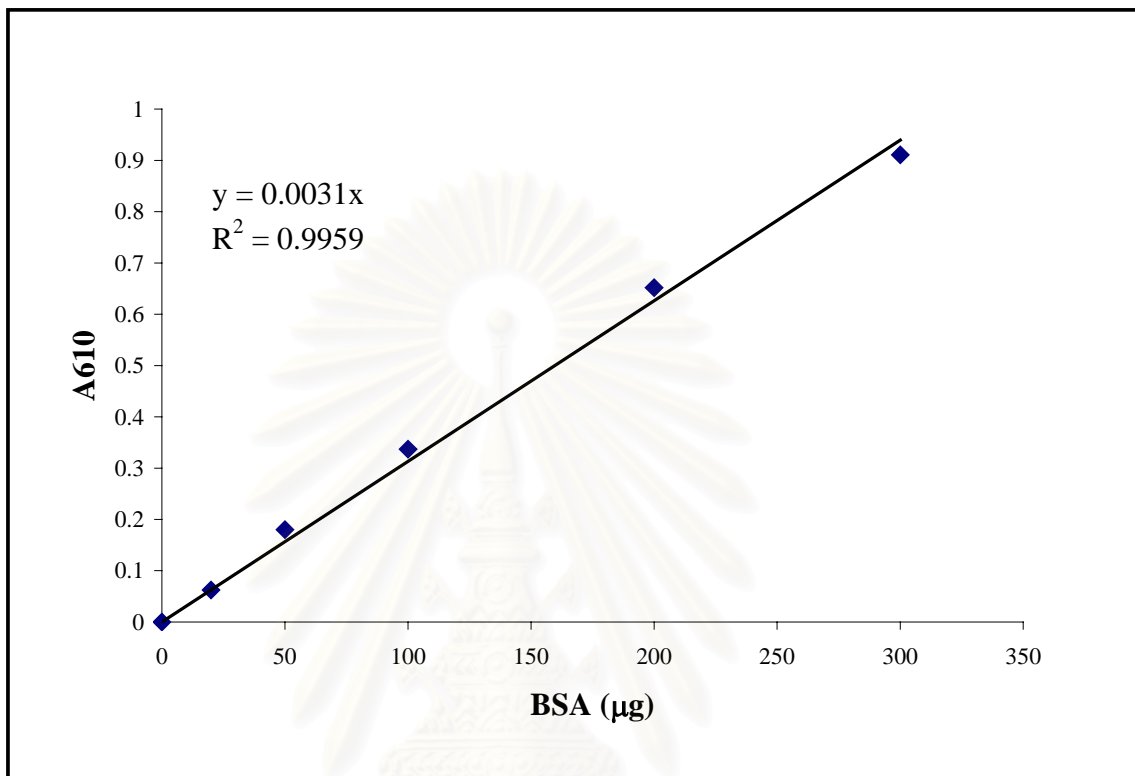
Signal G:1841 A:846 T:565 C:1502
DT377(BDv3)v1.mob
BD_MatrixV3.mtx
Points 1020 to 10616 Pk 1 Loc: 1020

Page.....of..... Page 1 of 2
Fri, Jul 11, 2003 8:02 AM
Thu, Jul 10, 2003 7:54 AM
Spacing: 10.13{10.13}



(1)

จุฬาลงกรณ์มหาวิทยาลัย

APPENDIX H**Standard curve for protein determination by Lowry's Method (1951)**

สถาบันวิทยบริการ
จุฬาลงกรณ์มหาวิทยาลัย

BIOGRAPHY

Mr. Jeerapan Machaopa was born on October 4, 1977. He graduated with the degree of Bachelor of Science from the department of Biochemistry at Srinakarinwirot University in 1999. He has studied for the degree of Master of Science at the Department of Biochemistry, Chulalongkorn University since 2000.



สถาบันวิทยบริการ
จุฬาลงกรณ์มหาวิทยาลัย